

Comparing the Kinematic and Kinetic Outputs from Digital Human Modeling Tools to a Lab-Based Rigid-Link Model for the Investigation of Musculoskeletal Disorder Hazards During Patient Handling

by

Uma Lad

A thesis
presented to the University of Waterloo
in fulfillment of the
thesis requirement for the degree of
Master of Science
in
Kinesiology

Waterloo, Ontario, Canada, 2018

©Uma Lad 2018

Author's Declaration

I hereby declare that I am the sole author of this thesis. This is a true copy of the thesis, including any required final revisions, as accepted by my examiners.

I understand that my thesis may be made electronically available to the public.

Abstract

Patient repositioning tasks expose healthcare providers (HCPs) to high bone-on-bone forces, resulting in the development of musculoskeletal disorders (MSDs) (Fragala,2011). Researchers have been able to estimate biomechanical exposures during patient turning using kinematic and kinetic data collected from HCPs (e.g., Marras et al., 1999); however, many of these laboratory-based studies require considerable time and resources to execute and it also remains challenging to gather reliable data (Jäger et al., 2013). Digital human modeling (DHM) may offer unique advantages over direct measurement to estimate biomechanically relevant exposures. Investigators have used DHM to evaluate MSD hazards (Cao et al., 2013; Potvin, 2017); however, there is limited evidence on the fidelity of their outputs. The objective of this study was to compare the kinematic and kinetic outputs produced by two commercial DHM software packages against those generated using a lab-based motion-capture driven approach when analyzing HCPs performance of patient turns.

Twenty-five (25) HCPs (eight males) performed a patient turn in the laboratory using a hospital bed with a live 82kg male patient. Whole body kinematics and sagittal plane video were collected. External peak hand force was measured using a force gauge. An accelerometer was placed on the sternum of the patient to identify point of initial patient motion which was assumed to represent the time-point of peak hand force application. Whole body kinematics were used to drive a rigid linked segment model for each participant using Visual3D (C-Motion Inc., Germantown, USA). Measured peak hand force was divided by two and applied to the model at the grip center of each hand at the frame of peak force application. A top down modeling approach was used to calculate trunk and shoulder joint angles and L4-L5 and shoulder joint

moments about the flexion/extension axis. These outputs were extracted and compared against DHM software outputs.

Siemens Jack (V 8.4) and Santos Pro DHM software packages were used to simulate the patient turn. The static patient turn posture used by the HCP was modeled using the manual joint manipulation, posture prediction and motion capture data importing approaches available in both software. Anthropometrics and peak hand force gathered from the laboratory experiment were inputted into the digital models. trunk and shoulder joint angles and L4-L5 and shoulder joint moments were computed and extracted about the flexion/extension axis from each digitally modeled posture. RMANOVAs, Pearson Product Moment correlation coefficients and Bland Altman analyses were used to compare DHM outputs to the lab-based model outputs.

Results from this investigation indicate that the use of Siemens Jack's (V 8.4) manual joint manipulation approach estimated low back and shoulder kinematics and kinetics that were in agreement with lab-based model outputs. The kinematics and kinetics computed using the posture prediction and motion capture driven approaches to modeling the patient repositioning task, using both Siemens Jack (V 8.4) and Santos Pro were not in agreement with the lab-based outputs. This may have been a result of differences in kinematic modeling assumptions related to the structure of skeletal linkage models, joint decompositions, degrees of freedom in each model and anthropometrics used in DHM software. The use of DHM tools for biomechanical analyses of patient repositioning tasks has the possibility to aide in the investigation of MSD exposures; however, it is important for investigators to understand the purpose of each DHM modeling approach as well as the underlying assumptions of digital human models that may affect kinematic and kinetic outputs used to quantify the exposure to MSDs.

Acknowledgements

I would first like to thank my thesis supervisor Dr. Steven Fischer. The door to Steve's office was always open whenever I ran into trouble or had a question about my research. Steve recognized biomechanics wasn't my true passion in life, but still went beyond his supervisor duties to support my learning. He steered me in the right direction whenever I was about to skid off the tracks. He was there for me to support me through my struggles and was there with me to celebrate my greatest achievements. Thank you for introducing me to the research world during my undergraduate education and providing me with the confidence to further advance my education into graduate studies; I'm grateful for learning and growing as an academic alongside you. You taught me the tricks of the trade and challenged me to "think outside the box." It was an absolute privilege and blessing to have come across such a kind-hearted, down to earth and passionate supervisor like Steve. Thanks Fishy!

I would like to thank my thesis advisory committee, Dr. Clark Dickerson and Dr. Carolyn MacGregor. Their support and contributions strengthened my thesis document.

I would also like to acknowledge members of the Occupational Biomechanics and Ergonomics Lab: Daniel Armstrong, Claragh Pegg, Nick Patrick, Nathalie Oomen and Laura Healey. I appreciated all the advice, feedback and troubleshooting assistance provided by all of you throughout my thesis project. As well, thanks for making my dull days brighter with all of your trolling jokes, memes and GIFs!

Thank you, Aleksandra Budarick, for all the technical and logistical support you provided me during my data collections and ongoing guidance throughout the writing process of my thesis. It was a pleasure working alongside Aleks, and I could not have successfully completed this thesis without her support!

I would also like to acknowledge the undergraduate research volunteers who helped with piloting and data collections. Specifically, thank you to Justin Davidson, Sarah Remedios, Chris Moore and Oliver Clark.

I am thankful to have come across Dr. Suryapratim Banerjee during my thesis project. I'm not the strongest in statistics, but he managed to teach me everything I needed to know about statistics in order to analyze my data. As an external academic supporter to my thesis, he always reminded me that the research I was doing was important, and always brought reassurance to me whenever I had doubt in my abilities as a researcher. He was an awesome guy to chat to when life got stressful in the biomechanics world. I appreciate all the time and effort he invested in me during my thesis project.

Thank you to Craig McDonald for assisting me with all the technical issues related to the digital human software used in this thesis. This thesis could not have been completed without your diligent help.

I must express my very profound gratitude to my parents for providing me with a roof over my head, food, bed and car (all free of charge) throughout my years of study and through the process of researching and writing this thesis. This accomplishment would not have been possible without their support.

Finally, I must thank my little sister Kirti for supporting me through my graduate studies. She helped me solve all my mathematical related problems and helped me destress with her procrastination tactics. I wouldn't have made it through without her in the background!

Thank you all!

Table of Contents

List of Figures	x
List of Tables	xvi
List of Abbreviations	xvii
1.0 Introduction	1
1.1 Patient Handling and Musculoskeletal Disorders	1
1.2 Challenges Measuring Biomechanical Exposures During Patient Handling Tasks	2
1.3 Digital Human Modelling: An Alternative to Comprehensive Direct Measurement	4
1.4 Research Objective	6
1.5 Research Questions	6
1.6 Research Hypotheses	7
1.7 Prioritization of Outcome Variables	10
1.8 Rationale for Research	11
2.0 Review of Relevant Literature	13
2.1 Patient Repositioning and Workplace Musculoskeletal Disorders	13
2.2 Biomechanical Studies on Patient Reposition Tasks	14
2.3 Challenges and Limitations when Performing Biomechanical Investigations on Patient Handling Tasks	15
2.4 Digital Human Modeling: An Alternate Approach to Estimate MSD Hazards for High Risk Jobs ..	16
2.5 DHM Applications in Manufacturing Industries	18
2.6 DHM Applications in the Healthcare Sector	20
2.7 Avatar Posturing and Control Approaches	22
2.7.1 Manual Joint Manipulation	22
2.7.2 3D Kinematic Data Importing	24
2.7.3 Posture Prediction	24
2.8 Advanced Digital Human Modeling Software Packages	26
2.8.1 Siemens Jack (V 8.4)	26
2.8.2 Santos Pro	28
2.9 Validation of Avatar Posturing Approaches for Healthcare Applications	30
2.10 Relevance of Current Research	31
3.0 Methodology	32
3.1 Participants	32
3.2 Instrumentation and Laboratory Setup	33

3.2.1 Motion Capture – 3D Kinematic Data	33
3.2.2 Video.....	35
3.2.3 External Hand Force Measure.....	35
3.2.4 Acceleration	37
3.3 Experimental Protocol	37
3.4 Data Processing.....	40
3.4.1 3D position data	40
3.4.2 Acceleration data.....	40
3.5 Calculating and Extracting Lab-Based Outcome Measures: Visual 3D Model Development and Analysis	40
3.6 Computing and Extracting Digital Human Model Outcome Measures	42
3.6.1 Kinematic Data Importing	44
3.6.2 Manual Posturing	44
3.6.3 Posture Prediction	45
3.7 Statistical Analyses	47
4.0 Results.....	50
4.1 Direct Motion Capture Data Importing.....	51
4.1.1 Kinematics	51
4.1.2 Kinetics	54
4.2 Manual Joint Manipulation	58
4.2.1 Kinematics	58
4.2.2 Kinetics	61
4.3 Posture Prediction	65
4.3.1 Kinematics	65
4.3.2 Kinetics	68
5.0 Discussion.....	72
5.1 Summary of Key Findings	72
5.2 Manual Joint Manipulation	75
5.3 Posture Prediction	79
5.4 Direct Motion Capture Data Importing.....	81
5.5 Summary of Factors Associated with Digital Models that Resulted in Differences Between Lab-based and DHM Biomechanical Outputs.....	84
5.5.1 Skeletal Linkage Model	85
5.5.2 Kinematic Degrees of Freedom	86
5.5.3 Joint Decomposition	87

5.5.4 Anthropometrics.....	88
5.6 Use of DHM Kinematic and Kinetic Outputs for the Investigation of MSD Hazards.....	90
6.0 Limitations	95
6.1 Implications of Future Research	97
7.0 Conclusions.....	99
References.....	101
Appendix I	120
Appendix II.....	121
Appendix III.....	123

List of Figures

Figure 1. Illustration of user control across the three posturing approaches	10
Figure 2. Skeletal linkage model of Jack (V 8.4)	27
Figure 3. Skeletal linkage model of Santos	29
Figure 4. Schematic diagram of the laboratory setup used to for the patient reposition task.....	34
Figure 5. Vicon reflective marker placement	35
Figure 6. Diagram of the rigid metal bar that was inserted into the sheet to facilitate hand force measurements using a force gauge	36
Figure 7. Critical patient care hospital bed	38
Figure 8. Block diagram of the experimental protocol used for the lab-based study	39
Figure 9. Block diagram of the flow of collected data that were used as inputs when digitally modeling the patient reposition task in Jack and Santos.....	43
Figure 10. Virtually simulating the static posture of the HCP at the initiation of the patient turn in Jack and Santos	46
Figure 11. Left – scatter plot illustrating the relationship between trunk angles (+ extension) estimated using Jack’s motion capture data importing approach and the lab-based RLM (V3D). Regression equation and Pearson’s correlation coefficient (r) are displayed on the plot. Right – Bland-Altman plot illustrating the differences between trunk angles (+ extension) produced by the lab-based RLM (V3D) and Jack’s motion capture data importing approach vs. the mean of the two measures. Red line is the systematic error produced by Jack, grey dashed lines are the limits of agreement from -1.96SD to +1.96SD, black dotted line is the line of equality.	52
Figure 12. Left - scatter plot illustrating the relationship between trunk angles (+ extension) estimated using Santos’ motion capture data importing approach and the lab-based RLM (V3D). Regression equation and Pearson’s correlation coefficient (r) are displayed on the plot. Right – Bland-Altman plot illustrating the differences between trunk angles (+ extension) produced by the lab-based RLM (V3D) and Santos’ motion capture data importing approach vs. the mean of the two measures. Red line is the systematic error produced by Santos, grey dashed lines are the limits of agreement from -1.96SD to +1.96SD, black dotted line is the line of equality.	52
Figure 13. Left – scatter plot illustrating the relationship between shoulder joint angles (+ flexion) estimated using Jack’s motion capture data importing approach and the lab-based RLM (V3D). Regression equation and Pearson’s correlation coefficient (r) are displayed on the plot. Right – Bland-Altman plot illustrating the differences between shoulder joint angles (+ flexion)	

produced by the lab-based RLM (V3D) and Jack’s motion capture data importing approach vs. the mean of the two measures. Red line is the systematic error produced by Jack, grey dashed lines are the limits of agreement from -1.96SD to +1.96SD, black dotted line is the line of equality..... 53

Figure 14. Left – scatter plot illustrating the relationship between shoulder joint angles (+flexion) estimated using Santos’ motion capture data importing approach and the lab-based RLM (V3D). Regression equation and Pearson’s correlation coefficient (r) are displayed on the plot. Right – Bland-Altman plot illustrating the differences between shoulder joint angles (+ flexion) produced by the lab-based RLM (V3D) and Santos’ motion capture data importing approach vs. the mean of the two measures. Red line is the systematic error produced by Santos, grey dashed lines are the limits of agreement from -1.96SD to +1.96SD, black dotted line is the line of equality. 54

Figure 15. Left – scatter plot illustrating the relationship between L4-L5 joint moments (+ extensor) estimated using Jack’s motion capture data importing approach and the lab-based RLM (V3D). Regression equation and Pearson’s correlation coefficient (r) are displayed on the plot. Right – Bland-Altman plot illustrating the differences between L4-L5 joint moments (+ extensor) produced by the lab-based RLM (V3D) and Jack’s motion capture data importing approach vs. the mean of the two measures. Red line is the systematic error produced by Jack, grey dashed lines are the limits of agreement from -1.96SD to +1.96SD, black dotted line is the line of equality..... 55

Figure 16. Left – scatter plot illustrating the relationship between L4-L5 joint moments (+ extensor) estimated using Santos’ motion capture data importing approach and the lab-based RLM (V3D). Regression equation and Pearson’s correlation coefficient (r) are displayed on the plot. Right – Bland-Altman plot illustrating the differences between L4-L5 joint moments (+ extensor) produced by the lab-based RLM (V3D) and Santos’ motion capture data importing approach vs. the mean of the two measures. Red line is the systematic error produced by Santos, grey dashed lines are the limits of agreement from -1.96SD to +1.96SD, black dotted line is the line of equality. 55

Figure 17. Left – scatter plot illustrating the relationship between shoulder joint moments (+ flexor) estimated using Jack’s motion capture data importing approach and the lab-based RLM (V3D). Regression equation and Pearson’s correlation coefficient (r) are displayed on the plot. Right – Bland-Altman plot illustrating the differences between shoulder joint moments (+ flexor) produced by the lab-based RLM (V3D) and Jack’s motion capture data importing approach vs. the mean of the two measures. Red line is the systematic error produced by Jack, grey dashed lines are the limits of agreement from -1.96SD to +1.96SD, black dotted line is the line of equality..... 56

Figure 18. Left – scatter plot illustrating the relationship between shoulder joint moments (+ flexor) estimated using Santos’ motion capture data importing approach and the lab-based RLM (V3D). Regression equation and Pearson’s correlation coefficient (r) are displayed on the plot. Right – Bland-Altman plot illustrating the differences between shoulder joint moments (+ flexor)

produced by the lab-based RLM (V3D) and Jack’s motion capture data importing approach vs. the mean of the two measures. Red line is the systematic error produced by Santos, grey dashed lines are the limits of agreement from -1.96SD to +1.96SD, black dotted line is the line of equality..... 57

Figure 19. Left – scatter plot illustrating the relationship between trunk angles (+ extension) estimated using Jack’s manual joint manipulation approach and the lab-based RLM (V3D). Regression equation and Pearson’s correlation coefficient (r) are displayed on the plot. Right – Bland-Altman plot illustrating the differences between trunk angles (+ extension) produced by the lab-based RLM (V3D) and Jack’s manual joint manipulation approach vs. the mean of the two measures. Red line is the systematic error produced by Jack, grey dashed lines are the limits of agreement from -1.96SD to +1.96SD, black dotted line is the line of equality. 59

Figure 20. Left – scatter plot illustrating the relationship between trunk angles (+ extension) estimated using Santos’ manual joint manipulation approach and the lab-based RLM (V3D). Regression equation and Pearson’s correlation coefficient (r) are displayed on the plot. Right – Bland-Altman plot illustrating the differences between trunk angles (+ extension) produced by the lab-based RLM (V3D) and Santos’ manual joint manipulation approach vs. the mean of the two measures. Red line is the systematic error produced by Santos, grey dashed lines are the limits of agreement from -1.96SD to +1.96SD, black dotted line is the line of equality. 59

Figure 21. Left – scatter plot illustrating the relationship between shoulder joint angles (+ flexion) estimated using Jack’s manual joint manipulation approach and the lab-based RLM (V3D). Regression equation and Pearson’s correlation coefficient (r) are displayed on the plot. Right – Bland-Altman plot illustrating the differences between shoulder joint angles (+ flexion) produced by the lab-based RLM (V3D) and Jack’s manual joint manipulation approach vs. the mean of the two measures. Red line is the systematic error produced by Jack, grey dashed lines are the limits of agreement from -1.96SD to +1.96SD, black dotted line is the line of equality. 60

Figure 22. Left – scatter plot illustrating the relationship between shoulder joint angles (+ flexion) estimated using Santos’ manual joint manipulation approach and the lab-based RLM (V3D). Regression equation and Pearson’s correlation coefficient (r) are displayed on the plot. Right – Bland-Altman plot illustrating the differences between shoulder joint angles (+ flexion) produced by the lab-based RLM (V3D) and Santos’ manual joint manipulation approach vs. the mean of the two measures. Red line is the systematic error produced by Santos, grey dashed lines are the limits of agreement from -1.96SD to +1.96SD, black dotted line is the line of equality. 61

Figure 23. Left – scatter plot illustrating the relationship between L4-L5 joint moments (+ extensor) estimated using Jack’s manual joint manipulation approach and the lab-based RLM (V3D). Regression equation and Pearson’s correlation coefficient (r) are displayed on the plot. Right – Bland-Altman plot illustrating the differences between L4-L5 joint moments (+ extensor) produced by the lab-based RLM (V3D) and Jack’s manual joint manipulation approach vs. the mean of the two measures. Red line is the systematic error produced by Jack, grey dashed lines are the limits of agreement from -1.96SD to +1.96SD, black dotted line is the line of equality. 62

Figure 24. Left – scatter plot illustrating the relationship between L4-L5 joint moments (+ extensor) estimated using Santos’ manual joint manipulation approach and the lab-based RLM (V3D). Regression equation and Pearson’s correlation coefficient (r) are displayed on the plot. Right – Bland-Altman plot illustrating the differences between L4-L5 joint moments (+ extensor) produced by the lab-based RLM (V3D) and Santos’ manual joint manipulation approach vs. the mean of the two measures. Red line is the systematic error produced by Santos, grey dashed lines are the limits of agreement from -1.96SD to +1.96SD, black dotted line is the line of equality. 62

Figure 25. Left – scatter plot illustrating the relationship between shoulder joint moments (+ flexor) estimated using Jack’s manual joint manipulation approach and the lab-based RLM (V3D). Regression equation and Pearson’s correlation coefficient (r) are displayed on the plot. Right – Bland-Altman plot illustrating the differences between shoulder joint moments (+ flexor) produced by the lab-based RLM (V3D) and Jack’s manual joint manipulation approach vs. the mean of the two measures. Red line is the systematic error produced by Jack, grey dashed lines are the limits of agreement from -1.96SD to +1.96SD, black dotted line is the line of equality. 63

Figure 26. Left – scatter plot illustrating the relationship between shoulder joint moments (+ flexor) estimated using Santos’ manual joint manipulation approach and the lab-based RLM (V3D). Regression equation and Pearson’s correlation coefficient (r) are displayed on the plot. Right – Bland-Altman plot illustrating the differences between shoulder joint moments (+ flexor) produced by the lab-based RLM (V3D) and Jack’s manual joint manipulation approach vs. the mean of the two measures. Red line is the systematic error produced by Santos, grey dashed lines are the limits of agreement from -1.96SD to +1.96SD, black dotted line is the line of equality. 64

Figure 27. Left – scatter plot illustrating the relationship between trunk angles (+ extension) estimated using Jack’s posture prediction approach and the lab-based RLM (V3D). Regression equation and Pearson’s correlation coefficient (r) are displayed on the plot. Right – Bland-Altman plot illustrating the differences between trunk angles (+ extension) produced by the lab-based RLM (V3D) and Jack’s posture prediction approach vs. the mean of the two measures. Red line is the systematic error produced by Jack, grey dashed lines are the limits of agreement from -1.96SD to +1.96SD, black dotted line is the line of equality. 66

Figure 28. Left – scatter plot illustrating the relationship between trunk angles (+ extension) estimated using Santos’ posture prediction approach and the lab-based RLM (V3D). Regression equation and Pearson’s correlation coefficient (r) are displayed on the plot. Right – Bland-Altman plot illustrating the differences between trunk angles (+ extension) produced by the lab-based RLM (V3D) and Santos’ posture prediction approach vs. the mean of the two measures. Red line is the systematic error produced by Santos, grey dashed lines are the limits of agreement from -1.96SD to +1.96SD, black dotted line is the line of equality. 66

Figure 29. Left – scatter plot illustrating the relationship between shoulder joint angles (+ flexion) estimated using Jack’s posture prediction approach and the lab-based RLM (V3D). Regression equation and Pearson’s correlation coefficient (r) are displayed on the plot. Right – Bland-Altman plot illustrating the differences between shoulder joint angles (+ flexion) produced

by the lab-based RLM (V3D) and Jack's posture prediction approach vs. the mean of the two measures. Red line is the systematic error produced by Jack, grey dashed lines are the limits of agreement from -1.96SD to +1.96SD, black dotted line is the line of equality..... 67

Figure 30. Left – scatter plot illustrating the relationship between shoulder joint angles (+ flexion) estimated using Santos' posture prediction approach and the lab-based RLM (V3D). Regression equation and Pearson's correlation coefficient (r) are displayed on the plot. Right – Bland-Altman plot illustrating the differences between shoulder joint angles (+ flexion) produced by the lab-based RLM (V3D) and Santos' posture prediction approach vs. the mean of the two measures. Red line is the systematic error produced by Santos, grey dashed lines are the limits of agreement from -1.96SD to +1.96SD, black dotted line is the line of equality. 68

Figure 31. Left – scatter plot illustrating the relationship between L4-L5 joint moments (+ extensor) estimated using Jack's posture prediction approach and the lab-based RLM (V3D). Regression equation and Pearson's correlation coefficient (r) are displayed on the plot. Right – Bland-Altman plot illustrating the differences between L4-L5 joint moments (+ extensor) produced by the lab-based RLM (V3D) and Jack's posture prediction approach vs. the mean of the two measures. Red line is the systematic error produced by Jack, grey dashed lines are the limits of agreement from -1.96SD to +1.96SD, black dotted line is the line of equality. 69

Figure 32. Left – scatter plot illustrating the relationship between L4-L5 joint moments (+ extensor) estimated using Santos' posture prediction approach and the lab-based RLM (V3D). Regression equation and Pearson's correlation coefficient (r) are displayed on the plot. Right – Bland-Altman plot illustrating the differences between L4-L5 joint moments (+ extensor) produced by the lab-based RLM (V3D) and Santos' posture prediction approach vs. the mean of the two measures. Red line is the systematic error produced by Santos, grey dashed lines are the limits of agreement from -1.96SD to +1.96SD, black dotted line is the line of equality. 69

Figure 33. Left – scatter plot illustrating the relationship between shoulder joint moments (+ flexor) estimated using Jack's posture prediction approach and the lab-based RLM (V3D). Regression equation and Pearson's correlation coefficient (r) are displayed on the plot. Right – Bland-Altman plot illustrating the differences between shoulder joint moments (+ flexor) produced by the lab-based RLM (V3D) and Jack's posture prediction approach vs. the mean of the two measures. Red line is the systematic error produced by Jack, grey dashed lines are the limits of agreement from -1.96SD to +1.96SD, black dotted line is the line of equality. 70

Figure 34. Left – scatter plot illustrating the relationship between shoulder joint moments (+ flexor) estimated using Santos' posture prediction approach and the lab-based RLM (V3D). Regression equation and Pearson's correlation coefficient (r) are displayed on the plot. Right – Bland-Altman plot illustrating the differences between shoulder joint moments (+ flexor) produced by the lab-based RLM (V3D) and Jack's posture prediction approach vs. the mean of the two measures. Red line is the systematic error produced by Santos, grey dashed lines are the limits of agreement from -1.96SD to +1.96SD, black dotted line is the line of equality. 71

Figure 35. Joint position data from the lab-based model mapped onto anthropometrically scaled avatars in Jack (left) and Santos (right). In Santos, the green circles show the avatar joint centers of rotation and the red circles are the joint centers of rotation of the lab-based skeletal model, red lines show the mapping errors 84

Figure 36. A summary of factors associated with digital models that resulted in differences between lab-based and DHM biomechanical outputs. Each model-related factor influenced the kinematic and kinetic outputs across the posturing approaches; however, this flow chart illustrates where each influencing factor was revealed in this investigation. 90

List of Tables

Table 1. Participant demographics.....	32
Table 2. Outline of the independent and dependent variables assessed in the RANOVA	47
Table 3. Relationships assessed between the lab-based model and DHM outcome measures.....	49
Table 4. Summary of the mean differences found between kinetic and kinematic measures estimated using the lab-based RLM (V3D) and DHM software packages' direct motion capture data importing approach. Asterisks indicate significant differences between models. The calculated smallest detectable change within 95% confidence intervals is reported for each pair.	51
Table 5. Summary of the mean differences found between kinetic and kinematic measures estimated using the lab-based RLM (V3D) and DHM software packages' manual joint manipulation approach. Asterisks indicate significant differences between models. The calculated smallest detectable change within 95% confidence intervals is reported for each pair.	58
Table 6. Summary of the mean differences found between kinetic and kinematic measures estimated using the lab-based RLM (V3D) and DHM software packages' posture prediction approach. Asterisks indicate significant differences between models. The calculated smallest detectable change within 95% confidence intervals is reported for each pair.	65

List of Abbreviations

HCP.....	Health care provider
MSD.....	Musculoskeletal disorder
L4-L5.....	4th/5th lumbar vertebrae joint
RLM.....	Rigid linked model
DHM.....	Digital human model
IK.....	Inverse kinematics
CAD.....	Computer aided design
HF&E.....	Human factors & engineering
GEBOD.....	Generator of Body Data
ROM.....	Range of motion
NIOSH.....	National Institute of Occupational Safety and Health
RULA.....	Rapid upper limb assessment
REBA.....	Rapid entire body assessment
OWAS.....	Ovako working posture assessment system
MTM.....	Methods-time measurement
DOF.....	Degrees of freedom
ANSUR.....	Anthropometric survey
NHANES.....	National Health and Nutrition Examination Survey
ATB.....	Articulated Total Body
MOO.....	Multi-objective optimization
RANOVA.....	Repeated analysis of variance

1.0 Introduction

1.1 Patient Handling and Musculoskeletal Disorders

Patient handling activities expose healthcare providers (HCPs) to musculoskeletal disorder (MSD) hazards. HCPs, including registered nurses, nursing assistants and personnel support workers have one of the highest rates of MSDs. According to 2014 Ontario health care sector injury statistics, 24% of lost time injury claims in nursing services were a result of MSDs associated with patient handling (lifting, transferring and repositioning patients/residents/clients) (Health Care Sector Injury Statistics, 2016). In particular, researchers have found that repositioning patients in a bed is one of the highest risk activities for injuries among HCPs (Fragala & Bailey, 2003; Pompeii, Lipscomb, Schoenfisch, & Dement, 2009; Weiner, Alperovitch-Najenson, Ribak, & Kalichman, 2015). Repositions require HCPs to laterally slide the patient in their bed, reposition their limbs and turn them over from supine to lateral recumbent position. Patient repositioning has been reported as a task that involves frequent lifting, pulling, pushing, awkward postures and handling of heavy loads (Weiner, Kalichman, Ribak, & Alperovitch-Najenson, 2017). These are all MSD hazards that increase the risk of developing MSDs, including low back pain and shoulder injury (Fragala, 2011; Nelson, Lloyd, Menzel, & Gross, 2003; OSHA, 2009).

Intervening on patient handling related MSDs first requires quantification of exposures. To determine the factors that increase the physical demands of the task the most, postures, durations, frequencies, and loads handled by HCPs during patient repositioning tasks have been analyzed to estimate biomechanical loading on HCPs. Researchers have evaluated the effects of patient repositioning actions on the compressive and shear forces acting at the 4th/5th lumbar

vertebrae joint (L4-L5) in a laboratory setting. Biomechanical studies have found that at peak exposures during repositioning can result in L4-L5 compressive forces over 3400N (W. S. Marras, Davis, Kirking, & Bertsche, 1999; Schibye et al., 2003); surpassing the NIOSH action limit for compressive loading on the spine (Waters, Putz-Anderson, Garg, & Fine, 1993). A research group from Denver investigated the effects of patient weight (59kg, 83kg and 109kg) and patient disability type (hemiplegia, paraplegia and near-paralysis) on spine forces during lateral transferring of patients. The study found that increased patient weight and disability imposed higher L4-L5 compressive and shear forces on HCPs (Skotte & Fallentin, 2008). Jäger et al. (2013) and Theilmeier, Jordan, Luttmann, & Jäger, (2010) used a specially designed hospital bed integrated with force sensors to more accurately quantify the hand forces exerted by HCPs when performing patient repositioning actions. Hand forces and postures used by HCPs resulted in low back compressive forces, that again, exceed recommended thresholds (Jäger et al., 2013; Theilmeier et al., 2010).

1.2 Challenges Measuring Biomechanical Exposures During Patient Handling Tasks

Our knowledge of biomechanical exposures during patient handling comes from the application of a traditional lab-based occupational biomechanics approach. Using this approach, researchers can directly measure kinetics (e.g., ground reaction forces) and kinematics (via 3D motion capture) as participants perform an occupational task of interest. These measured data provide inputs into biomechanical models (e.g., rigid linked segment models and joint models), which can yield estimates of net joint moments and bone-on bone forces. Despite previous efforts to apply this occupational biomechanics-based approach to health care, challenges persist when applying this approach to understand exposure profiles during patient handling activities.

Researchers have been able to estimate biomechanical exposures during patient repositioning using kinematic and kinetic data collected from HCPs; however, many of the studies have suffered from challenges affecting the ability to gather reliable data for a sufficiently wide range of situations. For example, HCPs have stepped off the force platforms during the performance of the patient repositioning actions (Schibye et al., 2003; Skotte et al., 2002), altering the ground reaction force profiles necessary to support a rigid-linked modeling approach. Additionally, with the use of passive motion capture systems, the ability to view the reflective markers placed on the HCPs can be obstructed by the limbs of the HCP or by the patient (Jäger et al., 2013; Theilmeier et al., 2010), affecting the postural data profiles necessary to support modeling efforts. These challenges emphasize the difficulty in obtaining reliable biomechanical data for a wide array of situations as is required to explore new and novel designs and approaches to address MSD risks among HCPs associated with patient handling.

Researchers have recognized that traditional biomechanical instrumentation can also be cumbersome or sometimes impossible to use in health care facilities including hospitals, clinics and long-term care homes (Cao, Jiang, Han, & Khasawneh, 2013; Jimerson, Park, Jiang, & Stajsic, 2016). Physical instrumentation to gather data as required to estimate levels of biomechanical exposure can disrupt or impede the natural performance of patient handling tasks or the standardized work processes of HCPs (Winkel & Mathiassen, 1994). Challenges performing occupational biomechanical investigations in health care facilities include shared working environments, facility regulations, security and privacy concerns (Hall, Longhurst, & Higginson, 2009). Due to this unique and dynamic environment, it is difficult for investigators to control co-founding factors such as patient weight or time of day, threatening the internal validity of findings.

1.3 Digital Human Modelling: An Alternative to Comprehensive Direct Measurement

Digital human modeling (DHM) may offer unique advantages over direct measurement to estimate biomechanically relevant exposures. DHM allows users to investigate the relationship between workplace/tasks parameters and human factor elements, such as patient weight, hospital bed height, etc., quickly and efficiently. DHM simulates humans anthropometrically and biomechanically in 3D space. Avatars, representing humans, have integrated rigid-link skeletal models powered by an inverse kinematics (IK) algorithm to simulate real-time joint positions. Additionally, leveraging inverse kinetics and built in joint models, DHMs can provide estimates of bone-on-bone joint forces as well. DHM enables users to conduct occupational biomechanical evaluations on human – environment interactions with minimal to no disruption to the work process, obstructing physical instrumentation or extensive use of physical models (e.g. vehicle or machine prototype).

Researchers, engineers and ergonomist have utilized DHM for design and injury risk assessments in aerospace, automotive, manufacturing and health care industries (Chaffin, 2008). Using a design-of-experiments approach, experts can run a variety of simulations, manipulating factors such as the physical environments, avatar anthropometry and task requirements, such as external loads, to effectively analyze and estimate their effects on MSD exposures. This advantage addresses the limitation of traditional lab-based assessments that are often restricted to the analysis of only a subset of conditions. For example, to model a manual work task, the user can position the joints of the virtual avatar to simulate a lift, carry or walking tasks in its specifically designed virtual environment, such as a warehouse. The user can then analyze the effects of different postures and loads or anthropometric parameters used in the simulation on biomechanical exposures such as joint forces experienced by the worker, providing evidence

about relationships between design parameters, movement behaviours and MSD exposure likelihood. With the ability to virtually mock up workplace environments and work processes to inform better designs, companies have reduced costs, time and lost time injury claims (Demirel & Duffy, 2007; Fritzsche, 2010).

Different DHM software packages have been developed that include a variety of capabilities; some including, Delmia, RAMSIS and 3DSSPP. Currently, Siemens Jack (V 8.4) and Santos Pro are commercially available DHM software packages with the latest developments in virtual simulation capabilities, including a wide range of anthropometric databases, advanced human posturing controls and IK and kinetics algorithms, improved rigid link models (RLMs), and ergonomics analysis tools (Chaffin, 2005). These features, allow users to create static or dynamic simulations of avatars interacting with their environment, physical objects or with other simulated humans. Furthermore, Jack (V 8.4) and Santos Pro offer three avatar control approaches to simulate human kinematics. These include manual joint manipulation, direct motion capture data importing and posture prediction (Santoshuman Inc. Software, 2009; Siemens PLM Software, 2016). Each of these posturing approaches yields a set of joint angles for the rigid link human model integrated in the avatar of Jack and Santos; however, validation of these posturing approaches for the application in healthcare sector is still required.

DHM has been widely applied in automotive and manufacturing industries, but it also has a strong prospect for increased applications within the healthcare sector. Investigators have used DHM to evaluate the MSD hazards associated with patient handling activities (Cao et al., 2013; Jimerson et al., 2016; L. Zhang, Niu, Feng, Xu, & Li, 2013); however, some users found that the DHM software was limited, as it could not simulate the HCP's preferred movement strategies (Paul & Quintero-Duran, 2015). While many investigators have used DHM to evaluate MSD

hazards in a variety of occupational tasks, there is limited evidence on the validity of their outputs. We do not know if the avatar control approaches used to simulate whole body postures are realistic. This thesis describes a study that compared the joint angles and joint moments estimated by Jack (V 8.4) and Santos, using each of their three posturing approaches, relative to those calculated using a traditional lab-based occupational biomechanics approach, as HCPs perform a patient repositioning task.

1.4 Research Objective

1. The objective of this study was to compare the low back and shoulder kinematic and kinetic outcomes produced using Siemens Jack (V 8.4) and Santos Pro software package's avatar control approaches; manual joint manipulation, direct motion capture data importing and posture prediction approaches to those calculated using a lab-based rigid-link segmental model when modeling HCPs performance of a patient repositioning task.

1.5 Research Questions

1. How do L4-L5 and shoulder flexor/extensor joint moments and trunk and shoulder flexion/extension joint angles of HCPs during the performance of a patient reposition differ, when estimated using:
 - a. Siemens Jack (V 8.4) and Santos Pro software package's manual joint manipulation approach;
 - b. Siemens Jack (V 8.4) and Santos Pro software package's direct motion capture data importing approach; and
 - c. Siemens Jack (V 8.4) and Santos Pro software package's posture prediction approach

relative to when calculated using a lab-based rigid-linked segment model approach driven by directly measured kinematics and hand forces?

2. Are L4-L5 and shoulder flexor/extensor joint moments and trunk and shoulder flexion/extension joint angles of HCPs when repositioning a patient estimated using Siemens Jack (V 8.4) or Santos Pro correlated with those estimated using a lab-based rigid-linked segment model approach?

1.6 Research Hypotheses

1. There will be significant differences between L4-L5 and shoulder flexor/extensor joint moments and trunk and shoulder flexion/extension joint angles estimated using Siemens Jack (V 8.4) and Santos Pro, relative to those calculated using a lab-based rigid-linked segment model approach when using the posture prediction approach to simulate HCPs repositioning a patient, but no differences when using the manual joint manipulation and direct motion capture approaches.
 - i. The posture prediction approach estimates a set of joint angles (whole body posture) for the avatar using software specific algorithms. Therefore, posture prediction provides users with the least control when simulating a posture. Therefore, it is hypothesized that joint angles and moments produced using the posture prediction approach will be significantly different from the lab-based RLM outputs. In turn, when importing motion capture directly into the DHM or when manually manipulating the avatar, the user is offered greater control over posturing. As a result, it was anticipated that when DHMs were used in manual joint manipulation or

motion capture importing modes, it would result in outcome measures that would be similar to the lab-based RLM (Figure 1).

2. When considering correlations between L4-L5 and shoulder flexor/extensor joint moments and trunk and shoulder flexion/extension joint angles:
 - a. Manual joint manipulation will result in outcome measures that are moderately correlated ($0.5 \leq r \leq 0.7$) to those calculated using a lab-based rigid-linked segment model approach driven by directly measured kinematics and hand forces when modeling HCPs repositioning a patient.
 - i. Since posturing is based on the sagittal image of the participant, there may be differences in output variables. Position of the avatar segments according to the video image may produce differing results relative to the lab-based RLM because the geometric segments (with clothing) will be positioned. This could produce differing shoulder and trunk joint angles and moments. While this limitation may cause differences in the output joint angles and moments relative to the lab-based RLM, it is predicted this method will still produce relatively similar results to the lab-based RLM outputs as the user has control over joint/segment positioning.
 - b. Direct motion capture data importing will result in outcome measures that are strongly correlated ($r > 0.7$) with those calculated using a lab-based rigid-linked segment model approach driven by directly measured kinematics and hand forces when modeling HCPs repositioning a patient.

- i. Joint and segment positions gathered from the laboratory collection using motion capture will be mapped onto the anthropometrically scaled virtual avatar. Jack and Santos should compute similar shoulder and L5-L5 angles and moments. It is hypothesized that anthropometric databases and linkage model differences within Jack and Santos may produce some error in the joint angles and moments when using this approach

- c. Posture prediction will result in outcome measures that are weakly correlated ($r < 0.5$) with those calculated using a lab-based rigid-linked segment model approach driven by directly measured kinematics and hand forces when modeling HCPs repositioning a patient.
 - i. Since there is very little control over the posture predicted by the DHM when using the posture prediction approach, it is anticipated that there will be high variability in kinematic and kinetic model outputs relative to the lab-based RLM. Both Jack and Santos use unique algorithms to predict human postures (statistical and optimization-based approaches respectively); however, very little control of the inputs into the software packages is required by the user relative to the direct motion capture approach and manual joint manipulation approach. Therefore, since there is less control in the model parameter inputs, it is hypothesized that posture prediction approach will produce weakly correlated joint angles and moments.

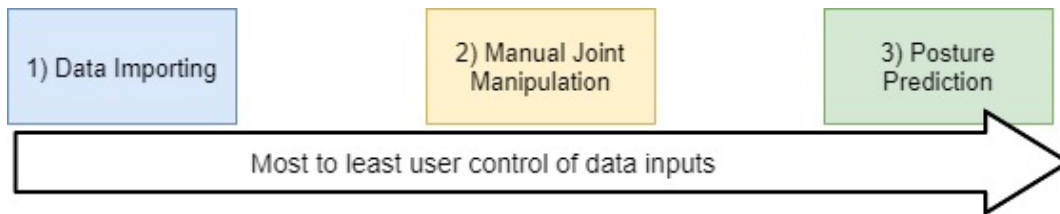


Figure 1. Illustration of user control across the three posturing approaches

1.7 Prioritization of Outcome Variables

The outcome variables (biomechanical measures) of interest in this study will be prioritized based on their value towards the investigation of MSD Hazards in HCPs (clinical significance). The output variables will be ranked as follows:

- 1) L4-L5 flexor/extensor joint moments (moment produced in the sagittal plane about the L4-L5 joint)
- 2) Shoulder flexor/extensor joint moments (moment produced in the sagittal plane about the shoulder joint center)
- 3) Trunk flexion/extension angles (angle formed between the trunk segment and pelvis segment, in the sagittal plane)
- 4) Shoulder flexion/extension joint angles (angle formed between the humerus segment and trunk segment, in the sagittal plane)

L4-L5 and shoulder joint flexor/extensor joint moments were prioritized over the trunk and shoulder flexion/extension joint angles because joint moments are often used by ergonomist and researchers to quantify the risk of injuries, as it is a measure that describes the amount of torque applied to each joint of the musculoskeletal system. L4-L5 flexor/extensor moments was ranked first because there is a higher risk for low back injuries in HCPs during patient repositioning over shoulder injuries (Fragala, 2011; Nelson et al., 2003; OSHA, 2009). Incidence rate for back injuries involving lost work days was 181.6 per 10 000 full-time HCPs (Nelson et

al, 2003). L4-L5 flexor/extensor joint moments are important biomechanical variables used to calculate low back compression forces, which is an objective measure used often in spine research to predict the risk of development of low back injuries (Marras, Davis, Kirking, & Bertsche, 1999; Schibye et al., 2003). Shoulder injuries and pain are commonly reported by nursing personnel during the performance of patient handling tasks (Black, Shah, Busch, Metcalfe, & Lim, 2011). HCPs are exposed to high peak and cumulative shoulder demands during patient reposition tasks, increasing their risk of sustaining a shoulder injury (Belbeck, Cudlip, & Dickerson, 2014). As a result, shoulder flexor/extensor moments were selected as an outcome to validate as it is a biomechanical measure that has been used by researchers to assess the risk of injury to the shoulder during occupational tasks (Bjelle, Hagberg, & Michaelson, 1981).

Joint angles are measures commonly used in physical ergonomics to define and classify working postures adapted by individuals during the performance of occupational tasks (Lowe, Weir, & Andrews, 2014), as a result trunk and shoulder flexion/extension joint angles were ranked with least prioritization. The trunk and shoulder have been most commonly observed deviating from neutral position during patient handling tasks such as patient turning (Freitag et al., 2012), therefore angles at these sites will be useful for identifying determinants of injury risk such as biomechanical loading (moments) of joints and tissues (Marras & Karwowski, 2006). Since joint angles are commonly used to assess risk, they had least priority in this investigation.

1.8 Rationale for Research

This research will generate new knowledge regarding the ability of digital human modeling tools, and inherent modeling approaches, to simulate and estimate biomechanical exposures relevant to a patient handling task. Comparing Jack (V 8.4) and Santos Pro digital

human model kinematic and kinetic outputs to laboratory data-based rigid-link model outputs will provide preliminary evidence towards the validity of DHM software package's ability to adequately evaluate MSD exposures within a patient handling context. If we can verify which of the three avatar control approaches available in Jack (V 8.4) and Santos are valid for simulating and analyzing the kinematics and kinetics of HCPs performing patient handling activities, it could potentially support the utility of DHM as a cost-efficient and effective tool to investigate MSDs in the healthcare sector, and also to inform the design of new tools and products to reduce MSD exposures the HCPs.

2.0 Review of Relevant Literature

2.1 Patient Repositioning and Workplace Musculoskeletal Disorders

HCPs are exposed to MSD hazards when performing patient handling tasks. HCPs, including registered nurses, nursing assistants and personal support workers routinely perform physically demanding tasks, including lifting, transferring and repositioning patients. Epidemiological studies report that providing direct patient care involves frequent exposure to MSD hazards including: manual handling, awkward postures and repeated handling of heavy loads (Estrynebehar et al., 1990). These hazards have been associated with high spine forces when performing patient handling tasks (Gagnon, Chehade, Kemp, & Lortie, 1987; Skotte & Fallentin, 2008; Ulin et al., 1997). Specifically, biomechanical studies have indicated that patient repositioning tasks expose HCPs to L4-L5 compressive and shear forces above recommended threshold limit values (W. S. Marras, Davis, Kirking, & Bertsche, 1999; Schibye et al., 2003).

Repositioning of immobile patients involves several patient handling actions, including laterally sliding the patient to the side of the bed, adjusting their limbs and turning the patient from supine to lateral recumbent position. These patient handling actions have been observed to involve the use of frequent and forceful pushing, pulling and lifting exertions by the HCP (Weiner et al., 2015). Exposure to pushing, pulling and lifting can increase the risk of exposure to MSD hazards in HCPs (Fragala, 2011; Nelson et al., 2003; OSHA, 2009).

Manually repositioning patients helps to prevent the development of bedsores as a result of prolonged pressure to the skin and underlying tissue (Bergstrom et al., 2013; Griffiths, 2012). HCPs have been observed repositioning patients at least 15 times over a 24hour period, highlighting the tasks frequency (Latimer, Chaboyer, & Gillespie, 2015). Since repositioning

patients is frequently performed, it increases a HCP's frequency of exposure to MSD hazards (high loads, awkward postures), consequently, increasing their risk for developing MSDs

2.2 Biomechanical Studies on Patient Reposition Tasks

Several studies have investigated MSD exposures associated with patient handling activities. Schibye et al. (2003) reported peak L4-L5 joint compressive forces above 3400N, in addition to high shear and net joint moments when HCPs perform patient repositioning. Similarly, researchers from Denmark found that patient reposition actions including lateral transfers and lifting resulted in L4-L5 compressive and shear forces exceeding injury thresholds (Skotte et al., 2002; Skotte & Fallentin, 2008). Further, increased weight and decreased mobility of patients were directly linked to increased spine loading on HCPs. Lindbeck & Engkvist (1993) estimated the L5-S1 joint moments as a function of time for a two HCP team when turning a patient from supine to lateral recumbent position. At the instant of estimated peak force application, spine moments up to 96Nm were imposed on the lead HCP.

Researchers have utilized unique biomechanical instrumentation and equipment to characterize the kinematics and kinetics associated with patient repositioning actions. Caboor et al. (2000) used an electrogoniometer, combined with electromyography to assess the change in postural and muscular demands of HCPs when performing patient handling tasks at different bed heights. The study did not observe changes in spinal motions or muscular demands as a result of bed height adjustments. Marras, Davis, Kirking, & Bertsche (1999) used a Lumbar Motion Monitor and electromyography (EMG) to gather kinematic and kinetic data to calculate internal spinal forces experienced by HCPs during patient transfer tasks. An EMG-assisted model estimated compressive forces at the L4-L5 joint over 3400N when using a partnered patient transfer technique.

Since patient repositioning involves the use of multiple maneuvering actions and forceful exertions, researchers have created in-house hospital bed mock ups with integrated force sensors to estimate the forces exerted by HCPs. A research group from Germany developed a hospital bed with tri-axial force sensors imbedded into the bedspring frame to record the forces exerted by the HCPs during the performance of patient repositioning actions (Jäger et al., 2013; Theilmeyer et al., 2010). Using external force recordings and postural data gathered using motion capture system, researchers were able to calculate spinal forces. The study found high L4-L5 compressive forces and spine moments that were a result of excessive spine flexion and lateral force exertions used during patient repositioning actions (Jäger et al., 2013; Theilmeyer et al., 2010).

2.3 Challenges and Limitations when Performing Biomechanical Investigations on Patient Handling Tasks

While researchers have been able to measure the external and estimate the internal forces imposed on the musculoskeletal system of HCPs during patient handling activities, multiple challenges and limitations have been reported. For example, researchers who have used in ground force platforms to gather kinetic measures during patient handling tasks have faced challenges when the HCP had stepped off the force plate during the task (Lindbeck & Engkvist, 1993; Skotte et al., 2002). Studies using passive motion capture systems to gather kinematic data found that the reflective markers attached to the HCP were occasionally obstructed by their own limbs or the patient during the performance of patient reposition tasks (Jäger et al., 2013; Theilmeyer et al., 2010). Additionally, while the use of laboratory-based mock ups are useful for characterizing the biomechanical exposures experienced by HCPs during patient repositioning

actions, these studies are costly and time consuming, limiting the number of experimental conditions, or alternate approaches that could be considered.

Though some research exists, as noted above, much less information is available about the biomechanics of patient handling, relative to general lifting, likely due to the challenges and limitations associated with characterizing exposures during the performance of unique patient handling tasks. Due to the complexity of patient handling tasks, researchers have issues gathering reliable human kinetic and kinematic data required to compute biomechanical measures that are used to estimate MSD exposures. Specifically, performing biomechanical investigations directly within health care facilities can pose challenges due to the dynamic environment, time constraints, costs and anonymity of patients (Hall et al., 2009; Winkel & Mathiassen, 1994). However, digital human models (DHMs) offers an alternative approach to estimate and characterize the kinematics and kinetics associated with patient handling activities. DHMs offers the ability to virtually simulate human behaviours as they interact with tools and equipment in a target environment. DHMs provide users with a method to simulate the postures and external loads experienced by real life humans and to derive the associated biomechanical measures required to evaluate MSD risks.

2.4 Digital Human Modeling: An Alternate Approach to Estimate MSD Hazards for High Risk Jobs

DHMs bridge the gap between computer aided designs (CAD) and human factors and ergonomics (HF&E). DHM software packages have the capabilities of emulating humans anthropometrically and biomechanically by using scaled avatars within representative 3D computer generated environments. DHM software packages draw on databases of anthropometry allowing users to scale an avatar's body segments to match the work population using regression

equations (Blanchonette, 2010). Alternatively, some DHM software packages have used the Generator of Body Data (GEBOD) (Cheng, Obergefell, & Rizer, 1994) to generate scaled geometric human body segments.

Avatars created in DHM software packages have complex kinematic linkage models that closely resemble the human skeletal structure with joints that obey physiological range of motion (ROM) restrictions and geometric shape. Avatars have integrated IK algorithms that are used to configure and drive avatars to produce human postures (described by a set of joint angles) and motions. IK models use external exposure data (force or pressure) along with anthropometric data to calculate net joint moments and forces experienced by the avatar (Duffy, 2008). The avatar's body is represented as a set of articulating links in a kinematic chain, therefore intersegmental joint moments and forces are calculated from forces measured at the top of the chain (top down inverse kinetics model) 3D dynamic model (Duffy, 2008). Alongside the inverse dynamic models, some DHM software packages also have integrated complex spine models to compute peak compression, shear and moments at the L4-L5 joint. Nuanced differences in modeling approaches between different commercially available DHMs may yield meaningful differences in estimated biomechanical exposure outputs underpinning the need for this comparative study.

Ergonomic analysis tool kits have also been integrated into DHM software packages to help users identify, evaluate and interpret MSD hazard risks. These include assessment tools such as National Institute of Occupational Safety and Health's (NIOSH) lifting equation, Rapid Upper Limb Assessment (RULA) tool, Rapid Entire Body Assessment (REBA) tool, Ovako Working Posture Analysis System (OWAS) and Methods Time Measurement (MTM) system and Porter's Comfort Rating Scale (Woldstad, 2006). However, the outcome of each tool

depends on how well the underlying DHM model replicates the kinematics and kinetics associated with the simulated behaviour. The ability to produce valid kinematic and kinetic estimates is crucial to the long-term utility and sustainability of DHM to support the consideration of HF&E into high-demand tasks like patient handling.

2.5 DHM Applications in Manufacturing Industries

DHM was first adopted by the aerospace industry, followed by the automotive engineering sectors (Demirel & Duffy, 2007). Through the virtual interaction of 3D objects/humans in a 2D computational interface, engineers have been able to utilize DHM for work station and product design as well as the optimization of work systems. Several researchers have successfully applied DHM to digitally mock up cock pit and crew work station designs to assess HF&E metrics (Karmakar, Pal, Majumdar, & Majumdar, 2012; Rune, Hongjun, & Bifeng, 2008; Sanjog, Karmakar, Patel, & Chowdhury, 2015; Sun, Gao, Yuan, & Zhao, 2011). Analysis emphasized cockpit design on vision and accessibility across variable anthropometrics of crew members. Through digital mock ups, engineers have analyzed human-machine interactions and incorporated them into design drawings in CAD (Demirel & Duffy, 2007; Naumann & Roetting, 2007), eliminating the need for physical mock-ups, shortening design cycle times and decreasing development costs for companies.

DHM is most commonly used to facilitate proactive HF&E investigations within automotive manufacturing, allowing companies to simulate realistic postures in order to evaluate efficiency of the work processes and systems. Specifically, industrial engineers have widely used DHM to simulate humans in CAD vehicle designs to account for human factors. Parameters such as passenger comfort, visibility, ingress/egress, reach capability have been evaluated in the design process of new vehicles (Naumann & Roetting, 2007). Reed & Huang (2008) modeled the

human motions used during the stages of ingress/egress of vehicles during their design process in DHM to identify design issues associated with the variability in human anthropometrics and motions. DHM has also been used to simulate and analyze workers' postures and motions used when performing specific tasks on automotive assembly lines in order to improve the efficiency of the assembly line design (Dan Lämkkull, Hanson, & Roland Örtengren, 2009).

DHM has also been used to facilitate proactive ergonomic investigations within manufacturing tasks to predict musculoskeletal demands. Fritzsche (2010) and (Lämkkull, Hanson, & Roland Örtengren (2009) found that DHM process simulations provided correct estimates of physical demands relative to real life estimates when evaluating the static postures of vehicle assembly line workers. Chang & Wang (2007) simulated automobile assembly tasks using CAD objects of the vehicle parts. The integrated ergonomic and biomechanical analysis tools identified MSD hazards associated with individual task operations (Chang & Wang, 2007).

DHM allows users to perform predictive simulations to improve and support manual materials handling tasks. Regazzoni & Rizzi, (2013) generated multiple simulations of a manual loading operation across a 5th and 50th percentile female and 50th and 95th percentile male to predict the reachability of different workers in order to optimize the height of a loading platform. Hanson, Högberg, & Söderholm (2012) illustrated the iterative process involved when solving for the optimal work posture to minimize joint stresses associated with a truck part assembly line. Anthropometrics, and joint positions were repeatedly adjusted to minimize stressors in order to identify the safest working posture. Case, Hussain, Marshall, Summerskill, & Gyi (2015) used DHM to model older adults with limited upper limb joint mobility when performing manufacturing tasks to identify acceptable and unacceptable strategies used to perform tasks given the joint demands. With the ability to instantly change anthropometrics, hand loads and

joint positions of the avatar during static or dynamic human simulations, users have been able to utilize DHMs to predict occupational task demands and optimize worker performance.

DHMs have enabled users to test a wider range of human machine/equipment interactions than physical mock-ups to explore issues related to assembly cycle times and worker safety (Naumann & Roetting, 2007). With the ability to adjust anthropometrics, postures and loads, engineers and ergonomists have been able to optimize product designs and work environments to minimize injury (Xudong Zhang & Chaffin, 2006). Furthermore, industry experts, at the administrative level have been able to efficiently solve and communicate health and safety related issues within the company to improve injury prevention strategies (Chaffin, 2008).

2.6 DHM Applications in the Healthcare Sector

While DHM has been effectively used in the automotive and manufacturing industries, improved virtual human modeling tools are beginning to see application in the healthcare sector. DHM has been employed to optimize healthcare facility design. Zhang, Xue, Li, & Kim, (2013) developed a virtual human torso model with 30 degrees of freedom (DOF) to evaluate the effect of surgical table heights. While the virtual model did provide insight into ergonomic guidelines, it was limited to posture analysis of the upper torso and used one standard anthropometric linkage model. Similarly, Paul & Quintero-Duran (2015) utilized Jack (V 7.1) to simulate a hospital bed pushing task to evaluate the influence of different anthropometric conditions of HCPs on hospital bed design. However, based on the simulation results, authors concluded that simulating complex healthcare tasks was limited in Jack (V 7.1) due to its inability to simulate an individual's movement preferences or motor control strategies (Paul & Quintero-Duran, 2015).

Investigators have also used DHM tools to assist in evaluating and identifying MSD hazards associated with patient handling activities. Jimerson, Park, Jiang, & Stajic (2016) used

Jack (V 7.1) to assess the low back forces experienced by HCPs when performing actions required to prepare immobile patients for transfer. But since Jack (V 7.1) lacks the ability to model human-to-human interactions, researchers used rudimentary CAD objects with calculated scaled body segment masses to simulate the patient. Similarly, Cao, Jiang, Han, & Khasawneh (2013) used Jack (V 7.1) to model and evaluate the low back forces imposed on HCPs when performing a barrow lift across different patient and HCP anthropometrics. Researchers constrained the trunk flexion angle of HCPs to 45 degrees and used a systematic bed height. Due to these simulation constraints, the study was not able to explore the effect of these independent variables on low back forces. Potvin (2017) used Jack (V 8.0) to evaluate the postures and loads imposed on HCPs when rotating a patient using a clinical assistive chair. While the investigation provided insights into the biomechanical demands imposed on HCPs, the data was limited by the extent to which it could be generalized. The study simulated and analyzed one posture that could be adopted by a 50th percentile female HCP when using the chair, while there could have been several possible postures adopted by HCPs depending on their motor control strategies and anthropometrics.

One known published study simulated a patient repositioning activity to evaluate and control the MSD hazard exposures on HCPs. Zhang, Niu, Feng, Xu, & Li (2013) used classic Jack (V 7.1) to simulate static and dynamic actions used by HCPs to turn patients from supine to lateral recumbent position. While researchers were able to simulate the postures associated with the dynamic task of turning a patient, external hand force exposures during each action were not included into the simulations. As mentioned previously, biomechanical evidence suggests that exposure to handling heavy loads (patients) during patient repositioning actions is one of the MSD hazards directly related to the increase in spinal forces imposed on HCPs (Skotte &

Fallentin, 2008). Future efforts to simulate patient handling should consider the influence of hand forces.

It is apparent that DHM has the capacity to be used in the automotive/manufacturing sectors, and the healthcare sector. HF&E experts practicing in healthcare have the ability to assess the influence of various health care tasks, work processes and medical device designs on MSD hazard exposures. However, very few studies have explored the validity of simulating complex healthcare tasks such as patient repositioning. There is a clear need to validate the utility of DHM for use in healthcare.

2.7 Avatar Posturing and Control Approaches

Over the past decade, simple single virtual human models have evolved into unique and powerful DHM software packages. Some of which include BOEMAN, MannequinPro, Siemens Jack, Safework, SAMMIE, RAMSIS, DELMIA, 3DSSPP and Santos (Raghunathan & R, 2016). DHM software packages have improved kinematic linkage models and algorithms that have increased efficiency, accuracy and control of the virtual avatar. To simulate the posture of the avatar, developers have integrated three different methods into DHM software packages to derive whole body linked segment joint positions. Three posturing approaches include; manual joint manipulation, 3D kinematic data importing and posture prediction (Duffy, 2008). Each of these avatar posturing approaches offer different levels of precision and fidelity.

2.7.1 Manual Joint Manipulation

In the early DHM software packages developed, users were required to manually articulate the avatar's joints independently to simulate whole body postures. With the improvements of rigid link models, users are now able to produce more realistic postures with increased degrees of freedom (DOF) at the joints, subjected to individual joint limits. As users

move individual segments, most DHM software packages use real time IK to determine the position of the linked segments/joints (Duffy, 2008).

Manual posturing approach is commonly used in reactive ergonomics to evaluate the risks associated with a job or task. Ergonomists have used manually postured DHM simulations to evaluate static postures and force exposures in order to provide estimates of physical demands imposed on individuals during real-life occupational tasks (Satheeshkumar & Krishnakumar, 2014). Since manual posturing is often used to assess and report the current risks associated with a task, it has been often used as descriptive tool in the ergonomics design process (Chang & Wang, 2007; Fritzsche, 2010; Rajput, Kalra, & Singh, 2013; Samson & Khasawneh, 2009). Jimerson and colleagues (2016) used postural and biomechanical data obtained from their digital simulations of HCPs preparing patients to make recommendations for equipment manufacturers and HCP/staff training to eliminate or control MSD hazards.

However, manually posturing can be laborious and an inconsistent process. For example, when a user is given the same goal posture to model, a different user may realize very different movement strategies based on knowledge of biomechanics and work processes (Duffy, 2008). Consequently, small deviations in postures caused through manual joint manipulation can result in large errors in the external joint moments and bone on bone forces produced by the biomechanical models (Chaffin, 2005). This can result in errors in prediction of MSD hazard exposures.

Manual manipulation of the avatar still remains one of the most common approaches to posturing avatars (Duffy, 2008), but is one of the most time-consuming components of DHM (Wegner, Chiang, Kemmer, Lämkuil, & Roll, 2007) due to the complexity of the joint linkages. Therefore, to avoid these inaccuracies and decrease the time taken for human model posturing,

developers have added alternative approaches for avatar posturing including direct 3D kinematic data importing into the DHM software to simulate more accurate postures.

2.7.2 3D Kinematic Data Importing

The most recently updated and developed DHM software packages, including Jack (V 8.4) and Santos, have the ability to drive motions and postures of the virtual avatar using kinematic data gathered from a motion tracking device. The unique add-on feature included in these packages allows users to import 3D motion capture data collected to recreate the posture in the DHM package. 3D position data of the subject's joints and segments are imported into the package which refines the avatar's posture to mimic the real life subject's postures or motions (Santoshuman Inc. Software, 2009; Siemens PLM Software, 2016). Data importing reduces simulation times for users as well as improves the accuracy of postures (joint angles) and captures variability in movement relative to manual joint manipulation approach (Duffy, 2008). However, this approach can only be used by researchers or industries that have access to motion capture technologies. Further, since this approach relies on importing of data through DHM, we do not know how potential errors or inaccuracies could arise when mapping motion capture data onto the computerized human avatar, motivating the need for this investigation.

2.7.3 Posture Prediction

To provide users with an alternate approach to decrease DHM simulation times, posture and motion prediction approaches have been integrated into DHM software packages to rapidly posture the avatar with minimal manual input. To generate a posture (set of joint angles) for a given task, such as grabbing an object, end effectors (point of interest on the human body, end of kinematic chain) and target contact (point or plane in space) must be identified first. Using these points throughout the iterative simulation process a statistical regression approach or an

optimization algorithm is applied to estimate the avatar's motion or posture (Abdel-Malek & Arora, 2013; Duffy, 2008).

Statistical regression (data-driven) approaches to predict postures, rely on pre-recorded motion data, anthropometrics and functional regression models to predict joint angles as a function of time (Duffy, 2008). Data driven posture prediction includes large data sets and multiple model parameters (human anthropometrics, target coordinates, etc.). This can result in increased risk of computational errors in the algorithm, causing reduced accuracy in the regressed postures. For example, if a user wanted to predict a posture for a target point that was not part of the experimental database, the algorithm would use extrapolation to obtain results. As a result, poor postures can be predicted if they do not fit the exact anthropometrics or motions included in the database (Duffy, 2008). Comparatively, the optimization-based approach to predict postures takes the biomechanics, physics of motion and human behaviour into consideration (Abdel-Malek & Arora, 2013). Joint angles are calculated for a single posture, or for a sequence of postures by solving a general optimization problem based on objective functions related to human performance criteria (Abdel-Malek et al., 2007).

The posture prediction approach can help facilitate the proactive ergonomics process. Where ergonomist and researchers have the ability to verify the suitability of a workplace or task during the development stages (Regazzoni & Rizzi, 2013). Users can predict how the worker will perform a task based on their anthropometrics, physical abilities or placement of interacting materials/tools. Posture prediction has been commonly used in the automotive industry to predict the reach capability of occupants during the design process of vehicle interiors (Chaffin, 2005; Xia & Gunther, 2011; Yang, Kim, et al., 2007)

Posture prediction is a time efficient approach for estimating human movement behaviour. However, since the human body is a highly redundant system, the avatar could adopt many different whole body joint angle configurations to achieve assigned task objectives that may not simulate the actual postures and motions used by subjects across different occupations and activities. Moreover, posture prediction can also be limited by the kinematic model's DOF. Research is required to determine the reliability of the posture generating feature in producing human body postures for complex tasks, such as patient handling. This is especially important when validating the utility of DHM for proactive HF&E investigations.

2.8 Advanced Digital Human Modeling Software Packages

According to the literature on the development of DHMs, the most advanced DHM software packages currently in the market for commercial use are Siemens Jack (V 8.4) and Santos. Both software packages have improved biomechanical models for enhanced avatar control, robust algorithms, updated anthropometric databases, realistic skeletal linkage models with greater DOF and computationally fast real-time simulations (Duffy, 2008).

2.8.1 Siemens Jack (V 8.4)

Siemens Jack remains as a popular, commercially available DHM package serving a range of clients within North America. The Jack human modeling tool was developed at the Center for Human Modelling and Simulation at the University of Pennsylvania (Badler, Phillips, & Webber, 1999a). The main impetus for the development of Jack was to support the inclusion of HF&E principles into the design and development of workspaces, emphasizing the optimization of human-machine interfaces. Avatars (Jack or Jill) are scaled based on regression equations that use comprehensive military civilian anthropometric survey (ANSUR) data. The database contains 132 anthropometric measures from 9000 military personnel (1774 men and

2208 female) (Raschke, Schutte, & Chaffin, 2000). The skeletal linkage model includes 71 segments and 64 joints with 135 DOF (Monheit & Badler, 1991). The shoulder is composed of two articulating joints (shoulder and sterno-clavicular joints) and the spine consists of 12 thoracic and 5 lumbar vertebrae (Monheit & Badler, 1991). Jack uses an IK model to compute whole body joint angles and an inverse dynamics approach (top-down) to calculate joint moments and reactions forces. To control the avatar, users have the options of manually manipulating the joints, importing motion capture data to drive Jack/Jill, or using the posture prediction command.

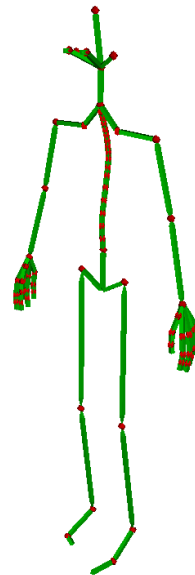


Figure 2. Skeletal linkage model of Jack (V 8.4)

Jack's posture prediction uses a data-driven statistical regression approach; therefore, it can only produce accurate results for a finite number of tasks/motions. An accumulation of more than 70 000 motions collected from subjects performing a variety of manual automotive related tasks were gathered to create a database for the model (Duffy, 2008; Faraway & Reed, 2007). Motions collected using 3D motion capture included reaching for controls in a vehicle, lifting

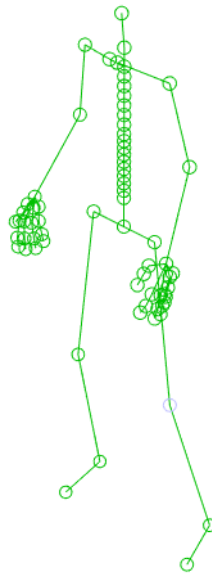
objects onto shelves and stepping around small areas (Faraway & Reed, 2007). Kinematic data from this is used to model functions as opposed to scalar/vector motions that are used to predict postures. Jack's built-in IK algorithms are used to determine how Jack will move based on the behavioural constraints selected (e.g., torso constrained, head/eye fixated on object), then the avatar can be moved to select the end effector, and the joints involved will be automatically adjusted using the IK algorithms (Duffy, 2008).

Digital environments can be created and modified using a range of native CAD object libraries (office furniture, automotive objects). Along with a range of ergonomic analysis tools available to support the assessment of workplace designs, Jack has also included a lumbar-torso model to calculate low back forces. Jack has integrated Raschke's (1996) neurophysiology-based model that estimates L4-L5 compression and shear forces. The biomechanical lumbar-torso model uses muscle recruitment based on a distributed moment histogram method to predict agonist and antagonist activity in the torso (Raschke, Martin, & Chaffin, 1996).

2.8.2 Santos Pro

Santos is emerging as a competitor DHM software in the North American market. This DHM package was developed at the Virtual Soldier Research Program at the University of Iowa (Abdel-Malek et al., 2007). Santos was developed with the primary focus of modeling realistic human characteristics; including whole body movement, appearance and feedback (Abdel-malek et al., 2008).

Avatars (Santos or Sophia) are scaled based on a GEBOD program that produces human and dummy body description data used by the Articulated Total Body (ATB) model (Cheng et al., 1994). Depending on the chosen subject type, the program computes the body segments' geometric dimensions, mass, joint locations and mechanical properties using regression equations developed from survey data (Cheng et al., 1994). Santos has a kinematic linkage model with 211 DOF (Abdel-malek et al., 2008). The shoulder model includes two articulating joints (shoulder and sterno-clavicular joint) and the spine model includes 17 vertebrae from the base of neck (Abdel-malek et al., 2008). Santos uses an IK model to compute whole body joint angles and an inverse dynamics approach (top-down) to calculate joint moments. Unlike Jack, Santos produces visually realistic humans with deformable skin to display the effects of the different postures. To control the avatar, users have the options of manually manipulating the joints, importing motion capture data to drive Santos/Sophia, or use the posture prediction command.



Santos' posture prediction approach was developed using a physics based multi-objective optimization (MOO) technique instead of pre-recorded data driven algorithms. Compared to

Figure 3. Skeletal linkage model of Santos

Jack, Santos' computational posture prediction model has the ability to estimate set of joint angles for an infinite number tasks (Abdel-Malek & Arora, 2013), presuming users can adequately adjust cost functions weights. The MOO approach uses physics factors that govern human movements, including gravity and potential energy (R. T. Marler, Arora, Yang, Kim, & Abdel-malek, 2009). Based on these physics factors, cost functions (human performance measures) were developed, including joint displacement, effort, change of potential energy, visual displacement and discomfort. (Abdel-Malek et al., 2007; R. T. Marler et al., 2009). Compared to IK approaches or experimental-based data driven approaches to posture prediction, Santos' MOO approach enforces human performance measures to predict the postures. As a result, it ensures autonomous movement regardless of the task scenario in real-time (Abdel-Malek et al., 2007).

Similar to Jack (V 8.4), Santos also has an integrated spine model. Santos estimates spine compression forces using a regression equation (McGill, Norman, & Cholewicki, 1996) originally developed as a surrogate to McGill's anatomically detailed spine model (McGill & Norman, 1986), which has noted limitations (Fischer, Albert, McClellan, & Callaghan, 2007).

2.9 Validation of Avatar Posturing Approaches for Healthcare Applications

Although DHM packages like Jack (V 8.4) and Santos have been applied across a diverse range of design problems and occupational tasks, only a limited number of published studies on the validation of Jack and Santos are available. To date, research efforts have concentrated on validating the anthropometric aspects of human modelling (Allen, Curless, & Popovic, 2004; Allen, Curless, & Popović, 2002; Kouchi & Mochimaru, 2004) and fine movement control of eyes (Kim & Martin, 2006; Ruspa, Quattrocolo, & Bertolino, 2007) and hands (Endo et al., 2007, 2009). Aside from the continuous validation of posturing algorithms (Yang, Rahmatalla, Marler,

& Abdel-malek, 2007), there is decreased attention towards establishing the fidelity of the kinematic simulations and their outputs.

One known published study from the United States Airforce research group validated Jack's (V 2.1) ability to simulate the postures of a front station crew in an F-16D (Duffy, 2008). Compared to field tests with humans, Jack yielded inaccurate results when attempting to determine accommodation limits for the aircraft cockpit (Duffy, 2008). Challenges posturing the avatar was a contributor to the errors reported in the validation phase.

2.10 Relevance of Current Research

Developers of Jack and Santos have updated the DHM software packages to help users simulate realistic human postures and motions. However, there is very little evidence supporting the validity of the kinematic and kinetic outputs produced by the posture control approaches integrated into Jack and Santos for the application of complex healthcare activities. The model outputs not only need to be realistic, but their results must be reproducible and verifiable. An important research area in biomechanics is determining the validity of instrumentation and associated models we use to predict and describe human motions and the forces that drive those postures. Therefore, by comparing the kinematic and kinetic outputs from manual posturing, kinematic data importing and posture prediction approaches against a lab-based rigid linked segment model will provide users with preliminary evidence to help determine the appropriateness of DHM to estimate MSD hazard exposures. The purpose of this research is to compare the kinematic and kinetic outputs produced using Siemens Jack (V 8.4) and Santos software package's avatar control approaches; manual whole body joint manipulation, direct motion capture data importing and posture prediction against lab-based rigid-linked segmental model outputs when modelling a HCP performing a patient repositioning task.

3.0 Methodology

3.1 Participants

Twenty-five (25) healthy HCPs (17 female) were recruited from local long-term care facilities and from Conestoga College to perform a patient repositioning task. All HCPs recruited had at least two years of standardized safe patient handling training in practical nursing school or through external training programs. Table 1 displays the participant demographics.

Based on a power analysis (G*Power 3.19.2, Düsseldorf, Germany), a minimum sample size of 23 was required to detect significant differences in kinematic and kinetic values between DHM software packages and the lab-based RLM within each posturing approach, with a medium to large effect size (partial $\eta^2=0.1$) using a one-way repeated measures analysis of variance (RMANOVA) and to detect significant correlation coefficients using Pearson's Product Moment correlation ($\alpha=0.05$, $1-\beta = 0.8$).

Table 1. Participant demographics

	Females (n=17)	Males (n=8)
Age (years)	37.6 ±14.0	34.9 ±12.5
Height (m)	1.66 ±0.09	1.77 ±0.08
Weight (kg)	68.6 ±9.5	83.9 ±18.0
Patient handling experience (years)	11.9 ±13.0	5.4 ±8.8

Prior to collection, participants were screened in person to determine eligibility for the study. The Nordic MSD Questionnaire (Kuorinka et al., 1987), and the Physical Activity Readiness Questionnaire (ParQ+) (Warburton et al., 2011) were completed to screen for individuals who had suffered from an injury that required rehabilitation in the last 12 months (exclusion criteria). A demographics form was filled out which asked participants the number of years they had with patient handling experience (minimum of 2 years required as exclusion

criteria). All participants recruited for this study met the inclusion criteria. Informed consent was acquired from each participant prior to the collection. The study was reviewed by the University of Waterloo Office of Research Ethics Committee and received approval (ORE # 22314) prior to recruitment and collections.

3.2 Instrumentation and Laboratory Setup

The outcome measures for this study were calculated based on data obtained from 3D motion capture, 2D video capture, hand force measurements, and a body worn accelerometer. The following sections describes the instrumentation and laboratory setup used to compute the kinematic (joint angles) and kinetic (joint moments) outcome variables.

3.2.1 Motion Capture – 3D Kinematic Data

Whole body 3D positional data of participating HCPs were collected at 60Hz using a 12-camera passive motion capture system (Vicon, Centennial, Co, USA). The collection space was calibrated according to Vicon specifications (Vicon, 2016) and the origin was set at the center of the laboratory space. The laboratory coordinate system was configured so that +Z was upwards, +X was backward and +Y was directed to the right of the origin (Figure 4). Prior to a static calibration process 44 individual passive reflective markers (14mm diameter spheres) were placed on anatomical landmarks as required to mathematically define local coordinate systems for each body segment (Figure 5) (Wu et al., 2002, 2005). Anatomical markers were accompanied by rigid body marker clusters (each with four reflective markers) attached to the trunk, upper arms, lower arms, pelvis, thighs and shank. The rigid body marker clusters remained on participants during active trials to track the movements of each segment during dynamic motion to minimize the effect of skin motion artefact.

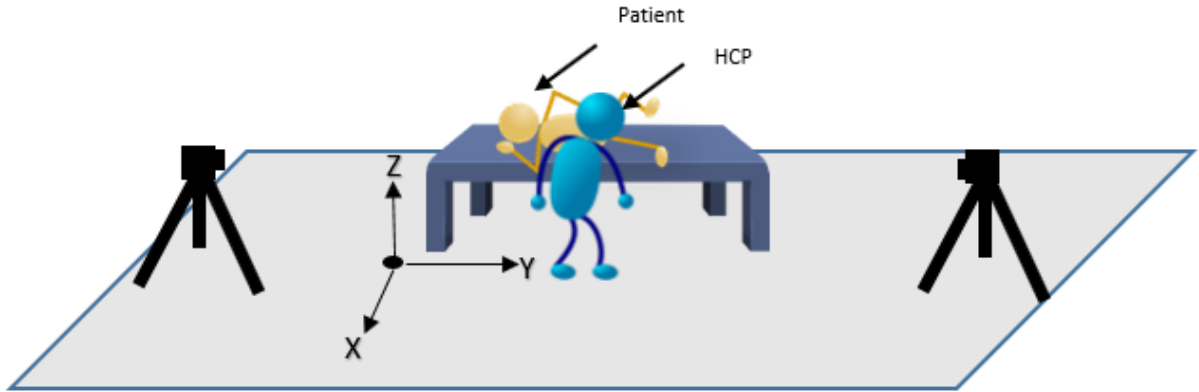


Figure 4. Schematic diagram of the laboratory setup used to for the patient reposition task

A combination of static and dynamic calibration trials were collected as per Vicon specifications (Vicon, 2016). A five second static calibration trial was collected for each participant in the space. Participants stood upright in anatomical position facing the positive axis of the of the laboratory space. This trial was used to express the segmental motions (tracked via clusters) relative to the segmental coordinate systems defined by the anatomical landmarks. The dynamic calibration trial was collected to capture the full range of motion (ROM) of the participant. Vicon Nexus software used the data gathered from the dynamic trial to track the movement of segments in subsequent trials.

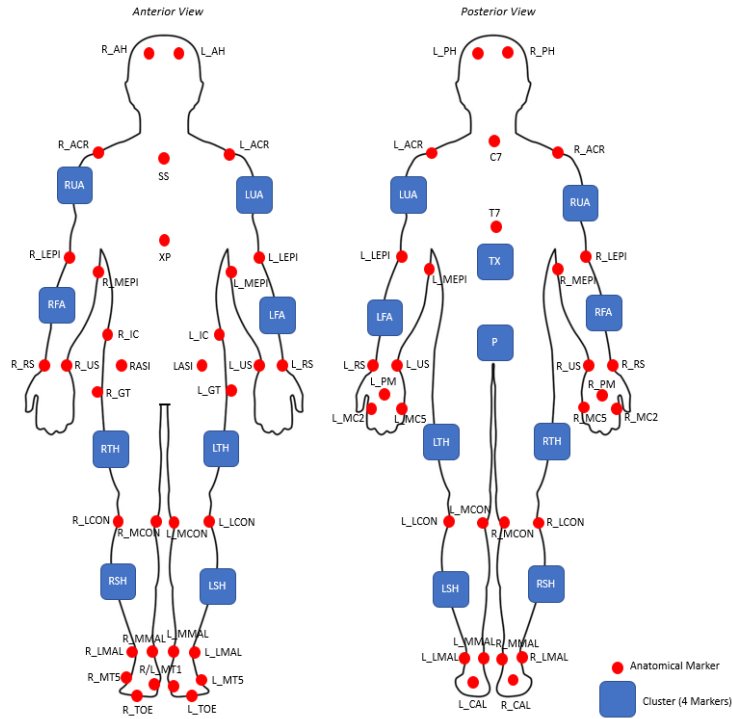


Figure 5. Vicon reflective marker placement

3.2.2 Video

Two Vicon Vue cameras, synchronized into Vicon’s motion capture system were used to capture 2D video data of the HCP performing the patient reposition task. Video data were sampled at 30Hz. The two cameras were secured to tripods and placed in the collection space to capture the sagittal plane, whole body motions of the HCP. The camera placement in the laboratory space can be seen in Figure 4.

3.2.3 External Hand Force Measure

Due to challenges in the collection of real-time direct hand forces, peak external hand force estimates were measured using a DFX-200 digital Chatillon force gauge (MRM Precision Instruments, Brampton, ON). Peak hand-held force gauge measurements have shown good reliability compared to a six strain gauge force transducer (Hoozemans, Van Der Beek, Frings-Dresen, & Van Der Molen, 2001). HCPs often use a sheet to facilitate the physical actions

required to reposition a patient, including the initiation of the patient turn. Therefore, forces exerted by the HCP were estimated to mimic the magnitude of force exertion when using a sheet. To estimate the peak external hand force exerted, a rigid metal bar (80cm x 4cm x 0.5cm) with a hole (1.5cm diameter) in the center, was securely sewn to the end of a sheet. The force gauge was attached to the center of the bar using a clamp attachment (Figure 6). The force gauge was configured to register the peak force. The gauge was pulled upward to lift the lateral right torso-pelvis region of the patient off the bed. The peak force registered by the force gauge was assumed to occur at the initiation of the turn, consistent with initial motion of the patient. The force applied at the initiation of the turn was the minimum force required to overcome inertia and move the patient's body against gravity in order to tilt the patient. Three trials were conducted during piloting, and the average of the three trials was used as the representative hand force measurement in subsequent analyses.

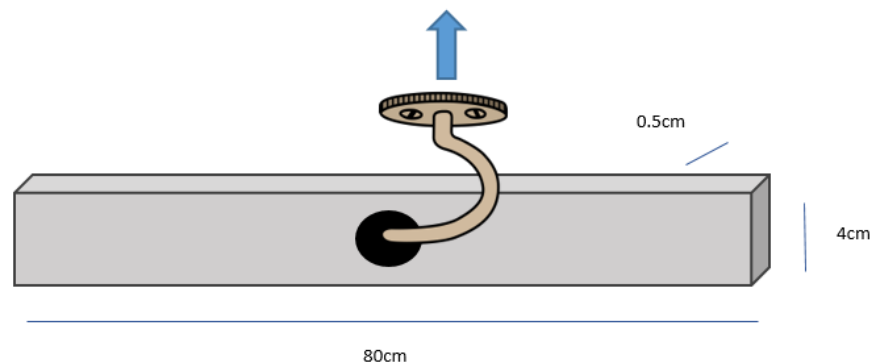


Figure 6. Diagram of the rigid metal bar that was inserted into the sheet to facilitate hand force measurements using a force gauge

3.2.4 Acceleration

To identify the point of initial patient motion (assumed as the point of peak external hand force), acceleration data were recorded from an accelerometer (Delsys Trigno, Natick, MA) placed on the sternum of the patient. Acceleration data (mm/s^2) were sampled at 148.1Hz, up-sampled to 2000Hz and synchronized to the motion capture system (analog sample rate 2100Hz). The accelerometer provided time series data that was used to determine when the patient's body began to move (initiation of the turn).

3.3 Experimental Protocol

Upon arrival, participants were asked to provide written and informed consent, complete a demographics questionnaire which asked them to provide details on their age, gender, weight (kg), height (m) and healthcare role. The hip height (vertical distance from the floor to the greater trochanter) of each participant was measured and recorded. A demonstration of the patient reposition task using a sheet was provided using a critical patient care hospital bed (Hill-Rom®, Chicago, IL) (Figure 7) where a live 60th percentile male (82kg) acted as the standardized patient (McDowell, Fryar, Ogden, & Flegal, 2008). Participants were given an opportunity to practice the patient repositioning activity before equipped with any instrumentation. Participants were then instrumented with full body passive reflective motion capture markers, including individual markers over requisite anatomical landmarks, and clusters of markers fixed to rigid bodies placed over body segments. Following instrumentation, participants performed static and dynamic (ROM) calibration trials in the capture space.



Figure 7. Critical patient care hospital bed

The hospital bed was first set to the hip height of the participant. Then, the participant was asked to simulate a patient reposition, which included the safe left-turn of an immobile patient. Three trials of were performed. Data acquisition (motion capture, video, accelerometer) for each trial began with participants standing at rest and ended once they had completed all the actions required to turn the patient (standing at rest). The experimental protocol is outlined in Figure 8.

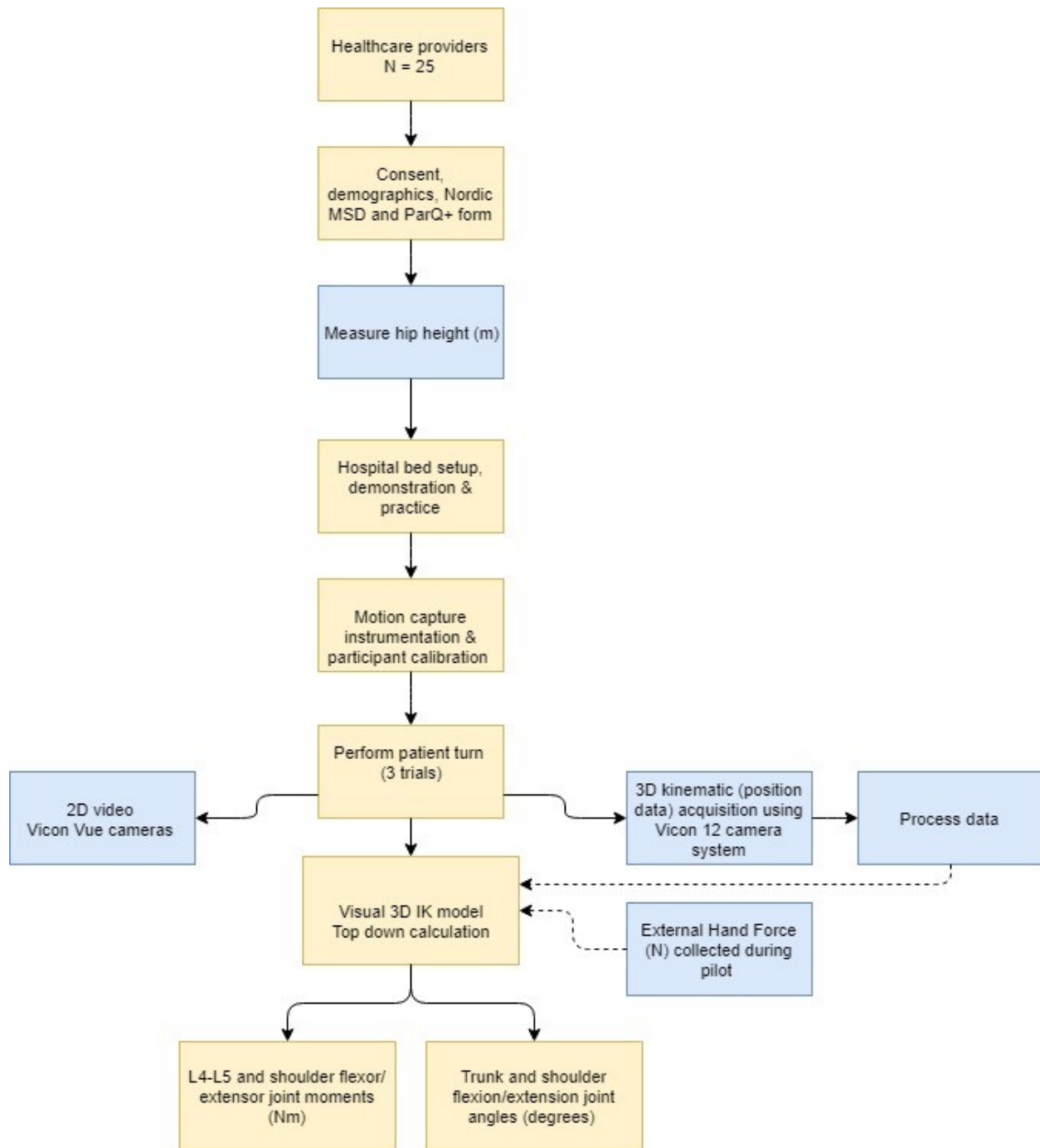


Figure 8. Block diagram of the experimental protocol used for the lab-based study

3.4 Data Processing

3.4.1 3D position data

Motion capture data were processed in Vicon Nexus 2.5 (Vicon, Centennial, CO, USA). Raw marker data captured for each participant's trial were reconstructed and labelled. Each reconstructed trial was then visually analyzed frame-by-frame to ensure that trajectories were properly labeled and free of any gaps. If trajectories were mis-labeled, they were manually re-labeled correctly. If any gaps emerged then a gap filling approach was applied, using the rigid body fill option in Vicon Nexus 2.5. Correctly labeled and gap-filled marker trajectory data were then filtered using a dual-pass, low pass digital Fourth Order Butterworth filter with a frequency cut off of 6Hz. Processed trajectory data were exported to Visual 3D V5 Software (C-Motion Inc., Germantown, USA) for additional analysis.

3.4.2 Acceleration data

Raw acceleration data gathered from the accelerometer was imported into Matlab R2015a software (Mathworks Inc., USA) for processing. Data from each trial was filtered using a dual-pass, low pass digital Fourth Order Butterworth filter with a frequency cut off of 3Hz. Based off visual inspection of the time-series acceleration data and whole-body motion capture data, a threshold in vertical acceleration was estimated to determine the frame at which the participant initiated the turn. A threshold of $\sim 6 \text{ mm/s}^2$ was used to identify the frame at which the patient turn was initiated in each trial.

3.5 Calculating and Extracting Lab-Based Outcome Measures: Visual 3D Model Development and Analysis

A 3D kinematic model was developed in Visual 3D V5 (V3D) Software using the processed position data from each participant's trial, where segments were defined based on the

anatomical landmarks. The model was customized to each participant by inputting their body mass (kg). Using the static calibration trial data, segment properties were computed. Joint centers of rotation were calculated using the anatomical landmarks where a stationary midpoint was calculated along a functional axis created between two relative segments (e.g. between the upper arm and forearm, an axis is created using the R_LEPI and R_MEPI landmarks (Figure 5 to calculate the elbow joint). The shoulder joint centre was estimated using the Nussbaum & Zhang, (2000) heuristic approach, locating the shoulder joint center 6 mm below the acromion on a line coincident with the long axis of the torso segment. Segment lengths were calculated using the proximal and distal ends defined for each segment using the anatomical landmarks. Dynamic patient turning trials were loaded, and the customized model was applied to the data set.

The frame at which peak force application was applied by the participant was identified in the time series data of the whole body positional data in each dynamic patient turning trial in V3D. This frame was the assumed static posture used by the participant at the initiation of the patient turn and used to compute model outputs.

The recorded peak external hand force (204N) measured was divided by two and applied to the approximate grip center of each hand segment. It was assumed that each participant had exerted an equally distributed force between both hands during the patient turn. Since only the magnitude of the force exerted was gathered, a vector was created to indicate the direction of force application in each hand. The hand force vector direction was assumed to be coincident to the long axis of the right and left forearms respectively at peak force application.

Using the IK model integrated in V3D, the right shoulder and trunk flexion/extension joint angles (degrees) were calculated at the selected frame. Joint angles were calculated based on definitions prescribed by the International Society of Biomechanics (Wu et al., 2002, 2005)

such that they could be referenced within a common orthopaedic convention (e.g., flexion/extension, internal/external rotation, etc.). The inverse-dynamics (top-down model) algorithm integrated in V3D calculated the joint moments from measured kinematic and estimate hand force data. The right shoulder and L4-L5 (trunk relative to pelvis) flexor/extensor net joint moments (Nm) were extracted for further analysis.

Among the three processed trials for each participant, the trial that included the best quality of data was selected. The trials that showed all the body segments constructed in V3D, along with accompanied video image that had minimal obstruction of view of the HCP at the target frame were selected. Joint angle and moment values at the instant of patient motion (i.e., peak force application) were exported from the selected trial and served as the lab-based RLM outcome measures

3.6 Computing and Extracting Digital Human Model Outcome Measures

The following sections describes the approach used to obtain biomechanical measures (kinematics and kinetics) from Jack and Santos software packages. There are three different posturing approaches available in Jack and Santos that were used to estimate the 3D joint angles and 3D joint moments at the instant of patient initiation; kinematic data importing, manual posturing and posture prediction. The steps taken to simulate the patient turning task in Jack and Santos using the three approaches are described below. Data gathered from the laboratory study were used as inputs and for reference to simulate the static posture of the HCP in a scaled virtual space.

Using the data gathered from the laboratory patient turning experiment, including the participant demographics, external hand force measure, hip height, video and 3D positional data, a static patient turn posture was simulated for each participant in Jack and Santos using

kinematic data importing, manual posturing and posture prediction approaches. An outline of the data inputs and outputs extracted from the digital human simulations performed in Jack and Santos are illustrated in Figure 9.

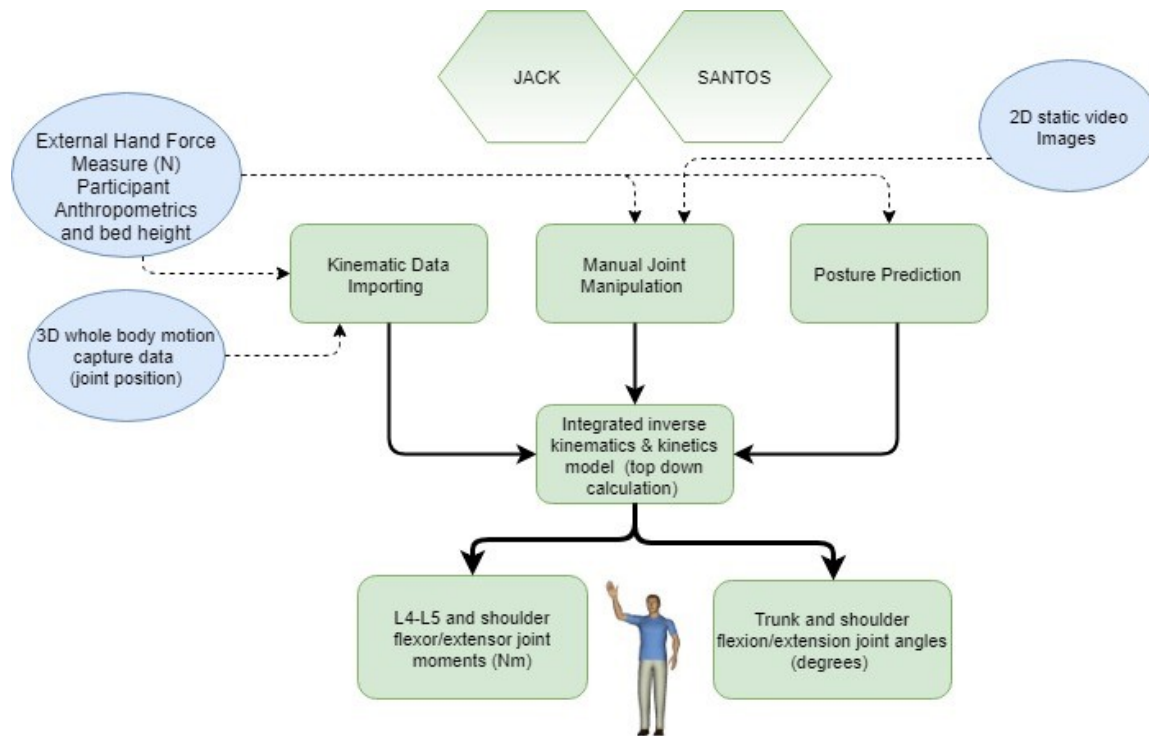


Figure 9. Block diagram of the flow of collected data that were used as inputs when digitally modeling the patient reposition task in Jack and Santos

A virtual scaled environment that simulated the laboratory investigation was first created in Jack and Santos. A scaled CAD model of the hospital bed (Hill-Rom®, Chicago, IL) that was used in the laboratory experiment was inputted into the virtual spaces of Jack and Santos. Two avatars were created to input into the virtual environment. A 60th percentile male avatar weighing 82kg was created in Jack and Santos and placed on the bed in supine position for each simulation. The second avatar was anthropometrically scaled to simulate the HCP in each

experimental trial. To scale the avatars in Santos and Jack, gender, weight and stature were adjusted. For each simulation, the average peak external hand force recorded during the patient turning trial was divided by two and applied to the left and right palm/hand centers of the virtual HCP. When inputting the external hand force into Jack or Santos, a vector appeared. The force vector was adjusted to align with the long axis of the forearm of the virtual HCP at peak force application.

3.6.1 Kinematic Data Importing

To simulate the static posture of the HCP performing the patient turn in Jack and Santos, the processed 3D joint position data computed using V3D at the instant of peak force application were mapped onto the virtual HCP. A table of the anatomical landmarks from the V3D model that were mapped onto the avatar in Jack and Santos is included in Appendix I. The right shoulder and trunk flexion/extension angles (degrees) and right shoulder and L4-L5 flexor/extensor joint moments (Nm) were extracted from the resulting posture assumed by the avatar using the kinematic data.

3.6.2 Manual Posturing

The 2D video collected from the selected trial of the patient turning task was used as reference to manually posture the limbs of the avatars in Jack and Santos. The frame at which the HCP was identified exerting peak force in the selected trial was used as the static sagittal frame image in the video data to inform posturing of the virtual HCP. Ergonomist routinely depend on video images previously collected from a work task as a visual reference to simulate the whole-body posture of the worker in DHM (Duffy, 2008).

Using the sagittal static image, the virtual HCP's limbs were adjusted to best match the posture of the lead HCP during the patient turn. The virtual HCP's joint positions, including the

shoulder, elbow, wrist, spine, hip, knee and ankles were articulated in the frontal, sagittal and transverse planes using the local coordinate systems of the avatar limbs. The right shoulder and trunk flexion/extension angles (degrees) and right shoulder and L4-L5 flexor/extensor joint moments (Nm) were exported from both software once the simulations were completed.

3.6.3 Posture Prediction

To simulate the static postures used by the HCP during the patient turn using the posture prediction approach, rudimentary CAD objects were used as the target positions that the HCP used in place of the sheet. Two CAD objects were positioned ~30cm above the bed and positioned directly above the right shoulder and lateral right hip of the patient for each simulation using posture prediction.

In Jack, the virtual HCP started in a neutral standing posture in front of the bed with the patient laying supine. A foot restriction zone of 60cm x 60cm was identified under the surface of the avatar's feet. The right hand was first identified as the end effector and the object above the lateral right hip was identified as the target. A command within Jack was used to instruct the virtual HCP to grasp the object (simulating the slide sheet boarder) (Siemens PLM Software, 2016). Then, the left hand was identified as the end effector and the object above the right shoulder was identified as the target. The virtual HCP was instructed to grasp the object simulating the border of the slide sheet with their left hand. Once a feasible posture was predicted by Jack, the right shoulder and trunk flexion/extension angles (degrees) and right shoulder and L4-L5 flexor/extensor joint moments (Nm) were exported.

In Santos, the virtual HCP also started in a neutral standing posture in front of the hospital bed. A foot restriction zone of 60cm x 60cm was identified under the surface of the avatar's feet. Then, to set up the initial optimization problem to predict the posture in Santos, the performance measures (objectives) were adjusted to prioritize the minimization of effort, discomfort, joint displacement, maximum joint torque and total joint torque for predicting postures. Then the right hand was identified as the first end effector and the object above the lateral right hip was identified as the target. Then, the left hand was identified as the second end effector and the object above the right shoulder was identified as the target. The posture prediction command was activated to automatically produce the predicted set of joint angles that represented the posture during the patient turn when using the slide sheet (Santoshuman Inc. Software, 2009). Once a feasible posture was predicted by Santos, the right shoulder and trunk flexion/extension angles (degrees) and right shoulder and L4-L5 flexor/extensor joint moments (Nm) were exported.

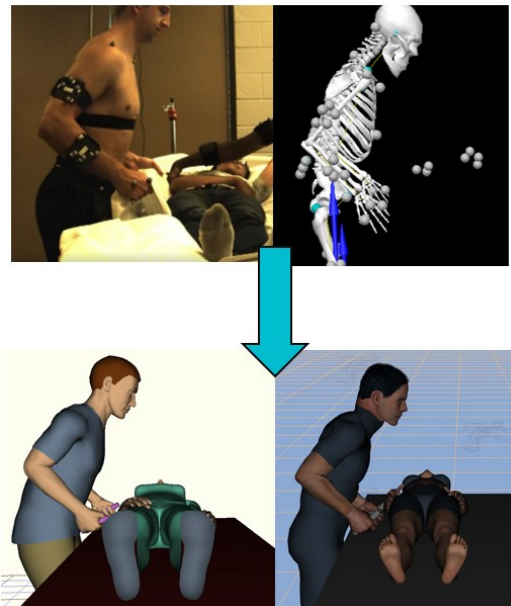


Figure 10. Virtually simulating the static posture of the HCP at the initiation of the patient turn in Jack and Santos

3.7 Statistical Analyses

Twelve independent, within subject one-way RANOVAs ($\alpha=0.05$, $1-\beta = 0.8$) were used to detect for a main effect of biomechanical modeling software on kinematic and kinetic outcome measures within each DHM posturing approach. Using SPSS software (IBM® SPSS®, 25.0, Armonk, NY, USA), three levels of the within-subject factor were considered in each ANOVA model (3 levels: V3D, Jack, Santos). The dependent measures considered in each model were the L4-L5 joint moment, shoulder joint moment, trunk angle and shoulder joint angle. Comparisons are summarized in Table 2. A Greenhouse-Geisser correction was applied if the assumption of sphericity was violated, according the Mauchly’s test of sphericity. When a significant main effect of biomechanical modeling software was found, pairwise comparisons were investigated using a Bonferonni correction to identify if differences emerged between the lab-based RLM (V3D) and the two DHM software packages.

Table 2. Outline of the independent and dependent variables assessed in the RANOVA

Dependent Variables	Independent Variables								
	V3D	Jack	Santos	V3D	Jack	Santos	V3D	Jack	Santos
Trunk flexion/extension joint angles (degrees)	Kinematic Data Importing			Manual Posturing			Posture Prediction		
Shoulder joint flexion/extension joint angles (degrees)									
L4-L5 joint flexor/extensor joint moments (Nm)									
Shoulder joint flexor/extensor joint moments (Nm)									

Pearson Product Moment correlation coefficients (r) were computed to assess the relationship between DHM software package (Jack and Santos) outcome measures and the V3D for each posturing approach. Relationships between outcome measures assessed are summarized in Table 3. Significant correlations were identified at a significance level of $p < 0.05$. Based on hypothesis two, it was predicted that the outputs computed using the direct motion capture

approach would have a strong correlation with the lab-based RLM, therefore DHM outputs would be proportional to the change observed across individuals from the lab-based RLM. And the outputs computed using the posture prediction approach would have a weak correlation with the lab-based RLM, therefore DHM outputs would not be proportional to the change observed across individuals from the lab-based RLM. Therefore, correlations between the DHM and lab-based modeled outputs were used to validate whether a linear relationship was present or absent in the data.

To further evaluate the DHM software's ability to estimate the same kinematic and kinetic measures as the lab-based RLM, Bland-Altman plots were created to evaluate the level of agreement between the outcome measures produced using each of the DHM posture simulating approaches and V3D. The differences between the DHM software and V3D (considered as the reference measure) outcomes were plotted against the averages of the DHM software and V3D outcome measures (Bland & Altman, 1999). The range of agreement within 95% ($\pm 1.96SD$) of the differences and the bias (mean difference) was calculated between V3D and software outcome measures and displayed on the graph. To determine if there was a significant proportional bias, a linear regression was calculated to predict the differences based on the means of each software outcome measure. Interpretation of Bland Altman plots can be found in Appendix II. The Bland-Altman analysis was used in this investigation to provide practitioners with practical and easily interpretable data such as the magnitude of the difference between DHM and lab-based outputs, trends in the outputs estimated by DHMs (underestimation/overestimation of measures), as well as measurement error. These data are useful in determining the ability of DHMs to produce realistic kinematic and kinetic data as well highlight any significant differences produced from the DHM modeling approaches.

Finally, the smallest detectable change (SDC) was computed to index the absolute measurement error in kinematic and kinetic outcome measures estimated using each DHM software. The SDC value was calculated by multiplying the standard deviation of the differences between V3D and DHM software outcome measures by 1.96 (Van Kampen et al., 2013).

Table 3. Relationships assessed between the lab-based model and DHM outcome measures

	DHM: Jack & Santos Posturing Approaches		
	Kinematic Data Importing	Manual Posturing	Posture Prediction
Reference model: Lab-based RLM (V3D)	Trunk flexion/extension angle (degrees)		
	Shoulder flexion/extension joint angle (degrees)		
	L4-L5 flexor/extensor moment (Nm)		
	Shoulder flexor/extensor moment (Nm)		

4.0 Results

The following section describes the results from this investigation. The results are separated into sections according to the DHM posturing approaches; 1) direct motion capture data importing, 2) manual joint manipulation and 3) posture prediction. Within each section the kinematic (trunk and shoulder joint angles) and kinetic (L4-L5 and shoulder joint moments) results are described for both Jack and Santos relative to the lab-based RLM (V3D) including a graphical representation of the results (side-by-side scatter and Bland Altman plots, for each respective dependent variable described). At the beginning of each section, a table is used to display a summary of the numerical results described in each section.

4.1 Direct Motion Capture Data Importing

Table 4. Summary of the mean differences found between kinetic and kinematic measures estimated using the lab-based RLM (V3D) and DHM software packages' direct motion capture data importing approach. Asterisks indicate significant differences between models. The calculated smallest detectable change within 95% confidence intervals is reported for each pair.

Model (Lab based)	Model (DHM)	Mean Difference (Lab based-DHM)	95% Confidence Interval for Difference		SDC \pm 95%
			Lower Bound	Upper Bound	
V3D Trunk Angle	Jack Trunk Angle	9.41*	3.78	15.04	6.06
	Santos Trunk Angle	2.81	-2.62	8.24	5.84
V3D Shoulder Angle	Jack Shoulder Angle	-35.51*	-42.74	-28.27	7.79
	Santos Shoulder Angle	-21.60*	-31.55	-11.65	10.71
V3D L4-L5 Moment	Jack L4-L5 Moment	4.43	-11.63	20.50	17.29
	Santos L4-L5 Moment	28.04*	8.40	47.68	21.14
V3D Shoulder Moment	Jack Shoulder Moment	6.77*	0.61	12.92	6.63
	Santos Shoulder Moment	6.66*	1.48	11.84	5.58

* $p < 0.05$

4.1.1 Kinematics

A main effect of DHM software was detected for trunk angles $F(2, 48) = 11.33, p < 0.001, \eta^2 = 0.32$. Pairwise comparisons indicated that trunk angles computed by Jack ($M=1.32, SD=5.08$) were significantly lower than V3D ($M=10.72, SD=12.26$) and Santos ($M=7.91, SD=9.32$). Correlation analysis revealed a positive, weak correlation between Jack and V3D ($r = 0.45, n = 25, p = 0.02$) and a positive, moderate correlation between Santos and V3D ($r = 0.56, n = 25, p < 0.001$) trunk angles. Bland Altman plots revealed poor agreement between trunk angles estimated using V3D and Jack and a significant proportional bias of 9.41 ($\beta = 0.75, t(24) = 5.38, p < 0.001$) (see Appendix III for regression results). However, moderate agreement was observed between trunk angles estimated using V3D and Santos with no significant proportional bias. The SDC $_{95\%}$ were $\pm 6.06^\circ$ and $\pm 5.84^\circ$ for Jack and Santos trunk angles respectively.

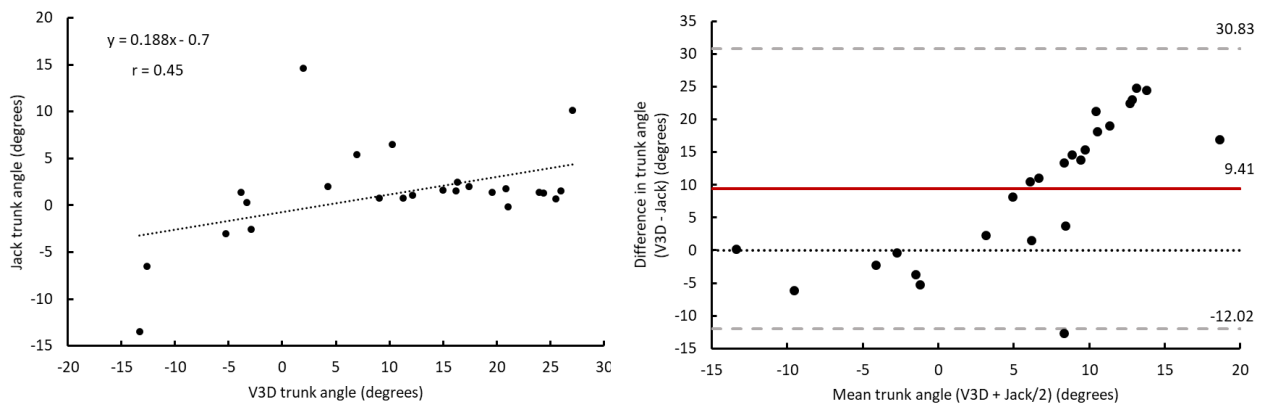


Figure 11. Left – scatter plot illustrating the relationship between trunk angles (+ extension) estimated using Jack’s motion capture data importing approach and the lab-based RLM (V3D). Regression equation and Pearson’s correlation coefficient (r) are displayed on the plot. Right – Bland-Altman plot illustrating the differences between trunk angles (+ extension) produced by the lab-based RLM (V3D) and Jack’s motion capture data importing approach vs. the mean of the two measures. Red line is the systematic error produced by Jack, grey dashed lines are the limits of agreement from $-1.96SD$ to $+1.96SD$, black dotted line is the line of equality.

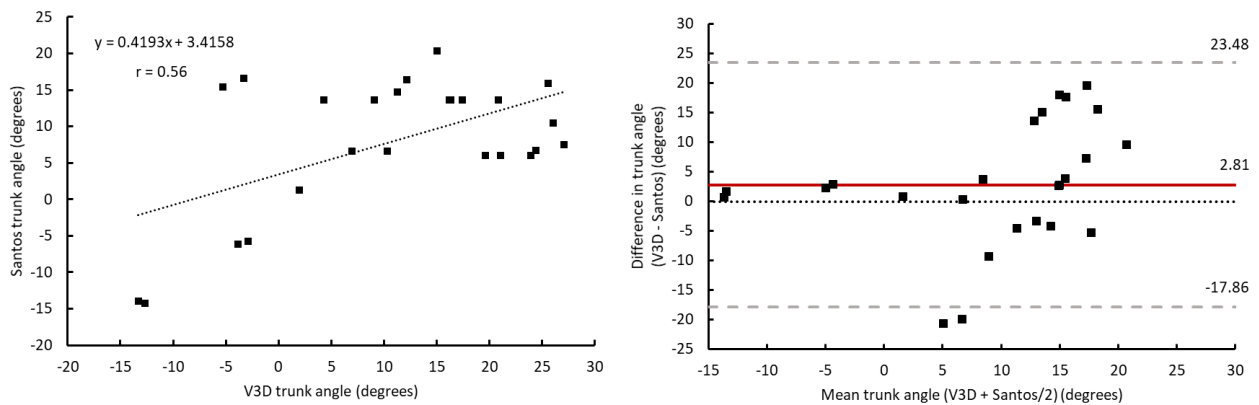


Figure 12. Left - scatter plot illustrating the relationship between trunk angles (+ extension) estimated using Santos’ motion capture data importing approach and the lab-based RLM (V3D). Regression equation and Pearson’s correlation coefficient (r) are displayed on the plot. Right – Bland-Altman plot illustrating the differences between trunk angles (+ extension) produced by the lab-based RLM (V3D) and Santos’ motion capture data importing approach vs. the mean of the two measures. Red line is the systematic error produced by Santos, grey dashed lines are the limits of agreement from $-1.96SD$ to $+1.96SD$, black dotted line is the line of equality.

A main effect of DHM software was detected for shoulder joint angles $F(2, 48) = 58.79$, $p < 0.001$, $\eta^2 = 0.71$. Pairwise comparisons indicated that shoulder angles computed by Jack ($M=56.54$, $SD=18.00$) and Santos ($M=42.64$, $SD=4.80$) were significantly higher than V3D ($M=21.04$, $SD=20.91$). There was a positive, strong correlation between Jack and V3D shoulder angles ($r = 0.75$, $n = 25$, $p < 0.001$) and a positive, but weak correlation between Santos and V3D ($r = 0.43$, $n = 25$, $p = 0.05$) shoulder joint angles. Bland Altman plots revealed disagreement between both DHM software and lab-based RLM, respectively; however, a significant proportional bias of -21.60 ($\beta = 0.92$, $t(24) = 10.95$, $p < 0.001$) was found between V3D and Santos shoulder angles. The $SDC_{95\%}$ were $\pm 7.79^\circ$ and $\pm 10.71^\circ$ Jack and Santos shoulder angles respectively.

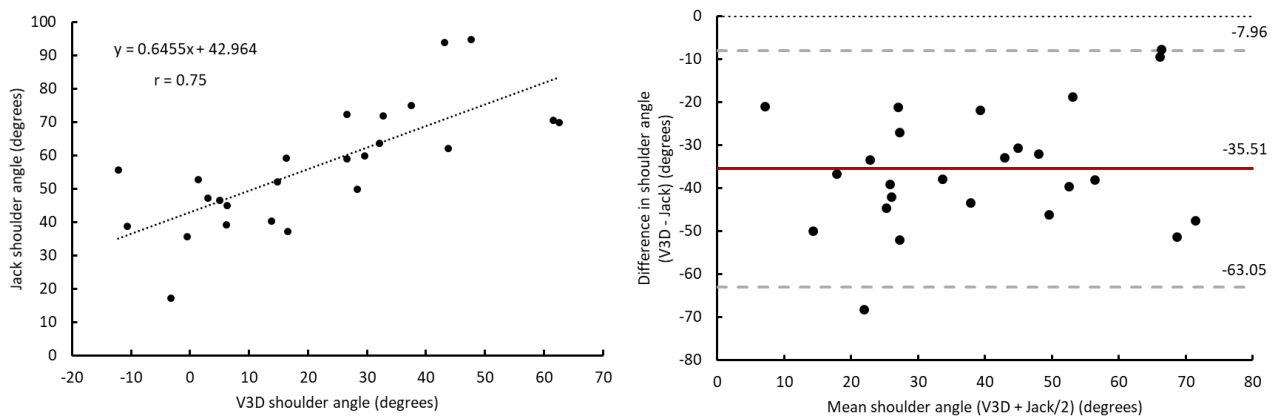


Figure 13. Left – scatter plot illustrating the relationship between shoulder joint angles (+ flexion) estimated using Jack’s motion capture data importing approach and the lab-based RLM (V3D). Regression equation and Pearson’s correlation coefficient (r) are displayed on the plot. Right – Bland-Altman plot illustrating the differences between shoulder joint angles (+ flexion) produced by the lab-based RLM (V3D) and Jack’s motion capture data importing approach vs. the mean of the two measures. Red line is the systematic error produced by Jack, grey dashed lines are the limits of agreement from $-1.96SD$ to $+1.96SD$, black dotted line is the line of equality.

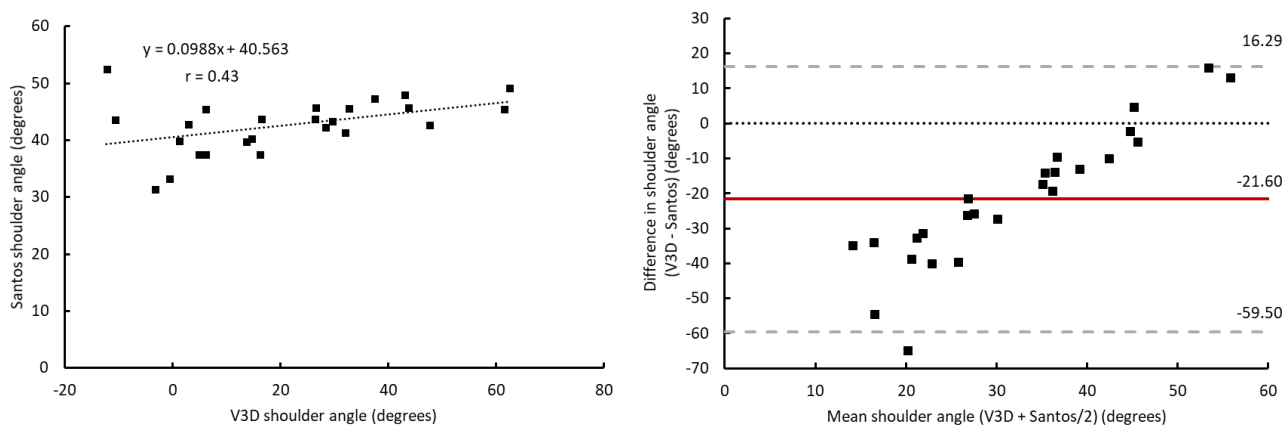


Figure 14. Left – scatter plot illustrating the relationship between shoulder joint angles (+flexion) estimated using Santos’ motion capture data importing approach and the lab-based RLM (V3D). Regression equation and Pearson’s correlation coefficient (r) are displayed on the plot. Right – Bland-Altman plot illustrating the differences between shoulder joint angles (+ flexion) produced by the lab-based RLM (V3D) and Santos’ motion capture data importing approach vs. the mean of the two measures. Red line is the systematic error produced by Santos, grey dashed lines are the limits of agreement from $-1.96SD$ to $+1.96SD$, black dotted line is the line of equality.

4.1.2 Kinetics

A main effect of DHM software package was detected for L4-L5 moments when using the direct motion capture data importing approach to simulate the patient turn $F(2, 48) = 10.86$, $p < 0.001$, $\eta^2 = 0.31$. Pairwise comparisons indicated that L4-L5 moments produced by Santos ($M=16.32$, $SD=8.48$) were significantly lower than V3D ($M=44.36$, $SD=41.45$) and Jack ($M=39.93$, $SD=28.68$). There were no significant differences between V3D and Jack L4-L5 moments. Correlation analysis revealed a positive, moderate correlation between Jack and V3D L4-L5 moments ($r = 0.66$, $n = 25$, $p < 0.001$), and a positive, but weak correlation between Santos and V3D L4-L5 moments ($r = 0.48$, $n = 25$, $p = 0.02$). Bland Altman plots revealed good agreement between L4-L5 moments estimated using V3D and Jack, with a significant proportional bias of 4.43Nm ($\beta = 0.45$ $t(24) = 2.40$, $p = 0.02$). However, only moderate agreement was observed between L4-L5 moments estimated using V3D and Santos, with a

significant proportional bias of 28.04Nm ($\beta = 0.94$ $t(24) = 12.77$, $p < 0.001$). The $SDC_{95\%}$ were ± 17.29 Nm and ± 21.14 Nm Jack and Santos L4-L5 moments, respectively.

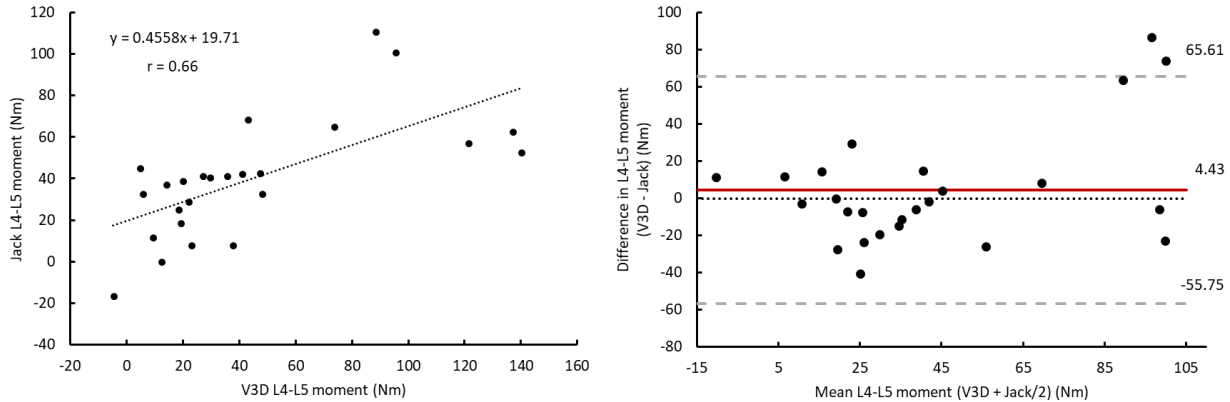


Figure 15. Left – scatter plot illustrating the relationship between L4-L5 joint moments (+ extensor) estimated using Jack’s motion capture data importing approach and the lab-based RLM (V3D). Regression equation and Pearson’s correlation coefficient (r) are displayed on the plot. Right – Bland-Altman plot illustrating the differences between L4-L5 joint moments (+ extensor) produced by the lab-based RLM (V3D) and Jack’s motion capture data importing approach vs. the mean of the two measures. Red line is the systematic error produced by Jack, grey dashed lines are the limits of agreement from $-1.96SD$ to $+1.96SD$, black dotted line is the line of equality.

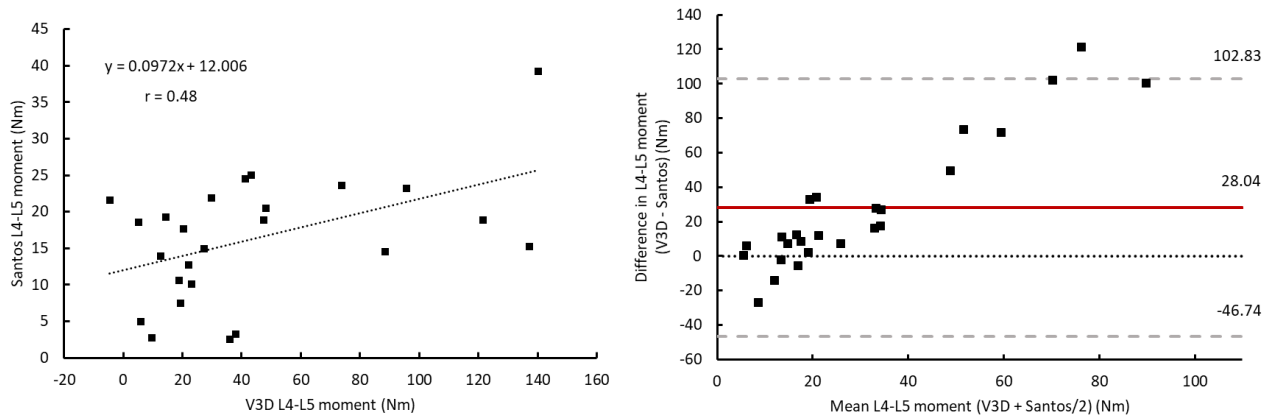


Figure 16. Left – scatter plot illustrating the relationship between L4-L5 joint moments (+ extensor) estimated using Santos’ motion capture data importing approach and the lab-based RLM (V3D). Regression equation and Pearson’s correlation coefficient (r) are displayed on the plot. Right – Bland-Altman plot illustrating the differences between L4-L5 joint moments (+ extensor) produced by the lab-based RLM (V3D) and Santos’ motion capture data importing approach vs. the mean of the two measures. Red line is the systematic error produced by Santos, grey dashed lines are the limits of agreement from $-1.96SD$ to $+1.96SD$, black dotted line is the line of equality.

Significant differences were detected in modeled shoulder moments. A main effect of DHM software package was detected $F(2, 48) = 5.84, p = 0.005, \eta^2 = 0.20$. Pairwise comparisons indicated that shoulder moments estimated by Jack ($M=20.64, SD=8.67$) and Santos ($M=20.75, SD=6.68$) were significantly lower than V3D ($M=27.41, SD=8.44$). No significant differences were found between Jack and Santos shoulder moments. There was a positive but weak correlation between Jack and V3D ($r = 0.02, n = 25, p = 0.91$), and Santos and V3D shoulder moments ($r = 0.13, n = 25, p = 0.54$); Bland Altman plots revealed disagreement between the software and lab-based RLM, respectively, with no significant proportional biases. The $SDC_{95\%}$ were $\pm 6.63\text{Nm}$ and $\pm 5.58\text{Nm}$ for Jack and Santos shoulder moments respectively.

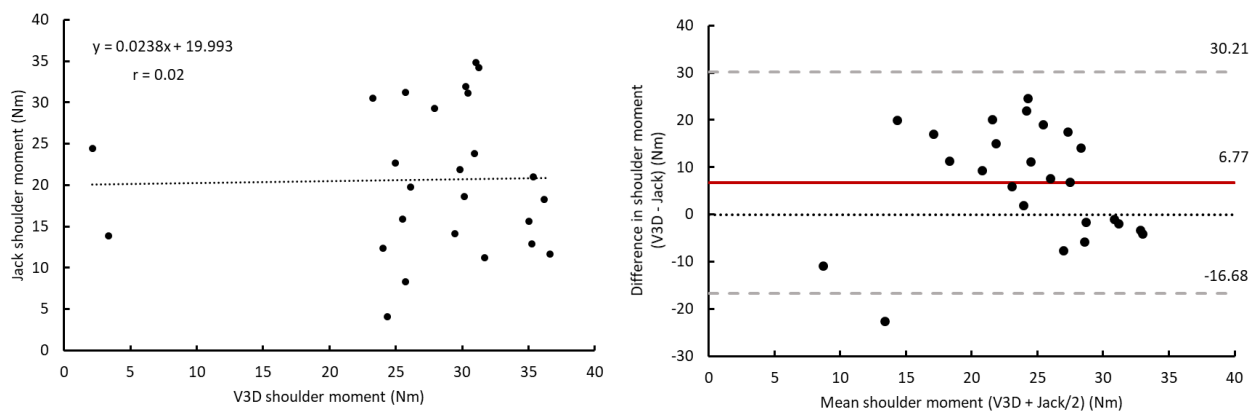


Figure 17. Left – scatter plot illustrating the relationship between shoulder joint moments (+ flexor) estimated using Jack’s motion capture data importing approach and the lab-based RLM (V3D). Regression equation and Pearson’s correlation coefficient (r) are displayed on the plot. Right – Bland-Altman plot illustrating the differences between shoulder joint moments (+ flexor) produced by the lab-based RLM (V3D) and Jack’s motion capture data importing approach vs. the mean of the two measures. Red line is the systematic error produced by Jack, grey dashed lines are the limits of agreement from $-1.96SD$ to $+1.96SD$, black dotted line is the line of equality.

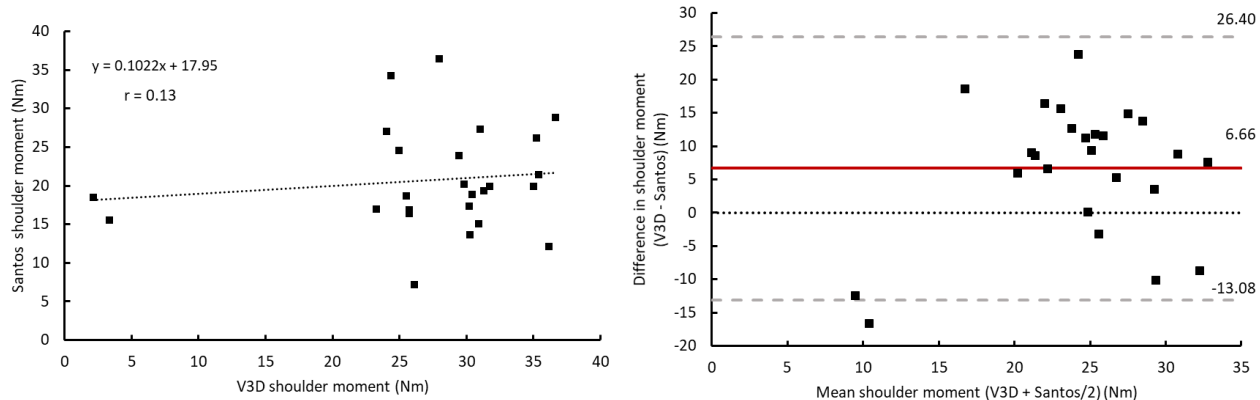


Figure 18. Left – scatter plot illustrating the relationship between shoulder joint moments (+ flexor) estimated using Santos’ motion capture data importing approach and the lab-based RLM (V3D). Regression equation and Pearson’s correlation coefficient (r) are displayed on the plot. Right – Bland-Altman plot illustrating the differences between shoulder joint moments (+ flexor) produced by the lab-based RLM (V3D) and Jack’s motion capture data importing approach vs. the mean of the two measures. Red line is the systematic error produced by Santos, grey dashed lines are the limits of agreement from $-1.96SD$ to $+1.96SD$, black dotted line is the line of equality.

4.2 Manual Joint Manipulation

Table 5. Summary of the mean differences found between kinetic and kinematic measures estimated using the lab-based RLM (V3D) and DHM software packages' manual joint manipulation approach. Asterisks indicate significant differences between models. The calculated smallest detectable change within 95% confidence intervals is reported for each pair.

Model (Lab based)	Model (DHM)	Mean Difference (Lab based- DHM)	95% Confidence Interval for Difference		SDC _{±95%}
			Lower Bound	Upper Bound	
V3D trunk Angle	Jack trunk Angle	1.08	-9.43	11.60	11.32
	Santos trunk Angle	7.59*	0.83	14.34	7.27
V3D Shoulder Angle	Jack Shoulder Angle	-7.76	-21.23	5.71	14.50
	Santos Shoulder Angle	3.81	-0.41	8.04	4.55
V3D L4-L5 Moment	Jack L4-L5 Moment	0.71	-7.99	9.42	9.37
	Santos L4-L5 Moment	28.25*	14.67	41.83	14.62
V3D Shoulder Moment	Jack Shoulder Moment	8.87*	3.34	14.39	5.94
	Santos Shoulder Moment	4.73*	0.00	9.46	5.09

* $p < 0.05$

4.2.1 Kinematics

A main effect of DHM software was detected for trunk angles $F(1.17, 28.02) = 3.68, p = 0.05, \eta^2 = 0.12$. Pairwise comparisons indicated that trunk angles computed by Santos ($M=3.13, SD=3.79$) were significantly lower than V3D ($M=10.72, SD=12.26$) and Jack ($M=9.64, SD=11.71$). Correlation analysis revealed a negative, weak correlation between Jack and V3D ($r = -0.45, n = 25, p = 0.02$) and Santos and V3D ($r = -0.08, n = 25, p = 0.71$) trunk joint angles. Bland Altman plots revealed moderate agreement between Jack and V3D trunk angles, with no significant bias detected, while poor agreement was observed between Santos and V3D trunk angles, with a significant proportional bias of 7.59 ($\beta = 0.83, t(24) = 7.02, p < 0.001$). The SDC_{95%} were $\pm 11.32^\circ$ and $\pm 7.27^\circ$ for Jack and Santos trunk angles respectively.

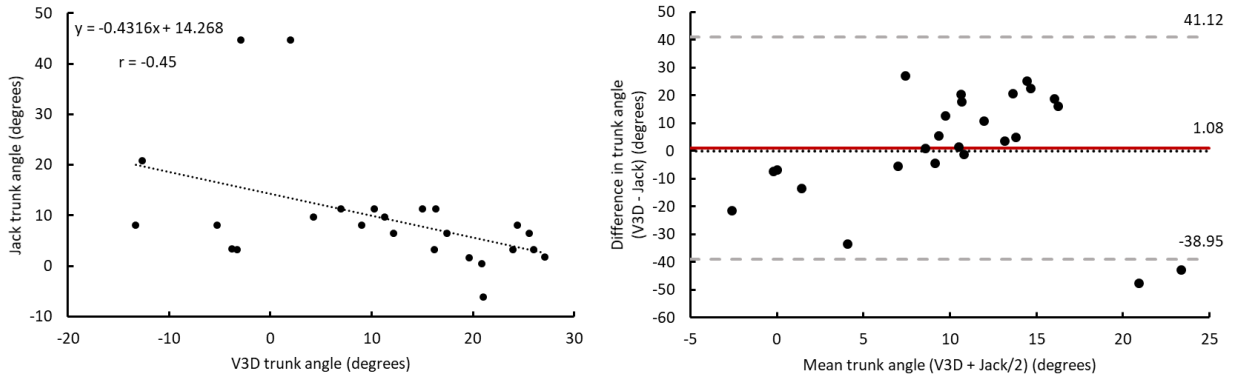


Figure 19. Left – scatter plot illustrating the relationship between trunk angles (+ extension) estimated using Jack’s manual joint manipulation approach and the lab-based RLM (V3D). Regression equation and Pearson’s correlation coefficient (r) are displayed on the plot. Right – Bland-Altman plot illustrating the differences between trunk angles (+ extension) produced by the lab-based RLM (V3D) and Jack’s manual joint manipulation approach vs. the mean of the two measures. Red line is the systematic error produced by Jack, grey dashed lines are the limits of agreement from $-1.96SD$ to $+1.96SD$, black dotted line is the line of equality.

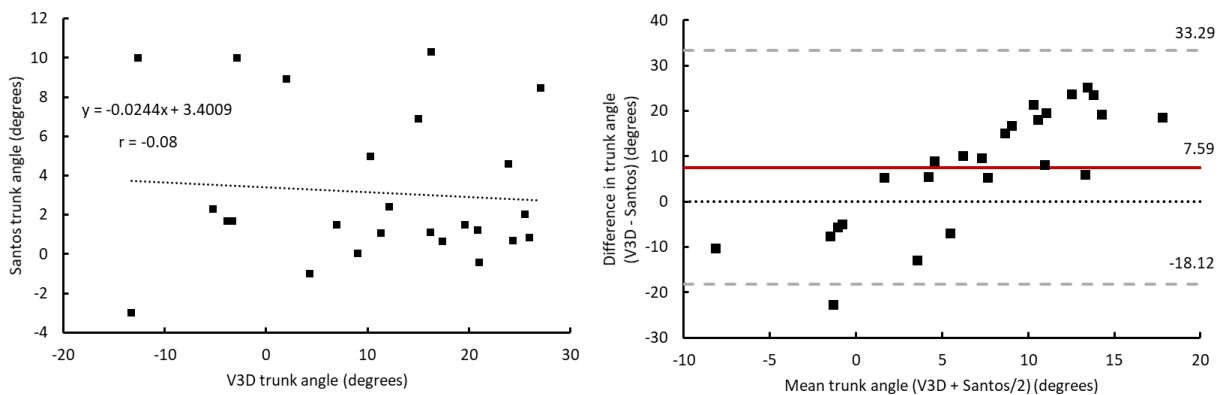


Figure 20. Left – scatter plot illustrating the relationship between trunk angles (+ extension) estimated using Santos’ manual joint manipulation approach and the lab-based RLM (V3D). Regression equation and Pearson’s correlation coefficient (r) are displayed on the plot. Right – Bland-Altman plot illustrating the differences between trunk angles (+ extension) produced by the lab-based RLM (V3D) and Santos’ manual joint manipulation approach vs. the mean of the two measures. Red line is the systematic error produced by Santos, grey dashed lines are the limits of agreement from $-1.96SD$ to $+1.96SD$, black dotted line is the line of equality.

Differences were not detected between Jack, Santos and V3D shoulder angles $F(1.14, 27.58) = 3.60, p = 0.06, \eta^2 = 0.13$. Correlation analysis revealed a positive, strong correlation between Jack and V3D ($r = 0.77, n = 25, p < 0.001$) and Santos and V3D ($r = 0.92, n = 25, p < 0.001$) shoulder joint angles. Bland Altman plots revealed moderate agreement between Jack and V3D shoulder angles with a significant proportional bias of -7.76 ($\beta = -0.71, t(24) = -4.85, p < 0.001$); however, good agreement was observed between Santos and V3D shoulder angles with no significant proportional bias. The $SDC_{95\%}$ were $\pm 14.50^\circ$ and $\pm 4.55^\circ$ for Jack and Santos shoulder angles respectively.

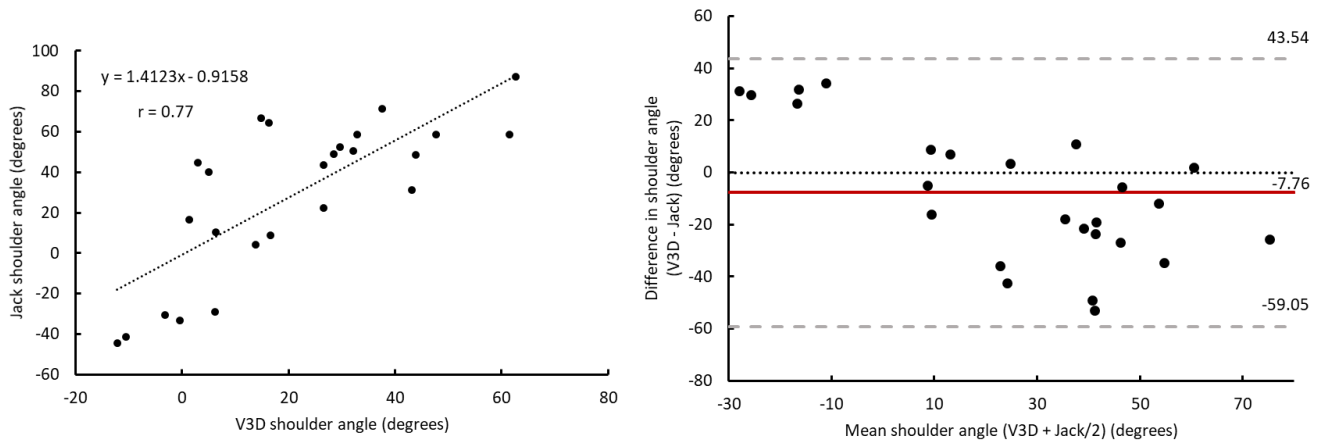


Figure 21. Left – scatter plot illustrating the relationship between shoulder joint angles (+ flexion) estimated using Jack’s manual joint manipulation approach and the lab-based RLM (V3D). Regression equation and Pearson’s correlation coefficient (r) are displayed on the plot. Right – Bland-Altman plot illustrating the differences between shoulder joint angles (+ flexion) produced by the lab-based RLM (V3D) and Jack’s manual joint manipulation approach vs. the mean of the two measures. Red line is the systematic error produced by Jack, grey dashed lines are the limits of agreement from $-1.96SD$ to $+1.96SD$, black dotted line is the line of equality.

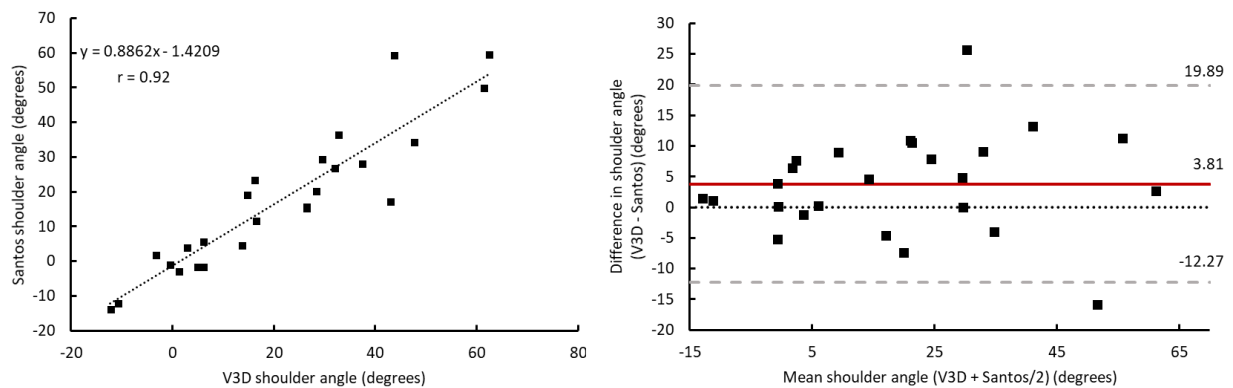


Figure 22. Left – scatter plot illustrating the relationship between shoulder joint angles (+ flexion) estimated using Santos’ manual joint manipulation approach and the lab-based RLM (V3D). Regression equation and Pearson’s correlation coefficient (r) are displayed on the plot. Right – Bland-Altman plot illustrating the differences between shoulder joint angles (+ flexion) produced by the lab-based RLM (V3D) and Santos’ manual joint manipulation approach vs. the mean of the two measures. Red line is the systematic error produced by Santos, grey dashed lines are the limits of agreement from $-1.96SD$ to $+1.96SD$, black dotted line is the line of equality.

4.2.2 Kinetics

A main effect of DHM software package was detected for L4-L5 moments when using the manual joint manipulation approach to simulate the patient turn $F(1.56, 37.40) = 28.23$, $p < 0.001$, $\eta^2 = 0.54$. Pairwise comparisons indicated that Santos L4-L5 moments ($M=16.11$, $SD=14.45$) were significantly lower than V3D ($M=44.36$, $SD=41.45$) and Jack ($M=43.65$, $SD=33.68$) L4-L5 moment. Correlation analysis revealed a positive, strong correlation between Jack and V3D L4-L5 moments ($r = 0.92$, $n = 25$, $p < 0.001$) and Santos and V3D L4-L5 moments ($r = 0.83$, $n = 25$, $p < 0.001$). Bland Altman plots revealed good agreement between Jack and V3D L4-L5 moments, with a significant proportional bias of 0.71Nm ($\beta = 0.47$, $t(24) = 2.54$, $p = 0.02$), but moderate agreement between Santos and V3D L4-L5 moments with a significant bias of 28.25Nm ($\beta = 0.79$, $t(24) = 6.15$, $p < 0.001$). The $SDC_{95\%}$ were $\pm 9.37\text{Nm}$ and $\pm 14.62\text{Nm}$ for Jack and Santos L4-L5 moments respectively.

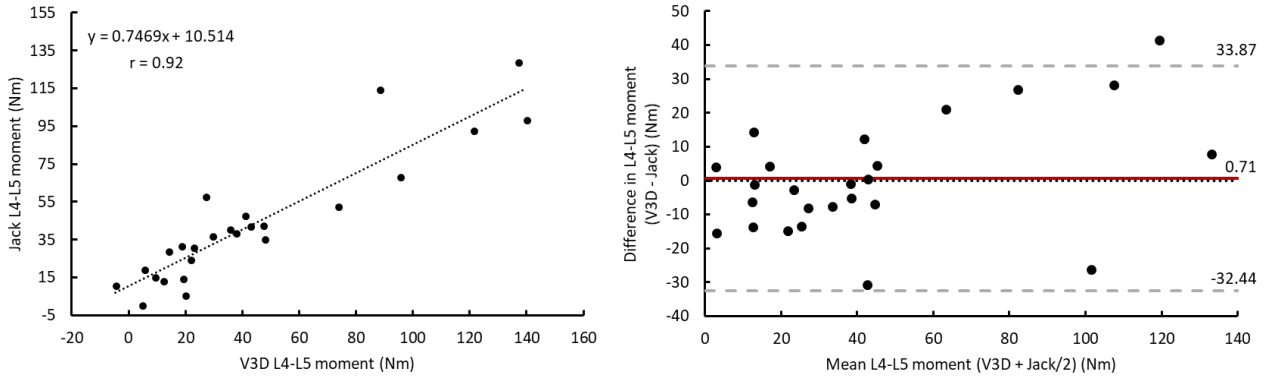


Figure 23. Left – scatter plot illustrating the relationship between L4-L5 joint moments (+ extensor) estimated using Jack’s manual joint manipulation approach and the lab-based RLM (V3D). Regression equation and Pearson’s correlation coefficient (r) are displayed on the plot. Right – Bland-Altman plot illustrating the differences between L4-L5 joint moments (+ extensor) produced by the lab-based RLM (V3D) and Jack’s manual joint manipulation approach vs. the mean of the two measures. Red line is the systematic error produced by Jack, grey dashed lines are the limits of agreement from $-1.96SD$ to $+1.96SD$, black dotted line is the line of equality.

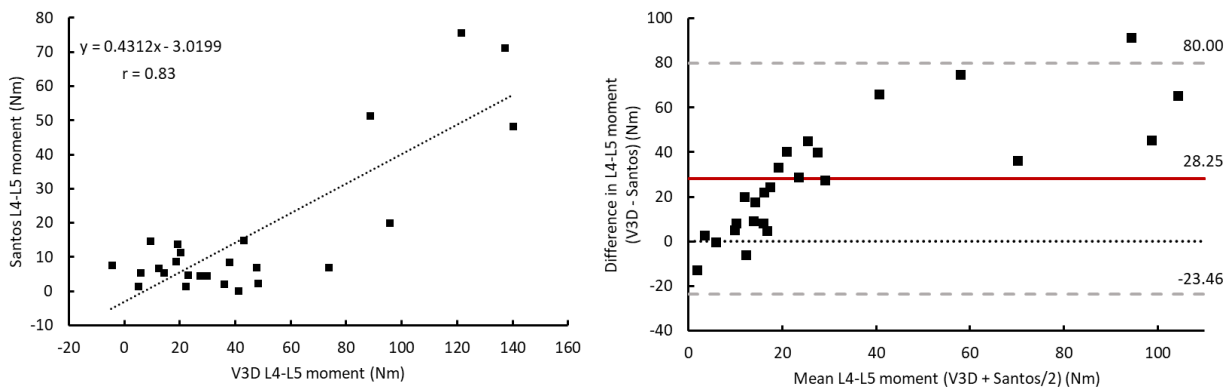


Figure 24. Left – scatter plot illustrating the relationship between L4-L5 joint moments (+ extensor) estimated using Santos’ manual joint manipulation approach and the lab-based RLM (V3D). Regression equation and Pearson’s correlation coefficient (r) are displayed on the plot. Right – Bland-Altman plot illustrating the differences between L4-L5 joint moments (+ extensor) produced by the lab-based RLM (V3D) and Santos’ manual joint manipulation approach vs. the mean of the two measures. Red line is the systematic error produced by Santos, grey dashed lines are the limits of agreement from $-1.96SD$ to $+1.96SD$, black dotted line is the line of equality.

Significant differences were detected for shoulder moments. A main effect of DHM software package was detected $F(2,48) = 11.96, p < 0.001, \eta^2 = 0.33$. Pairwise comparisons indicated shoulder moments produced by Jack ($M=18.54, SD=7.93$) and Santos ($M=22.68, SD=3.86$) were both significantly lower than V3D ($M=27.41, SD=8.44$). Significant differences were also found between Jack and Santos shoulder moment outputs. Correlation analysis revealed a positive, weak correlation between Jack and V3D ($r = 0.14, n = 25, p = 0.49$), and Santos and V3D shoulder moments ($r = 0.03, n = 25, p = 0.89$). Bland Altman plots revealed disagreement between both DHM software and V3D shoulder moment outputs; however, a significant proportional bias of 4.73Nm ($\beta = 0.65, t(24) = 4.15, p < 0.001$) was only found between Santos and V3D. The $SDC_{95\%}$ were ± 5.94 Nm and ± 5.09 Nm for Jack and Santos shoulder moments respectively.

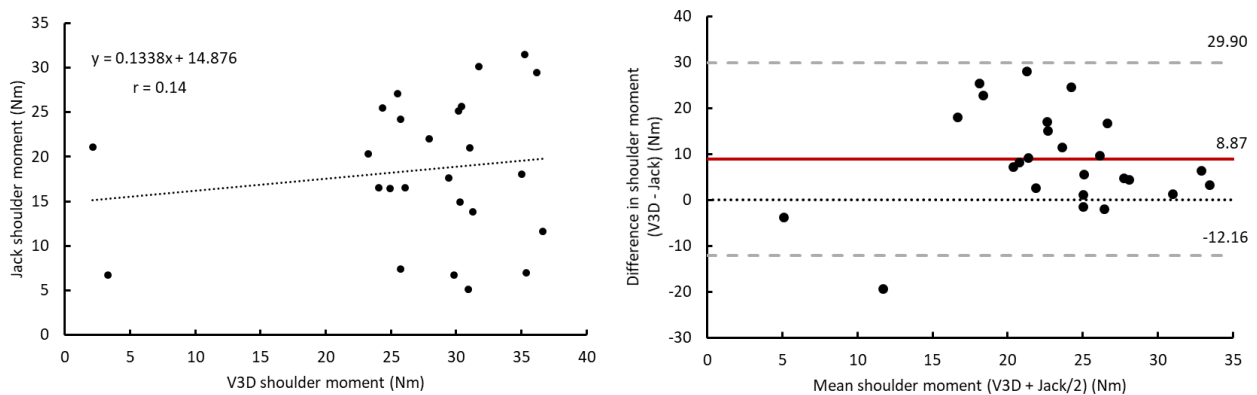


Figure 25. Left – scatter plot illustrating the relationship between shoulder joint moments (+ flexor) estimated using Jack’s manual joint manipulation approach and the lab-based RLM (V3D). Regression equation and Pearson’s correlation coefficient (r) are displayed on the plot. Right – Bland-Altman plot illustrating the differences between shoulder joint moments (+ flexor) produced by the lab-based RLM (V3D) and Jack’s manual joint manipulation approach vs. the mean of the two measures. Red line is the systematic error produced by Jack, grey dashed lines are the limits of agreement from $-1.96SD$ to $+1.96SD$, black dotted line is the line of equality.

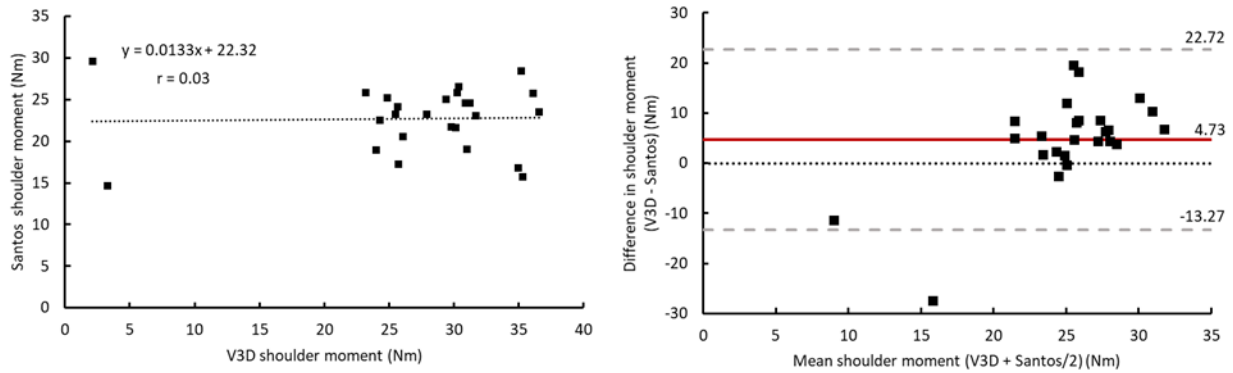


Figure 26. Left – scatter plot illustrating the relationship between shoulder joint moments (+ flexor) estimated using Santos’ manual joint manipulation approach and the lab-based RLM (V3D). Regression equation and Pearson’s correlation coefficient (r) are displayed on the plot. Right – Bland-Altman plot illustrating the differences between shoulder joint moments (+ flexor) produced by the lab-based RLM (V3D) and Jack’s manual joint manipulation approach vs. the mean of the two measures. Red line is the systematic error produced by Santos, grey dashed lines are the limits of agreement from $-1.96SD$ to $+1.96SD$, black dotted line is the line of equality.

4.3 Posture Prediction

Table 6. Summary of the mean differences found between kinetic and kinematic measures estimated using the lab-based RLM (V3D) and DHM software packages' posture prediction approach. Asterisks indicate significant differences between models. The calculated smallest detectable change within 95% confidence intervals is reported for each pair.

Model (Lab based)	Model (DHM)	Mean Difference (Lab based-DHM)	95% Confidence Interval for Difference		SDC _{±95%}
			Lower Bound	Upper Bound	
V3D Trunk Angle	Jack Trunk Angle	2.36	-3.97	8.69	6.81
	Santos Trunk Angle	8.21*	2.19	14.22	6.48
V3D Shoulder Angle	Jack Shoulder Angle	-47.65*	-59.62	-35.67	12.89
	Santos Shoulder Angle	5.52	-6.76	17.81	13.22
V3D L4-L5 Moment	Jack L4-L5 Moment	22.97*	2.73	43.21	21.78
	Santos L4-L5 Moment	29.14*	8.51	49.78	22.21
V3D Shoulder Moment	Jack Shoulder Moment	5.36*	0.76	9.95	4.95
	Santos Shoulder Moment	2.94	-2.29	8.18	5.64

* $p < 0.05$

4.3.1 Kinematics

A main effect of DHM software was detected for trunk angles $F(1.20, 28.70) = 8.74, p = 0.004, \eta^2 = 0.27$. Pairwise comparisons revealed that trunk angles computed by Santos ($M=2.51, SD=1.89$) were significantly lower than V3D ($M=10.72, SD=12.26$) and Jack ($M=8.36, SD=4.37$). Correlation analysis revealed a positive, weak correlation between Jack and V3D ($r = 0.17, n = 25, p = 0.42$) and Santos and V3D ($r = 0.37, n = 25, p = 0.07$) trunk angles; Bland Altman plots revealed disagreement between trunk angle outputs, respectively, with significant proportional biases of 2.36 ($\beta = 0.78, t(24) = 5.96, p < 0.001$) and 8.21 ($\beta = 0.96, t(24) = 16.28, p < 0.001$). The SDC_{95%} was $\pm 6.81^\circ$ and $\pm 6.48^\circ$ for Jack and Santos trunk angles respectively.

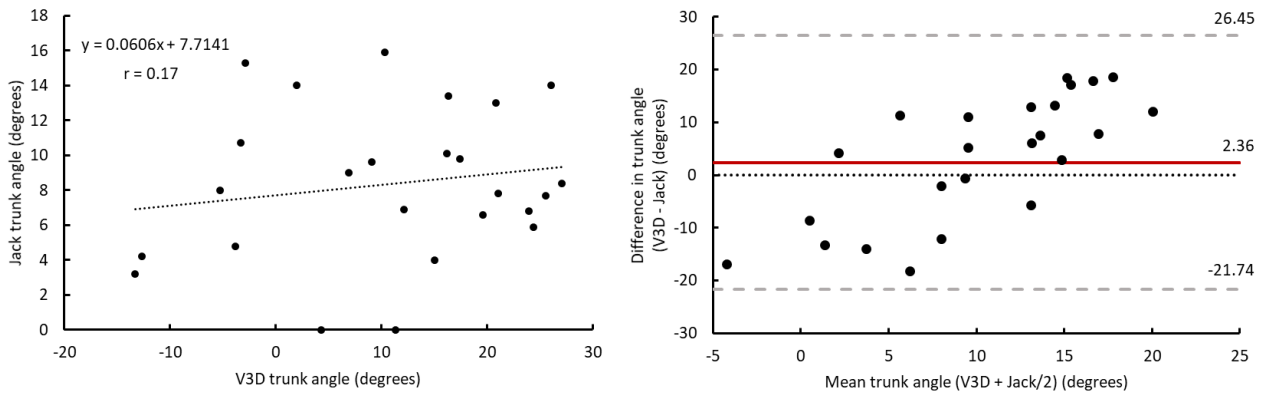


Figure 27. Left – scatter plot illustrating the relationship between trunk angles (+ extension) estimated using Jack’s posture prediction approach and the lab-based RLM (V3D). Regression equation and Pearson’s correlation coefficient (r) are displayed on the plot. Right – Bland-Altman plot illustrating the differences between trunk angles (+ extension) produced by the lab-based RLM (V3D) and Jack’s posture prediction approach vs. the mean of the two measures. Red line is the systematic error produced by Jack, grey dashed lines are the limits of agreement from $-1.96SD$ to $+1.96SD$, black dotted line is the line of equality.

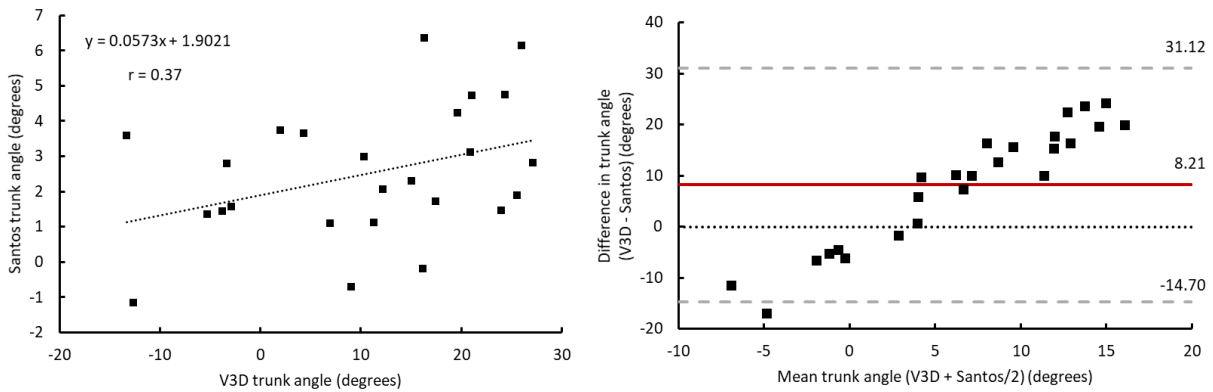


Figure 28. Left – scatter plot illustrating the relationship between trunk angles (+ extension) estimated using Santos’ posture prediction approach and the lab-based RLM (V3D). Regression equation and Pearson’s correlation coefficient (r) are displayed on the plot. Right – Bland-Altman plot illustrating the differences between trunk angles (+ extension) produced by the lab-based RLM (V3D) and Santos’ posture prediction approach vs. the mean of the two measures. Red line is the systematic error produced by Santos, grey dashed lines are the limits of agreement from $-1.96SD$ to $+1.96SD$, black dotted line is the line of equality.

A main effect of DHM software was detected for shoulder joint angles $F(2,48) = 88.60$, $p < 0.001$, $\eta^2 = 0.79$. Pairwise comparisons indicated that shoulder angles computed by Jack ($M=68.68$, $SD=12.64$) were significantly higher than V3D ($M=21.04$, $SD=20.91$) and Santos ($M=15.51$, $SD=11.18$). Correlation analysis revealed a weak correlation between Jack and V3D ($r = 0.11$, $n = 25$, $p=0.62$) and Santos and V3D ($r = -0.02$, $n = 25$, $p=0.93$) shoulder joint angles. Bland Altman plots revealed poor agreement between Jack and V3D shoulder angles, with a significant proportional bias of -47.65 ($\beta = 0.47$, $t(24) = 2.53$, $p=0.02$); however, moderate agreement was observed between Santos and V3D shoulder angles with a significant proportional bias of 5.52 ($\beta = 0.56$, $t(24) = 3.20$, $p < 0.001$). The $SDC_{95\%}$ were $\pm 12.89^\circ$ and $\pm 13.22^\circ$ for Jack and Santos shoulder angles respectively.

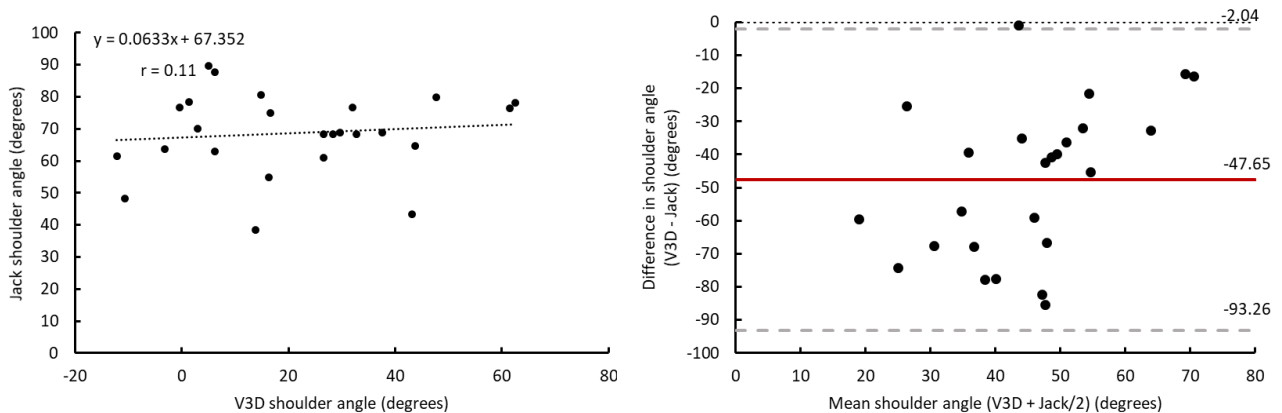


Figure 29. Left – scatter plot illustrating the relationship between shoulder joint angles (+ flexion) estimated using Jack’s posture prediction approach and the lab-based RLM (V3D). Regression equation and Pearson’s correlation coefficient (r) are displayed on the plot. Right – Bland-Altman plot illustrating the differences between shoulder joint angles (+ flexion) produced by the lab-based RLM (V3D) and Jack’s posture prediction approach vs. the mean of the two measures. Red line is the systematic error produced by Jack, grey dashed lines are the limits of agreement from $-1.96SD$ to $+1.96SD$, black dotted line is the line of equality.

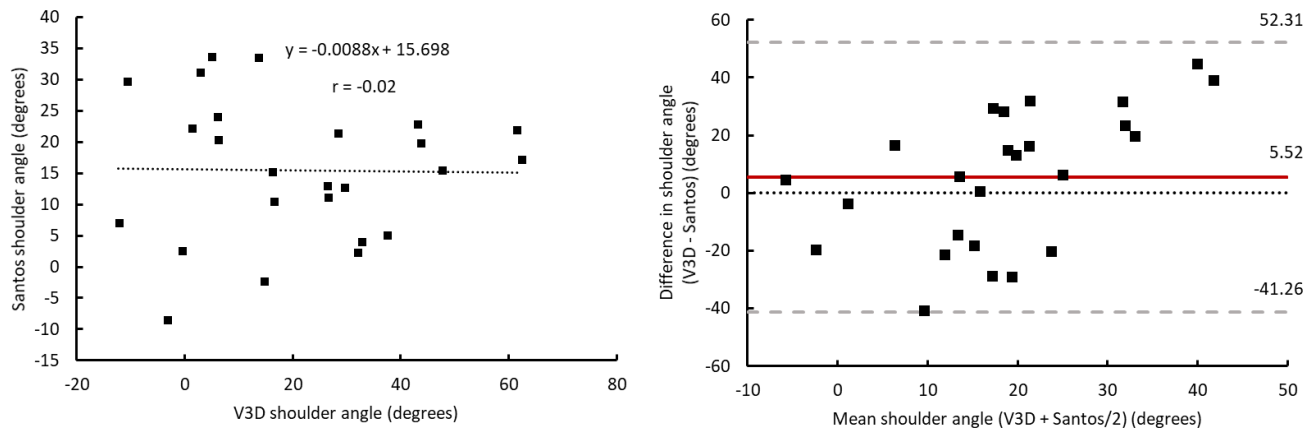


Figure 30. Left – scatter plot illustrating the relationship between shoulder joint angles (+ flexion) estimated using Santos' posture prediction approach and the lab-based RLM (V3D). Regression equation and Pearson's correlation coefficient (r) are displayed on the plot. Right – Bland-Altman plot illustrating the differences between shoulder joint angles (+ flexion) produced by the lab-based RLM (V3D) and Santos' posture prediction approach vs. the mean of the two measures. Red line is the systematic error produced by Santos, grey dashed lines are the limits of agreement from $-1.96SD$ to $+1.96SD$, black dotted line is the line of equality.

4.3.2 Kinetics

A main effect of DHM software package was detected for L4-L5 moments when using the posture prediction approach to simulate the patient turn $F(1.25, 29.92) = 10.39, p = 0.002, \eta^2 = 0.30$. Pairwise comparisons indicated that L4-L5 moments produced by Jack ($M=21.39, SD=14.13$) and Santos ($M=15.21, SD=10.13$) were significantly lower than V3D ($M=44.36, SD=41.45$). No significant differences were detected between Jack and Santos L4-L5 moment outputs. Correlation analysis revealed a positive, weak correlation between Jack and V3D L4-L5 moments ($r = 0.32, n = 25, p = 0.12$) and Santos and V3D L4-L5 moments ($r = 0.26, n = 25, p=0.22$). Bland Altman plots revealed disagreement between both Jack and Santos and V3D L4-L5 moments, as well as significant proportional biases of 22.97Nm ($\beta = 0.81 t(24) = 6.56, p<0.001$), and 29.14Nm ($\beta = 0.89 t(24) = 9.4, p<0.001$), respectively. The $SDC_{95\%}$ were ± 21.78 Nm and ± 22.21 Nm Jack and Santos L4-L5 moments respectively.

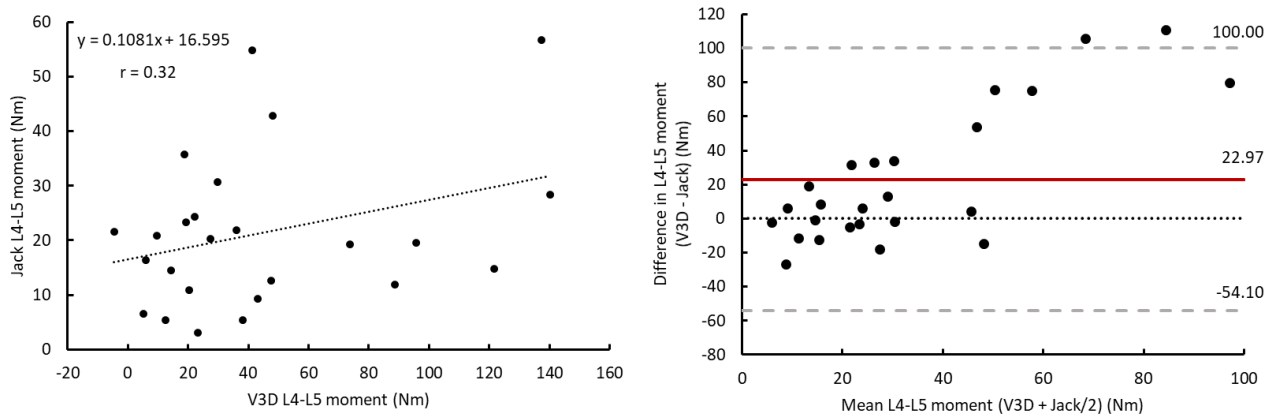


Figure 31. Left – scatter plot illustrating the relationship between L4-L5 joint moments (+ extensor) estimated using Jack's posture prediction approach and the lab-based RLM (V3D). Regression equation and Pearson's correlation coefficient (r) are displayed on the plot. Right – Bland-Altman plot illustrating the differences between L4-L5 joint moments (+ extensor) produced by the lab-based RLM (V3D) and Jack's posture prediction approach vs. the mean of the two measures. Red line is the systematic error produced by Jack, grey dashed lines are the limits of agreement from $-1.96SD$ to $+1.96SD$, black dotted line is the line of equality.

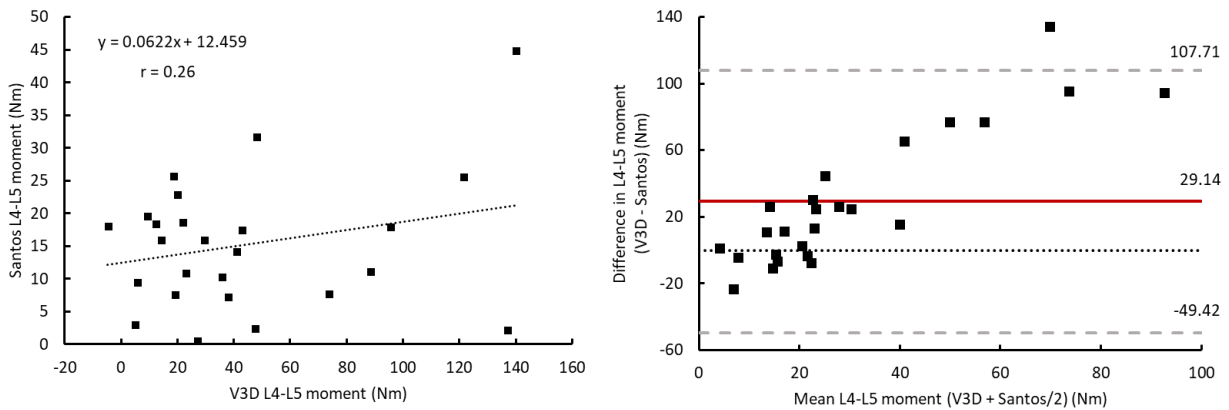


Figure 32. Left – scatter plot illustrating the relationship between L4-L5 joint moments (+ extensor) estimated using Santos' posture prediction approach and the lab-based RLM (V3D). Regression equation and Pearson's correlation coefficient (r) are displayed on the plot. Right – Bland-Altman plot illustrating the differences between L4-L5 joint moments (+ extensor) produced by the lab-based RLM (V3D) and Santos' posture prediction approach vs. the mean of the two measures. Red line is the systematic error produced by Santos, grey dashed lines are the limits of agreement from $-1.96SD$ to $+1.96SD$, black dotted line is the line of equality.

Significant differences were detected for shoulder moments. A main effect of DHM software package was detected $F(2,48) = 3.69, p = 0.03, \eta^2 = 0.13$. Pairwise comparisons indicated that shoulder moments produced by Jack ($M=22.05, SD=8.04$) were significantly lower than V3D ($M=27.41, SD=8.44$). Santos and V3D shoulder moment outputs were not significantly different. Correlation analysis revealed a positive, weak correlation between Jack and V3D ($r = 0.41, n = 25, p = 0.04$), and Santos and V3D shoulder moments ($r = 0.08, n = 25, p = 0.71$); Bland Altman plots revealed moderate agreement between the variables, respectively, with no significant proportional biases. The $SDC_{95\%}$ were $\pm 4.95\text{Nm}$ and $\pm 5.64\text{Nm}$ for Jack and Santos shoulder moments respectively.

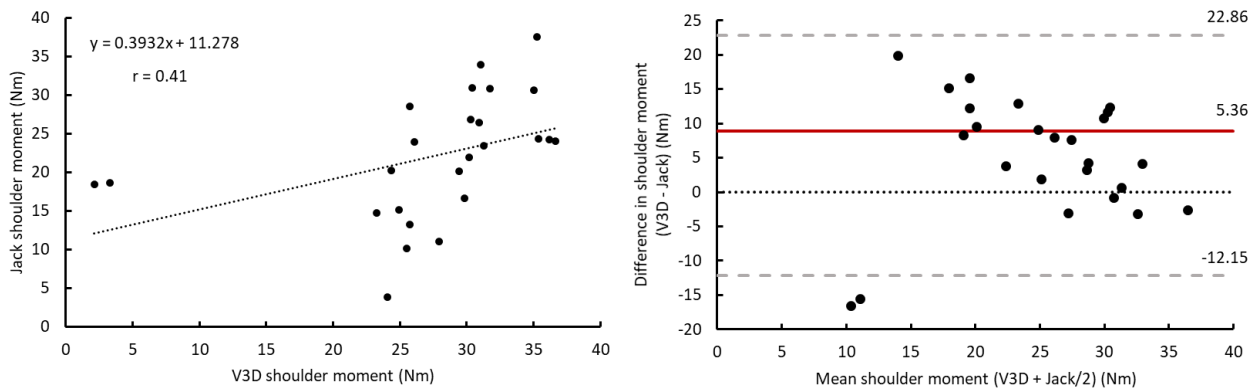


Figure 33. Left – scatter plot illustrating the relationship between shoulder joint moments (+ flexor) estimated using Jack’s posture prediction approach and the lab-based RLM (V3D). Regression equation and Pearson’s correlation coefficient (r) are displayed on the plot. Right – Bland-Altman plot illustrating the differences between shoulder joint moments (+ flexor) produced by the lab-based RLM (V3D) and Jack’s posture prediction approach vs. the mean of the two measures. Red line is the systematic error produced by Jack, grey dashed lines are the limits of agreement from $-1.96SD$ to $+1.96SD$, black dotted line is the line of equality.

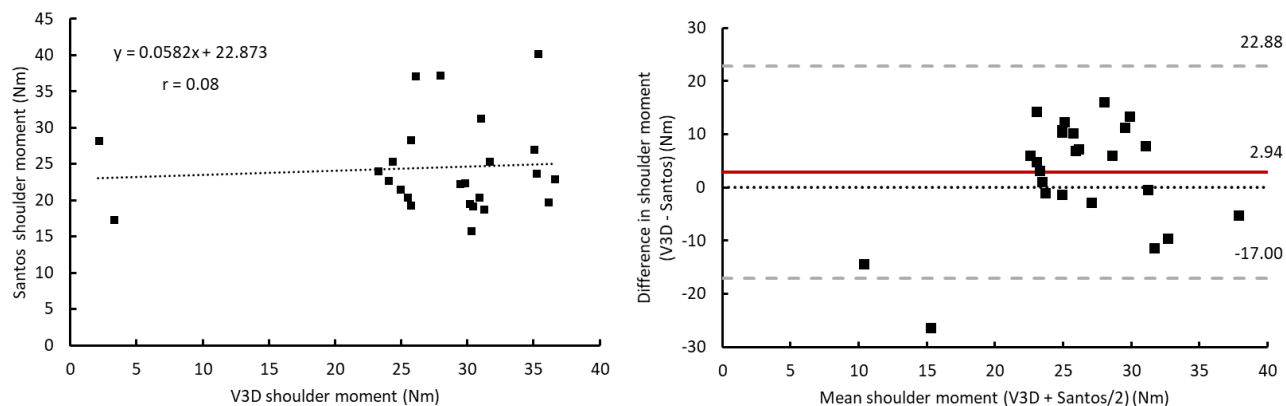


Figure 34. Left – scatter plot illustrating the relationship between shoulder joint moments (+ flexor) estimated using Santos' posture prediction approach and the lab-based RLM (V3D). Regression equation and Pearson's correlation coefficient (r) are displayed on the plot. Right – Bland-Altman plot illustrating the differences between shoulder joint moments (+ flexor) produced by the lab-based RLM (V3D) and Jack's posture prediction approach vs. the mean of the two measures. Red line is the systematic error produced by Santos, grey dashed lines are the limits of agreement from $-1.96SD$ to $+1.96SD$, black dotted line is the line of equality.

5.0 Discussion

5.1 Summary of Key Findings

Three different DHM posturing approaches were used in this investigation to simulate a static patient reposition task and estimate low back and shoulder kinematic and kinetic measures. Trunk and shoulder joint angles and moments estimated using these posturing approaches were compared to a lab-based rigid linked segment model (RLM). Posturing using Siemens Jack's (V 8.4) manual joint manipulation approach produced kinematic and kinetic outputs that agreed with the lab-based RLM outputs; however, Santos Pro's manual joint manipulation approach outputs did not agree with lab-based RLM. Kinematic and kinetic outputs estimated using both DHM software packages' posture prediction and direct motion capture data importing approaches differed from the lab-based RLM outputs likely due to differences associated with the link segment models as well factors associated with the posturing approaches.

It was expected that the estimated kinematic and kinetic outputs would be similar to the lab-based RLM outputs when using motion capture data importing and manual posturing to simulate the patient reposition task in Jack and Santos; however, the data only partially supported this hypothesis. When comparing Jack's outputs, the trunk angles and L4-L5 moments as well as shoulder angles produced using its manual posturing approach were similar to the lab-based RLM outputs as hypothesized; however, only L4-L5 moments estimated using its motion capture data importing approach were similar to the lab-based RLM outputs; partially supporting the hypothesis. It was believed that the motion capture data importing approach and manually posturing approaches would simulate realistic postures as a result of their increased user control, and ability to have maximum influence over the simulated posture. However, the lack of consistency in differences observed between these two approaches indicates that there may be

differences in the underlying models. Using a deductive reasoning approach, differences in the definition of Jack's RLM relative to the lab-based RLM could explain the variation observed. This explanation is discussed in more detail in the direct motion capture data importing section below.

In turn, when comparing Santos' outputs to lab-based RLM outputs, only the trunk angles produced by its motion capture data importing approach and shoulder joint angles produced using the manual posturing approach were similar, refuting hypothesis one. Contrary to the belief that increased user control would assist in simulating data similar to a lab-based model, these results clearly suggest that there are other influencing factors that may extend beyond simple posture manipulation. In particular to Santos' RLM, the multi-segmental model of the spine provided in the avatar may have acted as both an advantage and disadvantage when simulating the patient reposition task. It is believed that when using the motion capture data importing approach, the avatar was able to better adjust its spine (due to the increased DOF provided in the spine) with the given 3D position data from the lab-based RLM, to replicate the posture of the trunk segment. This may explain the similarities observed between the motion capture driven and lab-based RLM trunk angles. In turn, while the user was given a higher degree of control when manually posturing the spine of the avatar, this may have resulted in producing higher variation in trunk angles relative to the lab-based RLM.

When using the DHM software packages' posture prediction approach to simulate the patient reposition task, it was hypothesized that the estimated kinematic and kinetic joint measures would differ from the lab-based RLM outputs. Data indicated that the L4-L5 joint moments, shoulder joint angles and moments estimated using Jack's statistical driven posture prediction approach were different from lab-based RLM outputs, supporting hypothesis one.

However, only the trunk angles and L4-L5 moments estimated using Santos' optimization-based posture prediction approach were different from lab-based RLM outputs, partially supporting hypothesis one. When considering the differences between Jack and Santos' posture prediction results, there were apparent model differences that effected the predicted joint angles and moments. According to Faraway et al. (2006) Jack will attempt to minimize motion from the base of its kinematic chain (spine root), as a result, similar trunk angles may have been observed relative to the lab-based RLM. Comparatively, Santos' optimization model attempted to minimize joint displacement and moments when predicting whole body postures. Interestingly, the shoulder joint angles and moments estimated were similar to the lab-based RLM, suggesting that Santos may better predict upper extremity kinematics and kinetic but suffer in producing low back measures, in part due to the digital structure of the of the spine (increased degrees of freedom).

When evaluating the relationship between DHM estimated kinematics and kinetics using the posture prediction approach to lab-based RLM outputs, it was predicted that they would have a weak correlation. All four outcome measures of interest; trunk and shoulder joint angles and moments estimated using Jack and Santos' posture prediction approach had a weak correlation ($r < 0.50$) with lab-based RLM outputs, supporting hypothesis two. Large variation found between posture predicted DHM outputs and lab-based RLM can explain the lack of association and agreement between the variables. Interestingly, when evaluating the relationship between manual posturing outputs and lab-based RLM, a moderate correlation ($0.5 \leq r \leq 0.7$) was expected; however, a stronger relationship was found between L4-L5 joint moments and shoulder angles estimated by Jack and Santos, partially supporting the hypothesis. The differences between the relative variables were small, but still underestimated values, indicating that measurement error

during manually posturing effected results. Finally, a strong relationship was predicted between direct motion capture data estimated kinematics and kinetics to the lab-based RLM outputs; however, only the shoulder joint angles estimated by Jack had a strong correlation ($r > 0.7$), refuting hypothesis two. Again, the lack of association found between the variables can be explained by the variability observed in the outputs estimated by the motion capture data importing approach.

Based on the resultant data, it is clear that there are inherent features associated with DHM posturing approaches that limits their ability to simulate a patient handling task that would replicate a lab-based biomechanical investigation. Moreover, there are biomechanical modelling differences between DHMs and the lab-based RLM used in this study that effect the ability to directly compare the results of DHMs to those generated using a lab-based approach when estimating kinematic and kinetic joint outcome measures. Differences identified between the simulated data across the three posturing approaches as well as the implication of these differences towards the investigation of MSD hazard exposures in patient handling are further explained by posture approach, below.

5.2 Manual Joint Manipulation

Manual joint manipulation is a common approach used to digitally simulate postures in DHM environments, therefore it remains important to compare modeled joint kinematic and kinetic outputs to a lab-based modeling approach. When manually posturing in Jack, the kinematic and kinetic outputs estimated agreed with the lab-based model, while outputs estimated using Santos did not agree. Manually manipulating the avatar in Jack to simulate automotive assembly tasks have also shown good accuracy in kinematic and kinetic joint measures (Kajaks, Stephens, & Potvin, 2011). Data from this study demonstrated that Jack also

has the ability to simulate realistic postures adopted by HCPs during patient repositioning tasks when using its manual joint manipulation approach. Although, this is likely also dependent on the skill and practice of the user performing the manual joint manipulation.

Generally, in the field of biomechanics, there is no acceptable measurement error value for kinematic and kinetic joint measures. However, researchers in gait biomechanics have used $\pm 5^\circ$ in joint angles as an acceptable measure of error in results (Hassan, Jenkyn, & Dunning, 2007; McGinley, Baker, Wolfe, & Morris, 2009) and $\pm 10\text{Nm}$ has been previously used in the literature to evaluate the validity of low back moments estimated using a 3D RLM (Plamondon, Gagnon, & Desjardins, 1996). While both these acceptable limits are not directly related to the context of this investigation, they still provide a comparative value to interpret the errors produced in the biomechanical measures.

Users can expect to see a difference of at least $\pm 11.32^\circ$ and $\pm 14.50^\circ$ in trunk and shoulder joint angles respectively when using Jack to estimate angles, relative to a lab-based approach. In the context of occupational biomechanics, this magnitude of error in kinematic outputs (regardless of being outside the recommended range of error) would likely not influence to the interpretation of data when investigating MSD exposures. However, investigators should still use their own judgment and experience when evaluating the kinematic outputs from Jack. In turn, it is expected that Jack's manual posturing approach will produce an error of at least $\pm 9.37\text{Nm}$ in L4-L5 joint moments when simulating a patient handling task. This evidence further provides preliminary evidence to support the ability of Jack's manual posturing approach to estimate valid biomechanical demands used to investigate the exposures to MSD hazards in patient handling tasks.

Outputs estimated by Santos when manually posturing the avatar were not in agreement with the lab-based model. Only the shoulder angles estimated by Santos showed agreement and contained a small error of measurement ($\pm 4.55^\circ$). The lack of agreement observed between Santos and the lab-based model outputs when manually posturing the avatar may be attributed to the structure of its rigid linked segmental model. Santos' trunk is modeled using a multi-segmental approach to represent the vertebrae of the spine (Figure 3), while the trunk of the lab-based RLM and Jack were modeled as one rigid segment. These two different trunk modeling approaches have had varying effects on trunk kinematics and kinetics. Differences in trunk flexion/extension angles has been observed between the use of a single-segmental model of the trunk and the multi-segmental model (Kudo, Fujimoto, Sato, & Nagano, 2018). Differences observed between the trunk angles estimated using Santos relative the lab-based RLM may be explained by its spine structure during manual joint manipulation, as well as the posture prediction and motion capture approach.

In addition to trunk kinematic differences, differences in modeling approaches may have also manifest in trunk kinetics. Variability in anthropometric parameters (i.e. trunk segment length, joint center of rotation) calculated for the trunk segment has been found between the use of single-segmental and the multi-segmental trunk models. These differences can change the moment arms estimated from the L4-L5 joint COR to the hand load depending on the structure of the spine model resulting in differences in low back moments calculated (Desjardins, Plamondon, & Gagnon, 1998; Rao, Amarantini, Berton, & Favier, 2006; Riemer & Hsiao-Weckler, 2008). Therefore, differences in the trunk segment models between Santos and the lab-based model may well explain the differences in L4-L5 joint moments.

Furthermore, with Santos' multi-segmental spine model, a higher degree of freedom in spine motion was provided. This could also have attributed to differences observed in trunk angles and L4-L5 moments. With Santos' multi-segmental spine model, users are able to manipulate 17 single vertebral joints to simulate the posture adopted by the HCP during the patient handling task. Jack's spine was manipulated at a single joint (trunk over pelvis joint). Due to the higher degree of freedom, lower back and upper back curvature was better modeled in Santos, perhaps even better than the lab-based RLM approach. Vertebrae were individually positioned within the sagittal plane to best adjust the posture of the back to replicate the static image of the HCP. Due to this, trunk angles may have been underestimated (as more motion is taken up through other spine segments) and in turn, underestimated L4-L5 joint moments since the moment arm produced from the L4-L5 joint COR to the hand load is smaller to lower joint angles.

Finally, based on the magnitude of the trunk flexion/extension angles estimated by Santos, it is believed that the DHM may have been calculating and outputting intervertebral flexion/extension joint angles (angle produced between the L4 vertebrae and L5 vertebrae) rather than the trunk flexion/extension angles (trunk segment relative to the pelvis segment). Trunk angles estimated by Santos across all 25 individual manual simulations were under 10°. Studies evaluating the motions of intact human lumbar spines have reported that the total flexion/extension ROM between the L4 and L5 vertebral segments is approximately 12° (Cook, Yeager, & Cheng, 2015; Yamamoto, Panjabi, & Oxland, 1989). Prior to the use of Santos in this investigation and based on the commercially available documentation, it was assumed that Santos' kinematic model would output trunk flexion/extension angles; however, the resultant

data suggests that Santos may indeed be estimating intervertebral joint angles instead. This could also explain why trunk angles were underestimated by Santos.

5.3 Posture Prediction

Regardless of the posture prediction model (optimization-based in Santos, statistical-based in Jack), the DHM modeled low back and shoulder demands associated with a patient repositioning task were not in agreement with those estimated using a lab-based biomechanical modeling approach. While the goal of posture prediction is to provide users with a proactive method to simulate realistic human postures for any given task or design constraints (Abdel-Malek & Arora, 2013; Chaffin, 2005; Faraway & Reed, 2007), data from this investigation suggest that both Jack and Santos posture prediction models may still require improvement to robustly simulate postures adopted by HCPs. The lack of agreement observed in output measures can be explained by the underlying mathematical models used to drive the predicted set of joint angles and joint moments.

Jack's posture prediction model is driven by pre-recorded motion data and anthropometrics gathered from subjects performing manual automotive related tasks (Duffy, 2008; Faraway & Reed, 2007). As a result, it was not surprising to find that Jack was unable to predict realistic postures for a health care related task. However, it is interesting to note that the predicted shoulder angles contained a high bias (-47.65) relative to the other outputs. The human behaviour control framework integrated into Jack's existing empirical model could explain this (Faraway & Reed, 2007). To accurately produce postures for a complex task, an ergonomic control framework was developed based on hierarchical set of posture and motion modules that controlled human behavior (low back and shoulder biomechanical demands, upper and lower extremity inverse kinematics and torso motion) (Reed, Faraway, Chaffin, & Martin, 2006).

Based on this framework, it is believed that the model was attempting to predict postures that would minimize the demands at the low back. When the Jack avatar was reaching for the sheet to exert a force to move the patient, the distal end of the upper extremity kinematic chain moved first (hand, forearm, upper arm) followed by the torso, as necessary to complete the task. This likely caused increased variation in the shoulder angles, and an underestimation of trunk angles and L4-L5 moments. Interestingly, this pattern in limb trajectories used for the patient reposition task were similar to the trajectories described when predicting the seated reach in an automobile (Reed et al., 2006), where displacement of the low back was kept to a minimum. This further provides evidence to suggest that Jack has a tendency towards adopting postures used in automotive related tasks even when provided constraints to simulate a healthcare related task.

Santos uses an optimization methodology to predict postures. The optimization algorithm is dependent on how the user prioritizes competing objectives related to human performance measures (i.e., joint torque, discomfort, joint displacement) (Marler et al., 2009). For this investigation, it was assumed that HCPs attempted to optimize their postures to minimize joint stresses experienced when repositioning the patient. Ergonomic guidelines for safe patient handling suggest that HCPs should use safe postural strategies to minimize stresses to the musculoskeletal system (Nelson & Baptiste, 2004; OSHA, 2009). As a result, the weighting factors (based on percentage) of the objective functions were adjusted to prioritize the minimization of performance measures (e.g., 100% priority to minimizing joint torque, 100% to minimizing discomfort). L4-L5 and shoulder joint moments computed based on the predicted postures were lower than the lab-based RLM, demonstrating that the set objective functions did indeed minimize the joint torque. Similar to Lämkkull, Hanson, & Örtengren, (2008) findings, it is believed that the posture prediction approach was not used in its optimal manner. However, these

data do suggest that in order to predict the physical and biomechanical demands imposed on HCPs during a patient handling task, prioritization of performance measures need to be re-evaluated.

Unlike automotive or manual material handling tasks patient handling tasks do not always have the optimal conditions to use postural strategies that would minimize joint loading. This is primarily due to physically handling of humans versus industrial materials. As a result, joint torque may not be a factor that should be minimized when predicting postures for patient handling tasks. The postures adopted by HCPs during patient handling tasks need to be observed and analyzed in reality to determine appropriate objective weightings. When testing the fidelity of Santos' posture prediction model on a seated reach task, Marler & colleagues (2007) first determined the appropriate weights to assign to each performance measure by analyzing the postural strategies used by individuals via motion capture data collected during a seated reach task. While it was a fairly simple task, this approach did show similar joint angles produced to the motion capture study. The data from this study reinforce the importance of careful consideration when assigning weight factors in the optimization model in order to adequately generate realistic data. Analyzing the trends in kinematic and kinetic data of HCPs performing a patient handling tasks could be an option at determining the weight functions.

5.4 Direct Motion Capture Data Importing

While importing motion capture data into DHMs is not a common approach used to simulate postures, it was still included into this investigation to help uncover underlying differences between DHM and lab-based developed RLMs. Both Jack and Santos were unable to reproduce the postures of HCPs when mapping motion capture position data gathered from the lab investigation onto the avatar. Because the joint angles varied relative to the lab-based model,

the moment arms estimated from the shoulder and L4-L5 joint to the hand load likely also changed the joint moments calculated by the DHM models. The lack of agreement observed between the kinematic and kinetic outcome measures from both software is likely dependent on the differences in the kinematic linkage structures/joint decompositions of the DHM models and little to do with patient handling task simulated.

Shoulder joint angles estimated by both Jack and Santos were overestimated relative to the lab-based model. These results may be specific to differences in skeletal linkage models of the shoulder. In the lab-based RLM the center of joint rotation for the shoulder was identified at the glenohumeral joint and its axis of rotation were created based on the ISB standards. Jack and Santos' RLM model do not use the glenohumeral joint as the shoulder joint center, nor are their local joint coordinate systems created using ISB standard. Anatomically, the acromio-clavicular joint center (Robinette et al., 1991) was used as the shoulder joint and a robotics method (Denavit-Hartenberg) was used to create the local joint coordinate systems in both Jack and Santos (Badler, Phillips, & Webber, 1999b; Yang, Kim, et al., 2007). Due to these differences, there may have been errors produced when mapping the shoulder position data from the lab-based model onto the shoulder joint of the avatar. These difference in shoulder angles, may also be reflected in shoulder joint moments estimated by Jack and Santos, as the moment arm between the shoulder joint COR to the hand load likely changed, impacting the calculated joint moments.

When, comparing the low back joint kinematic and kinetic outputs from the DHM software a different trend in results was observed relative to the shoulder outputs. The trunk angles, computed by both Jack and Santos did not agree with the lab-based model angles; however, the L4-L5 joint moments estimated by Jack did show agreement with moments

estimated using the lab-based model. Since joint kinematics have a direct effect on joint kinetics, it is unusual to see that the differences produced in the trunk angles were not reflected in the joint moments. Similarities in the spine model structure between the lab-based RLM and Jack spine model discussed earlier could possibly explain similar L4-L5 joint moments estimated between Jack and the lab-based model. Again, differences between the conventions used to create local joint coordinate systems (ISB vs robotics) between the lab based and DHM RLM low back segment/joint may have also attributed to the errors produced in trunk angles and L4-L5 moments estimated using the motion capture data importing approach.

In addition to skeletal linkage model and/or joint angle decomposition differences, anthropometric differences were also found to have an impact on the kinematic and kinetic outputs estimated. When mapping the joint position data from lab-based RLM onto the avatar, visually, it was revealed that there were possible differences in skeletal linkage lengths between the lab-based model and DHM (Figure 35). This highlights how the use of anthropometric data bases in DHM software to derive skeletal linkage lengths of avatars (Raschke, Schutte, & Chaffin, 2000; Cheng et al., 1994) can produce varying anthropometric measures that may not exactly replicate the segment properties of modeled individuals.

Comparing the motion capture data driven postural data to lab based modelled postural data allowed for the investigation of potential sources of error within the DHM tools. Specifically, it allowed for the evaluation of the sensitivity of digitally modeled kinematics to differences in skeletal linkage models and joint angle decompositions. The analysis revealed that the differences in joint centers of rotations identified, local joint coordinate systems as well as anthropometrics (linkage length) used in digital human models influenced the resultant postural data simulated. Generally, these underlying differences found between commercial digital human

models versus a lab-based data constructed rigid link model highlights the potential limitations in using a digital model to investigate MSDs. Users should be aware of how these model differences could potentially influence the interpretation of their kinematic and kinetic outputs.



Figure 35. Joint position data from the lab-based model mapped onto anthropometrically scaled avatars in Jack (left) and Santos (right). In Santos, the green circles show the avatar joint centers of rotation and the red circles are the joint centers of rotation of the lab-based skeletal model, red lines show the mapping errors

5.5 Summary of Factors Associated with Digital Models that Resulted in Differences Between Lab-based and DHM Biomechanical Outputs

The results from this investigation demonstrated greater variability between the DHM and lab-based model estimated joint kinematic and kinetic measures than expected, across all posturing approaches. These unexpected differences are likely a result of several model related factors. The following section discusses specific model factors found within Jack and Santos that influenced their computed biomechanical outputs.

5.5.1 Skeletal Linkage Model

The kinetics of the digital spine in Jack and the lab-based RLM was modeled using a single rigid segment of the trunk while Santos' spine was modeled using a multi-rigid segment approach (kinematically and kinetically). A single segment modeling approach is typically used by researchers in the field of biomechanics to model and estimate the low back moments acting about the L4-L5 or L5-S1 joint (Marras, Davis, Kirking, & Granata, 1999; McGill & Norman, 1986; Reeves & Cholewicki, 2003), as it is a simplified approach. In turn, a multi-segmental spine allows for the user and the software to model the angular displacement of the lumbar and thoracic regions of the vertebrae. This can act as both a benefit and limitation to this particular study. Since HCPs adopt complex postures during patient handling tasks, using Santos allowed the user to better replicate the posture assumed through the upper and lower back when manually posturing the avatar. In retrospect, this did seem to better simulate the posture visually, but it impacted the quantitative biomechanical measures calculated from the model (trunk angles and L4-L5 moments).

Additionally, due to the multi-segmental spine model in Santos, the software computed trunk angles between vertebral segments, whereas the lab-based model and Jack computed trunk flexion/extension angles formed between the rigid trunk and pelvis segments. Furthermore, with a multi-segmental spine, comes increased degrees of freedom (DOF). As a result, when using the posture prediction approach in Santos, it is believed that the model utilized the increased DOF of the spine to assume a spine posture that would minimize the L4-L5 joint moments. Evidence from this study demonstrated how the use of the multi-segmented spine models in DHM can introduce differences when digitally modeling a patient handling task.

Based on the visual analysis of the upper body skeletal linkage models in Jack and Santos, it can be seen that a simple structure of the shoulder complex has been adapted. Both skeletal linkage models' shoulder joint position has been identified by model developers at the acromio-clavicular joint (scapula relative to clavicle) (Badler et al., 1999b; Robinette et al., 1991; Yang, Kim, et al., 2007). However, since there is no digital structure of the scapula in Jack and Santos, the rotation of the joint was modeled between the upper arm link and trunk segment. The shoulder joint center of rotation (COR) in the laboratory based RLM was defined at the glenohumeral joint (GH), which has been clinically identified as the axis where shoulder flexion/extension motion (humerus relative to the thorax) occurs. Anatomically, the position of acromio-clavicular joint is above the GH joint in the shoulder complex (this was evidently depicted in the motion capture data mapping in Figure 35). Therefore, it is likely that different moment arms were computed between the shoulder joint COR and the hand load between the DHM and lab-based model, resulting in difference in the shoulder joint moments calculated within each simulated posture of the HCP.

5.5.2 Kinematic Degrees of Freedom

In relation to the kinematic linkage model design, the differences in the DOF between the DHM and lab-based RLMs has been suspected as factor that resulted in differences as well. Increased DOF adds computational complexity to the kinematic model (Zhao & Badler, 1994). Mathematically, if a kinematic model has a high DOF, the rigid bodies have greater freedom to displace in space. However, when modeling human kinematics, this may introduce error in the predicted position and orientation of segments, as human joints are constrained by varying limits of degrees of motion (Zatsiorsky, 1998).

The lab-based RLM was developed with 34 DOF based on physiological parameters (i.e. no translation amongst segments); however, Jack (135DOF) and Santos (211DOF) included higher DOF in their kinematic linkage models (Abdel-Malek et al., 2007; Blanchonette, 2010). Differences produced as a result of increased DOF most likely influenced the postures simulated using the posture prediction approach in both Jack and Santos. Since the models are given fewer inputs (relative to manual manipulation and direct motion data importing), relying on the algorithm and kinematic linkage chain, the avatar likely utilized the full body DOF available to predict the postures in order to meet the objective of the task (turning a patient). While this increases the number of feasible simulations predicted by the software, it also increases the number of differences in joint angle outputs relative to the lab-based RLM.

However, when considering the limitations of previous studies that have used DHM to simulate patient handling tasks (Paul & Quintero-Duran, 2015; Potvin, 2017), having an increased DOF may be a benefit, as the avatar has the ability to predict several different postures depending on the constraints applied to the task. Broadly, this demonstrates the ability of the posture prediction approach to simulate the variability in movement strategies used by HCPs during patient handling tasks.

5.5.3 Joint Decomposition

Differences in the standards used to define local joint axis of joint may have also influenced the shoulder and trunk angles and L4-L5 moments estimated by the DHM software. The lab-based RLM was developed using the International Society of Biomechanics (ISB) standards for joint coordinate systems (Wu et al., 2002, 2005). When using this convention, each joint (i.e., elbow, knee, shoulder, L4-L5) has a different set of joint rotations defined to ensure that clinically meaningful joint angles and moments can be computed. In turn, the local joint

axes of rotation in Jack and Santos were developed using the Denavit-Hartenberg parameters (Badler et al., 1999b; Yang, Kim, et al., 2007). This convention is commonly used in the field of robotics to create reference frames for kinematic chains. The coordinate frames are attached to the joints between two links such that one transformation is associated with the joint and the second is associated with the link (Hartenberg & Denavit, 1955). The joints are modeled as either a hinged or sliding joint, whereas the ISB conventions were created based on the clinical joint type (i.e. GH joint modeled as ball and socket).

Since the Denavit-Hartenberg convention is based on mechanical properties rather than orthopedic properties of joints, it gives reason to believe that the shoulder and trunk angles and L4-L5 moments estimated by the DHM software may have error. Due to these differences, Jack and Santos may have also suffered from producing clinically meaningful joint angles and moments about the flexor/extensor axis. This could explain why a higher difference between joint angles and moments was observed at greater values between the DHM software and lab-based RLM. Consequently, when modeling HCPs who use postures with a greater range of motion (large shoulder or trunk flexion angle) may tend to underestimate these joint angles consequently impacting the fidelity of joint moments calculated as well.

5.5.4 Anthropometrics

The anthropometric databases in Jack and Santos (ANSUR, NHANES, GEBOD) used to scale the segment lengths of the virtual avatar may also have been a factor that resulted in differences. Kouchi & Mochimaru, (2004) found that the errors produced in anthropometric measures of avatars in DHM tools is dependent on the database and individual characteristic (race and body form, etc.). The lab-based RLM used the position data gathered from the anatomical landmarks and height of the subject to construct rigid body segments. In turn,

existing anthropometric measures (i.e. stature, hip height) directly measured from civilians or from 3D body scans are used to calculate the proportional length of rigid body segments of avatars based on the stature inputted into the software (Blanchonette, 2010; Duffy, 2008).

The potential influence of differences in anthropometric measures between the lab-based RLM and DHM RLMs was revealed when using the motion capture data importing approach to simulate the patient handling task. It was clear the link lengths estimated by both Jack and Santos were different from the lab-base model. Errors in link lengths may have influenced the joint angles produced by the DHM software, but likely had a greater influence on the joint moments estimated across each simulation, as the moment arms estimated from the shoulder and L4-L5 joint CORs to the hand load would differ as well. When considering anthropometric scaling, aside from other factors outlined, it is predicted to have the least influence on simulation results.

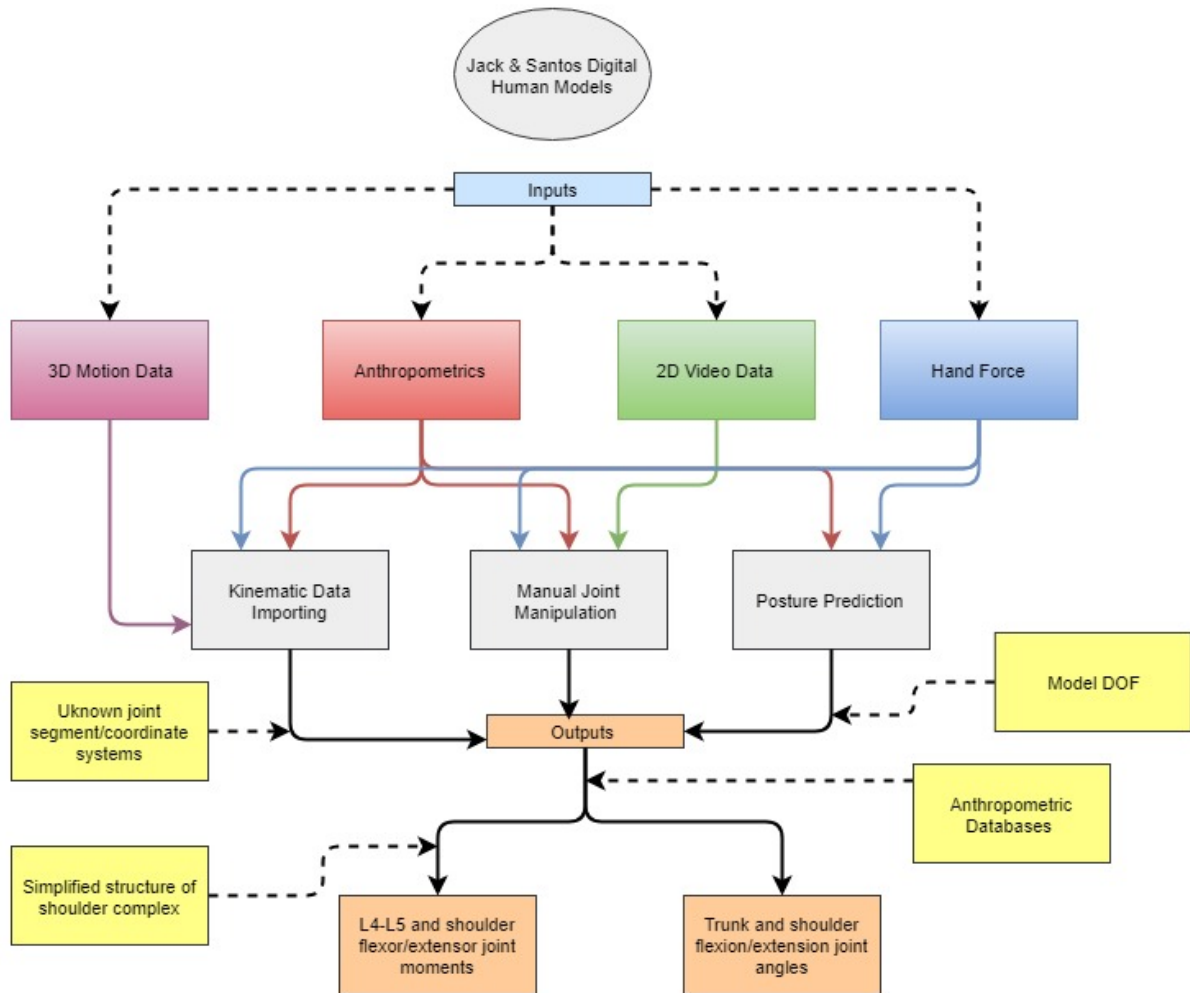


Figure 36. A summary of factors associated with digital models that resulted in differences between lab-based and DHM biomechanical outputs. Each model-related factor influenced the kinematic and kinetic outputs across the posturing approaches; however, this flow chart illustrates where each influencing factor was revealed in this investigation.

5.6 Use of DHM Kinematic and Kinetic Outputs for the Investigation of MSD Hazards

To investigate MSD hazard exposures in patient repositioning tasks, ergonomist and researchers need to have DHM tools that are able to accurately model and predict the biomechanical demands imposed on HCPs during patient repositioning tasks. Therefore, in this investigation, it was important to evaluate the practical applications of DHM estimated outcomes by comparing results directly to those obtained in a lab-based investigation. Lab-based modeled

joint angles and forces generated using 3D kinematics gathered from a motion capture system have been often used as the reference or “gold standard” measure in validation studies (Beravs, Reberšek, Novak, Podobnik, & Munih, 2011; Papi, Osei-Kuffour, Chen, & McGregor, 2015; Sutherland, Albert, Wrigley, & Callaghan, 2008). This is because measurements gathered directly from the human and are considered accurate.

Considering the differences found and measurement errors produced from each posturing approach, Jack’s manual posturing approach can be used as a descriptive tool to evaluate MSD hazards associated with patient repositioning tasks. The exposure to high risk external load moments to the low back is estimated at 74Nm (Marras et al., 1993; Marras et al., 1995). As a result, when practitioners are using Jack outputs from manual simulations to evaluate the biomechanical demands at the low back, a difference of ± 10 Nm would not likely impact the interpretation of L4-L5 joint moments when comparing the value to the low back moment injury threshold (74Nm). However, this investigation only calculated and compared the external moment produced about the flexion/extension axis at the low back. The impact of lateral/bending moments at the low back is also a measure to consider when assessing patient repositioning tasks, as these moments have been found to increase the biomechanical demands of the lumbar spine as well (Marras & Granata, 1997)

Postural data extracted from Jack’s manual simulations of a patient reposition can also be used as a measure to screen for exposures to MSD hazards. Practitioners can expect to see a difference of at least $\pm 11^\circ$ in sagittal plane trunk angles when modeling a patient reposition task. Exposure to trunk flexion angle greater than 45° (Punnett, Fine, Keyserling, Herrin, & Chaffin, 1991) and lumbar extension angle greater than 30° (Patel & Kinsella, 2017) have been classified as severe and associated with low back pain and disorders. While the majority HCPs observed in

the study produced trunk extension angles, a difference of $\pm 11^\circ$ in trunk flexion/extension angles produced by Jack would likely not impact the interpretation of exposure to the low back relative to the injury thresholds.

The shoulder flexion angle can be used by practitioners as a measure to determine the physical demands imposed at the shoulder during the performance of a patient reposition task. The 25th percentile female shoulder flexor strength moment is approximately 41Nm (Chaffin, Andersson, & Martin, 1991), where 25th percentile female strength is commonly used for ergonomic design guidelines. Both the shoulder flexion angle and load handled affect the moment strength produced by the shoulder. Considering the load handled in each hand by the HCP in this investigation (102N), the 25th percentile female HCP could produce the required shoulder flexion strength moment from $0^\circ - 25^\circ$ shoulder flexion angle to safely support the patient load (Chaffin, Andersson, & Martin, 1991). Jack's manual simulation produced a minimum difference of 15° in shoulder flexion angles when simulating HCPs perform a patient reposition task. Relative to the safe shoulder flexion angle ROM ($0^\circ - 25^\circ$) that can produce the required shoulder flexion strength, a difference of 15° may impact the interpretation of shoulder related MSD exposures during the ergonomic screening of a patient reposition task. In addition, it is important to highlight that the shoulder abduction/adduction and external/internal rotation at the shoulder was not explored in this investigation. Angles formed in these planes of motion at the shoulder can impact the physical loads imposed at the shoulder complex as well (Aarås, Westgaard, & Stranden, 1988; Punnett, Fine, Monroe Keyserling, Herrin, & Chaffin, 2000; Takagi et al., 2014). Practitioners should consider the shoulder movements produced by the HCP not only in the sagittal plane, but also the frontal and transverse plane when assessing the MSD exposures at the shoulder.

Compared to the posture prediction and motion capture driven approaches, the manual posturing approach in Jack could be utilized by practitioners to extract kinematic and kinetic data to help describe the exposures to MSD hazards during a patient repositioning task. Specifically, ergonomists and researchers could use Jack to manually simulate and evaluate several postures used by HCPs in their current practice when repositioning a patient. Information from the simulations can provide end-users with data on the postural and biomechanical demands imposed on HCPs that can be used to inform re-design of equipment or revised training programs for HCPs. Overall, increased user control provided when simulating the posture manually in Jack and the kinematic linkage structure of the avatar likely were factors that allowed the simulation of realistic joint kinematics and kinetics.

Although Jack and Santos' posture prediction approaches were not able to provide similar kinematic and kinetic outputs to the lab-based model outputs in this investigation, it still may be a potentially helpful approach for the proactive investigation of patient reposition tasks. In particular, Santos' optimization-based posture prediction approach has the capabilities of predicting how a HCP should safely perform a patient reposition. Practitioners could utilize this approach to determine the optimal task configurations (i.e. bed height, sheet position, hand position) that would minimize joint loading on the HCP during a patient turn. This predicted data could not only help re-design equipment and task parameters, it could also aide in the development of safe patient repositioning strategies that could reduce the exposure to MSD hazards. As well, with the simplicity of the approach, practitioners could determine the biomechanical demands imposed on HCPs from a distribution of population anthropometrics handling several different patient loads. This data could be used to determine load limits for safe handling.

Practitioners should use caution when interpreting low back kinematic data produced by DHMs. Considering the evidence found in this investigation, both Jack and Santos software packages calculate different low back angles due to their spine model structures. Where Jack calculates the trunk flexion/extension angle (trunk relative to the pelvis) and Santos calculates the intervertebral flexion/extension angle (L4 vertebrae relative to the L5 vertebrae). This model related factor highlights the importance of understanding the implications of DHM tools and their impact on outcome measures, particularly when comparing those measures to outcomes generated using a lab-based RLM for the investigation of MSD hazards.

6.0 Limitations

Despite the efforts made to control external factors and experimental conditions, limitations associated with the lab-based investigation may have had implications on the accuracy of the DHM simulations. During the collection of video data, only the sagittal, right upper body image and left lower body image of the HCP was captured during the performance of the patient reposition task. Consequently, this had implications towards the accuracy of simulations completed using the manual joint manipulation approach in Jack and Santos. This may have affected the low back kinematic and kinetic outputs estimated from manual joint manipulation approach. Additionally, segment positions about the transverse and frontal planes were not evaluated across the three DHM posturing approaches, consequently limiting the interpretation of data for MSD hazard investigations. Only the sagittal plane angles and joint moments produced at the low back and shoulder were evaluated in this investigation. Movements produced by the HCP during the patient reposition task varied about the three planes, which can impact the overall conclusion of severity of the MSD exposure.

The aim this thesis was to compare the kinematic and kinetic outputs estimated between DHMs and lab-based developed RLM. While lab-based models are commonly used as the criterion measure in many biomechanical investigations, the use of a lab-based RLM in this comparative study limited the extent to which practical comparisons could be made. Specifically, the structural and computational differences between DHMs and the lab-based RLM made it challenging to practically compare kinematic and kinetic outputs. For example, Jack and Santos DHMs were both developed based on robotics principles, included over a 100 DOF and used anthropometric databases to estimate link length. In turn, the lab-based constructed model was developed using biomechanical principles, included less than 50 DOF and used directly

measured data from human participants to calculate segment link lengths. Consequently, these significant model differences produced high variability in the dependent measures assessed, thus limiting the extent to which model-for-model comparisons could be made. As well, since both DHMs were pre-designed software packages, there was very limited ability provided to adjust the structural models of the avatars or computational approaches to match the lab-based model in order to make direct comparisons.

Furthermore, all three posturing approaches evaluated in this investigation provided different kinematics and kinetic results relative to the lab-based RLM. The manual posturing approach simulated the posture used by the HCP during lab-based investigation, which provided comparable results to the lab-based model. However, the posture prediction approach in both DHMs were predicting the postural strategies that would be used by a HCP, rather than modeling the posture used by the HCP during the lab-based investigation. This resulted in two differing data sets; where the lab-based model produced the real-life kinematics and kinetics of HCPs and the posture prediction approach produced the kinematics and kinetics associated with the optimal postural strategy that HCPs would use to perform the task. In retrospect, these data are therefore not the same and difficult to compare; however, it does highlight the unique differences between the uses of manual posturing and posture prediction approaches for different phases of HF&E investigations.

When using the correlation plots to compare the DHM and lab-based RLM outputs, there were several factors that may have skewed the interpretation of correlation coefficients. There were consistent extreme values that appeared in the correlation plots that may have affected the strength of the overall relationships. These consistent extreme joint angle or moment values may have been a result of characteristics of individual HCPs used in the study sample. In addition,

when comparing the relationship between outputs produced by both the posture prediction and motion capture approaches to the lab-based model, variability in the data sets may have attributed to the decreased size in the correlation coefficients estimated. Specifically, a skewed distribution in the posture predicted and motion capture driven DHM outputs likely affected the correlations.

Finally, this study only evaluated the static posture of a patient turn activity. This may hinder the extent to which the data can be generalized to other patient handling tasks. For example, the results may not reflect what would be seen in simulated data from lifting a patient. However, this investigation is the first to compare biomechanical measures estimated using DHM software packages to a lab-based modelled outputs specific to a patient repositioning task. Results from this study do provide preliminary evidence towards the validation of DHM tools as well as the independent factors associated with DHM modeling approaches that could impact the fidelity of biomechanical output measures commonly used to evaluate the presence or severity of MSD exposures.

6.1 Implications of Future Research

Through this comparative study, factors associated with the DHM software packages that could affect the fidelity of biomechanical measures were identified. An attempt was made at identifying the independent effect of each factor; however, due to the design of the experiment, it was not possible to quantify the effect of each model parameter on related difference in outcome measures. Further studies are required to investigate the magnitude of the effect of individual characteristics of digital models. Specifically, a detailed sensitivity analysis should be conducted to determine the effect of independent characteristics of DHM models on biomechanical measures.

Future studies should explore the effectiveness of DHM tools for both the reactive (descriptive) and proactive (prescriptive) investigation of MSD hazards for various patient handling tasks. As well, in addition to sagittal plane segment positioning, future studies should also consider modeling the frontal and transverse plane positions of limbs of HCPs during a patient reposition task. This would aide in estimating angles and moments about the low back and shoulder that are inclusive of the lateral bend, external/internal rotation and abduction/adduction limb motions used by HCPs. Further DHM investigations should also explore the use of directly measured segment lengths from live human participants that are being virtually simulated and input them into DHMs to scale the avatars. This could potentially minimize the errors produced in joint angles and moments as a result of anthropometric differences reported in this investigation.

7.0 Conclusions

The aim of this thesis was to compare the kinematic and kinetic measures produced using two commercial DHM software packages' manual joint manipulation, direct motion capture importing and posture prediction approaches against a lab-based rigid linked segmental model when modelling a patient repositioning task. Using Siemens Jack's (V 8.4) manual joint manipulation approach to simulate a patient turn task produced low back and shoulder joint kinematics and kinetics that agreed well with the lab-based rigid segment linked model outputs. Kinematics and kinetics estimated using the posture prediction and direct motion capture data importing approaches using Siemens Jack (V 8.4) and Santos Pro did not agree with the lab-based model outputs. Variation in shoulder and low back kinematic and kinetic measures observed across the three posturing approaches highlights the numerous factors associated with DHM software packages that could influence modeled biomechanical outcomes. Specifically, premise of each posturing approach (manual posturing vs. posture prediction) can provide either descriptive outputs or predictive outputs of a simulated patient reposition task. Furthermore, differences in the kinematic modeling assumptions related to structure of the skeletal linkage model, joint decomposition, anthropometry, and computational algorithms can all influence the biomechanical measures computed using DHM tools. The use of Siemens Jack (V 8.4) and Santos Pro software packages for biomechanical evaluation of patient repositioning tasks has the possibility to aide with the investigation of MSD exposures. However, it is important for practitioners to choose the appropriate posturing approach (reactive vs. proactive), depending on the goal of the MSD hazards investigation. As well, it is important for investigators to understand and consider the influence of model-related factors outlined in this investigation that

could affect their decisions when interpreting digitally modeled data that is used to determine exposures to MSD hazards

References

- Aarås, A., Westgaard, R. H., & Strandén, E. (1988). Postural angles as an indicator of postural load and muscular injury in occupational work situations. *Ergonomics*.
<https://doi.org/10.1080/00140138808966731>
- Abdel-Malek, K., & Arora, J. (2013). *Human Motion Simulation: Predictive Dynamics*.
Waltham, USA: Academic Press.
- Abdel-malek, K., Arora, J., Law, L. F., Swan, C., Beck, S., Xia, T., ... Obusek, J. P. (2008). Santos: a digital human in the making. *International Conference on Applied Simulation and Modeling*.
- Abdel-Malek, K., Yang, J., Kim, J. H., Marler, T., Beck, S., Swan, C., ... Arora, J. (2007). Development of the Virtual-Human Santos. In *Digital Human Modeling* (Vol. LNCS 4561, pp. 490–499). https://doi.org/10.1007/978-3-540-73321-8_57
- Allen, B., Curless, B., & Popovic, Z. (2004). Exploring the space of human body shapes : data-driven synthesis under anthropometric control. *Digital Human Modeling for Design and Engineering Symposium*, (c), 1–4. <https://doi.org/doi:10.4271/2004-01-2188>
- Allen, B., Curless, B., & Popović, Z. (2002). Articulated body deformation from range scan data. *ACM Transactions on Graphics*, 21(3). <https://doi.org/10.1145/566654.566626>
- Badler, N. I., Phillips, C. B., & Webber, B. L. (1999a). *Simulating Humans: Computer Graphics, Animation, and Control*.
- Badler, N. I., Phillips, C. B., & Webber, B. L. (1999b). *Simulating Humans: Computer Graphics, Animation, and Control*, (June 1993), 283.

- Belbeck, A., Cudlip, A. C., & Dickerson, C. R. (2014). Assessing the interplay between the shoulders and low back during manual patient handling techniques in a nursing setting. *International Journal of Occupational Safety and Ergonomics*, 20(1), 127–137. <https://doi.org/10.1080/10803548.2014.11077026>
- Beravs, T., Reberšek, P., Novak, D., Podobnik, J., & Munih, M. (2011). Development and validation of a wearable inertial measurement system for use with lower limb exoskeletons. In *IEEE-RAS International Conference on Humanoid Robots* (pp. 212–217). <https://doi.org/10.1109/Humanoids.2011.6100914>
- Bergstrom, N., Horn, S. D., Rapp, M. P., Stern, A., Barrett, R., & Watkiss, M. (2013). Turning for ulcer Reduction: A Multisite randomized clinical trial in nursing homes. *Journal of the American Geriatrics Society*, 61(10), 1705–1713. <https://doi.org/10.1111/jgs.12440>
- Bjelle, A., Hagberg, M., & Michaelson, G. (1981). Occupational and individual factors in acute shoulder-neck disorders among industrial workers. *British Journal of Industrial Medicine*, 38(4), 356–363. <https://doi.org/10.1136/oem.38.4.356>
- Black, T. R., Shah, S. M., Busch, A. J., Metcalfe, J., & Lim, H. J. (2011). Effect of Transfer, Lifting, and Repositioning (TLR) Injury Prevention Program on Musculoskeletal Injury Among Direct Care Workers. *Journal of Occupational and Environmental Hygiene*, 8(4), 226–235. <https://doi.org/10.1080/15459624.2011.564110>
- Blanchonette, P. (2010). Jack Human Modelling Tool: A Review. *Defence Science And Technology*. Air Operations Division, DSTO. Retrieved from <http://www.dtic.mil/dtic/tr/fulltext/u2/a518132.pdf>
- Bland, J. M., & Altman, D. G. (1999). Measuring agreement in method comparison studies.

Statistical Methods in Medical Research, 8(2), 135–160.

<https://doi.org/10.1191/096228099673819272>

Caboor, D. E., Verlinden, M. O., Zinzen, E., Van Roy, P., Van Riel, M. P., & Clarys, J. P.

(2000). Implications of an adjustable bed height during standard nursing tasks on spinal motion, perceived exertion and muscular activity. *Ergonomics*, 43(10), 1771–1780.

<https://doi.org/10.1080/001401300750004177>

Cao, W., Jiang, M., Han, Y., & Khasawneh, M. T. (2013). Ergonomic assessment of patient

Barrow lifting technique using digital human modeling. In *Digital Human Modeling* (Vol. 8026 LNCS, pp. 20–29). https://doi.org/10.1007/978-3-642-39182-8_3

Case, K., Hussain, A., Marshall, R., Summerskill, S., & Gyi, D. (2015). Digital Human

Modelling and the Ageing Workforce. *Procedia Manufacturing*, 3, 3694–3701.

<https://doi.org/10.1016/j.promfg.2015.07.794>

Chaffin, D. B. (2005). Improving digital human modelling for proactive ergonomics in design.

Ergonomics, 48(5), 478–491. <https://doi.org/10.1080/00140130400029191>

Chaffin, D. B. (2008). Digital human modeling for workspace design. In *Reviews of Human*

Factors and Ergonomics (p. 200). <https://doi.org/10.1518/155723408X342844>.

Chaffin, D. B. (2008). Digital Human Modeling for Workspace Design. *Reviews of Human*

Factors and Ergonomics, 4(1), 41–74. <https://doi.org/10.1518/155723408X342844>

Chang, S. W., & Wang, M. J. J. (2007). Digital human modeling and workplace evaluation:

Using an automobile assembly task as an example. *Human Factors and Ergonomics In Manufacturing*, 17(5), 445–455. <https://doi.org/10.1002/hfm.20085>

- Cheng, H., Obergefell, L., & Rizer, A. (1994). Generator of Body (GEBOD) Manual. Systems Research Laboratories, Inc.
- Cook, D., Yeager, M., & Cheng, B. (2015). Range of Motion of the Intact Lumbar Segment: A Multivariate Study of 42 Lumbar Spines. *International Journal of Spine Surgery*.
<https://doi.org/10.14444/2005>
- Demirel, H. O., & Duffy, V. G. (2007). Application of digital human modeling in industry. *Digital Human Modeling*, 824–832. https://doi.org/10.1007/978-3-540-73321-8_93
- Desjardins, P., Plamondon, A., & Gagnon, M. (1998). Sensitivity analysis of segment models to estimate the net reaction moments at the L5/S1 joint in lifting. *Medical Engineering and Physics*. [https://doi.org/10.1016/S1350-4533\(97\)00036-2](https://doi.org/10.1016/S1350-4533(97)00036-2)
- Duffy, V. G. (2008). *Handbook of Digital Human Modeling: Research for Applied Ergonomics and Human Factors Engineering*. Boca Raton, USA: CRC Press.
- Endo, Y., Kanai, S., Kishinami, T., Miyata, N., Kouchi, M., & Mochimaru, M. (2007). Virtual grasping assessment using 3D digital hand model. *10th Annual Applied Ergonomics Conference: Celebrating the Past - Shaping the Future*. Retrieved from <papers2://publication/uuid/EDDAB479-51F2-4390-9A59-681B4A4040DF>
- Endo, Y., Kanai, S., Miyata, N., Kouchi, M., Mochimaru, M., Konno, J., ... Shimokawa, M. (2009). An optimization-based approach for grasp posture generation of digital hand. In *2008 ASME International Design Engineering Technical Conferences and Computers and Information in Engineering Conference, DETC 2008* (Vol. 3, pp. 877–885).
<https://doi.org/10.1115/DETC2008-49749>

Estrynebar, M., Kaminski, M., Peigne, E., Maillard, M. F., Pelletier, a, Berthier, C., ... Leroux, J. M. (1990). Strenuous Working-Conditions and Musculoskeletal Disorders among Female Hospital Workers. *International Archives of Occupational and Environmental Health*, 62(Insee 1988), 47–57.

Faraway, J., & Reed, M. P. (2007). Statistics for Digital Human Motion Modeling in Ergonomics. *Technometrics*, 49(3), 277–290. <https://doi.org/10.1198/004017007000000281>

Fischer, S. L., Albert, W. J., McClellan, A. J., & Callaghan, J. P. (2007). Methodological considerations for the calculation of cumulative compression exposure of the lumbar spine: A sensitivity analysis on joint model and time standardization approaches. *Ergonomics*. <https://doi.org/10.1080/00140130701344042>

Fragala, G. (2011). Facilitating Repositioning in Bed. *AAOHN Journal*, 59(2), 63–68. <https://doi.org/10.3928/08910162-20110117-01>

Fragala, G., & Bailey, L. P. (2003). Addressing occupational strains and sprains: musculoskeletal injuries in hospitals. *AAOHN Journal*, 51(6), 252–259. Retrieved from http://ovidsp.ovid.com/ovidweb.cgi?T=JS&CSC=Y&NEWS=N&PAGE=fulltext&D=med4&AN=12846458%5Cnhttp://sdb-web2.biblio.usherbrooke.ca/web2/tramp2.exe/do_keyword_search/guest&SETTING_KEY=french&servers=1home&index=ISSN&query=0891-0162%5Cnhttp://sfxhosted.exlibris

Freitag, S., Fincke-Junod, I., Seddouki, R., Dulon, M., Hermanns, I., Kersten, J. F., ... Nienhaus, A. (2012). Frequent bending - An underestimated burden in nursing professions. *Annals of Occupational Hygiene*, 56(6), 697–707. <https://doi.org/10.1093/annhyg/mes002>

Fritzsche, L. (2010). Ergonomics Risk Assessment with Digital Human Models in Car

- Assembly: Simulation versus Real Life Lars Fritzsche. *Human Factors and Ergonomics in Manufacturing*, 20, 287–299. <https://doi.org/10.1002/hfm>
- Gagnon, M., Chehade, A., Kemp, F., & Lortie, M. (1987). Lumbo-sacral loads and selected muscle activity while turning patients in bed. *Ergonomics*, 30(7), 1013–1032. <https://doi.org/10.1080/00140138708965992>
- Griffiths, H. (2012). Adverse risk: A “dynamic interaction model of patient moving and handling.” *Journal of Nursing Management*, 20(6), 713–736. <https://doi.org/10.1111/j.1365-2834.2011.01276.x>
- Hall, S., Longhurst, S., & Higginson, I. J. (2009). Challenges to conducting research with older people living in nursing homes. *BMC Geriatrics*, 9(38), 1–6. <https://doi.org/10.1186/1471-2318-9-38>
- Hanson, L., Hogberg, D., & Soderholm, M. (2012). Digital test assembly of truck parts with the IMMA-tool - An illustrative case. *Work*, 41, 2248–2252. <https://doi.org/10.3233/WOR-2012-0447-2248>
- Hartenberg, R. S., & Denavit, J. (1955). A kinematic notation for lower-pair mechanisms based on metrics. *Transactions of the ASME. Journal of Applied Mechanics*. <https://doi.org/citeulike-article-id:7153318>
- Hassan, E. A., Jenkyn, T. R., & Dunning, C. E. (2007). Direct comparison of kinematic data collected using an electromagnetic tracking system versus a digital optical system. *Journal of Biomechanics*. <https://doi.org/10.1016/j.jbiomech.2006.03.019>
- Hoozemans, M. J. M., Van Der Beek, A. J., Frings-Dresen, M. H. W., & Van Der Molen, H. F.

- (2001). Evaluation of methods to assess push/pull forces in a construction task. *Applied Ergonomics*, 32(5), 509–516. [https://doi.org/10.1016/S0003-6870\(01\)00021-7](https://doi.org/10.1016/S0003-6870(01)00021-7)
- Jäger, M., Jordan, C., Theilmeier, A., Wortmann, N., Kuhn, S., Nienhaus, A., & Luttmann, A. (2013). Lumbar-load analysis of manual patient-handling activities for biomechanical overload prevention among healthcare workers. *Annals of Occupational Hygiene*, 57(4), 528–544. <https://doi.org/10.1093/annhyg/mes088>
- Jimerson, B., Park, E., Jiang, S., & Stajsic, D. (2016). Digital Human Modeling of Caretakers Preparing Patients for Patient Transfer Devices. *International Advanced Research Journal in Science, Engineering and Technology*, 3(12), 98–103. <https://doi.org/10.17148/IARJSET.2016.31219>
- Kajaks, T., Stephens, A., & Potvin, J. R. (2011). The effect of manikin anthropometrics and posturing guidelines on proactive ergonomic assessments using digital human models. *International Journal of Human Factors Modelling and Simulation*. <https://doi.org/10.1504/IJHFMS.2011.044512>
- Karmakar, S., Pal, M. S., Majumdar, D., & Majumdar, D. (2012). Application of digital human modeling and simulation for vision analysis of pilots in a jet aircraft: A case study. *Work*, 41(SUPPL.1), 3412–3418. <https://doi.org/10.3233/WOR-2012-0617-3412>
- Kim, K. H., & Martin, B. J. (2006). The Role of Visual and Manual Demand in Movement and Posture Organization and Engineering Conference. *Engineering Conference*, (724). <https://doi.org/10.4271/2006-01-2331>
- Kouchi, M., & Mochimaru, M. (2004). A Validation Method for Digital Human Anthropometry : Towards the Standardization of Validation and Verification, (724), 1–6.

- Kudo, S., Fujimoto, M., Sato, T., & Nagano, A. (2018). Quantitative evaluation of linked rigid-body representations of the trunk. *Gait & Posture*, 63(January), 119–123.
<https://doi.org/10.1016/j.gaitpost.2018.04.046>
- Kuorinka, I., Jonsson, B., Kilbom, A., Vinterberg, H., Biering-Sørensen, F., Andersson, G., & Jørgensen, K. (1987). Standardised Nordic questionnaires for the analysis of musculoskeletal symptoms. *Applied Ergonomics*. [https://doi.org/10.1016/0003-6870\(87\)90010-X](https://doi.org/10.1016/0003-6870(87)90010-X)
- Lämkkull, D., Hanson, L., & Örtengren, R. (2008). Uniformity in mannikin posturing: a comparison between posture prediction and manual joint manipulation. *International Journal of Human Factors Modelling and Simulation*.
<https://doi.org/10.1504/IJHFMS.2008.022478>
- Lämkkull, D., Hanson, L., & Roland Örtengren. (2009). A comparative study of digital human modelling simulation results and their outcomes in reality: A case study within manual assembly of automobiles. *International Journal of Industrial Ergonomics*, 39(2), 428–441.
<https://doi.org/10.1016/j.ergon.2008.10.005>
- Latimer, S., Chaboyer, W., & Gillespie, B. M. (2015). The repositioning of hospitalized patients with reduced mobility: a prospective study. *Nursing Open*, 2(2), 85–93.
<https://doi.org/10.1002/nop2.20>
- Lindbeck, L., & Engkvist, I.-L. (1993). Biomechanical analysis of two patient handling tasks. *International Journal of Industrial Ergonomics*, 12(1–2), 117–125.
[https://doi.org/10.1016/0169-8141\(93\)90043-D](https://doi.org/10.1016/0169-8141(93)90043-D)
- Lowe, B., Weir, P., & Andrews, D. (2014). Observation-Based Posture Assessment. *DHHS*

(NIOSH) Publication, 32. Retrieved from <http://www.cdc.gov/niosh/docs/2014-131/pdfs/2014-131.pdf>

Marler, R. T., Arora, J. S., Yang, J., Kim, J., & Abdel-malek, K. (2009). Use of multi-objective optimization for digital human posture prediction. *Engineering Optimization*, 41(10), 925–943. <https://doi.org/10.1080/03052150902853013>

Marler, T., Yang, J., Rahmatalla, S., Abdel-malek, K., & Harrison, C. (2007). Validation Methodology Development for Predicted Posture. *Design*. <https://doi.org/10.4271/2007-01-2467>

Marras, W., & Karwowski, W. (2006). *Fundamental and assessment tools for occupational ergonomics*. CRC Press, Taylor & Francis. <https://doi.org/10.1201/9781420003635>

Marras, W. S., Davis, K. G., Kirking, B. C., & Bertsche, P. K. (1999). A comprehensive analysis of low-back disorder risk and spinal loading during the transferring and repositioning of patients using different techniques. *Ergonomics*, 42(7), 904–926. <https://doi.org/10.1080/001401399185207>

Marras, W. S., Davis, K. G., Kirking, B. C., & Granata, K. P. (1999). Spine loading and trunk kinematics during team lifting. *Ergonomics*, 42(10), 1258–1273. <https://doi.org/10.1080/001401399184938>

Marras, W. S., & Granata, K. P. (1997). Spine loading during trunk lateral bending motions. *Journal of Biomechanics*. [https://doi.org/10.1016/S0021-9290\(97\)00010-9](https://doi.org/10.1016/S0021-9290(97)00010-9)

Marras, W. S., Lavender, S. A., Leurgans, S. E., Fathallah, F. A., Ferguson, S. A., Allread, W. G., & Rajulu, S. L. (1995). Biomechanical risk factors for occupationally related low back

disorders. *Ergonomics*. <https://doi.org/10.1080/00140139508925111>

Marras, W. S., Lavender, S. a, Leurgans, S. E., Rajulu, S. L., Allread, W. G., Fathallah, F. a, & Ferguson, S. a. (1993). The role of dynamic three-dimensional trunk motion in occupationally-related low back disorders. The effects of workplace factors, trunk position, and trunk motion characteristics on risk of injury. *Spine*. <https://doi.org/10.1097/00007632-199304000-00015>

McDowell, M., Fryar, C., Ogden, C., & Flegal, K. (2008). Anthropometric reference data for children and adults: United States, 2003-2006. *National Health Statistics Reports*, (10), 2003–2006. Retrieved from <https://www.cdc.gov/nchs/data/nhsr/nhsr010.pdf>

McGill, S. M., & Norman, R. W. (1986). Partitioning of the L4-L5 Dynamic Moment into Disc, Ligamentous, and Muscular Components During Lifting. *Spine*, *11*(7), 666–678.

McGill, S. M., Norman, R. W., & Cholewicki, J. (1996). A simple polynomial that predicts low-back compression during complex 3-d tasks. *Ergonomics*, *39*(9), 1107–1118.
<https://doi.org/10.1080/00140139608964532>

McGinley, J. L., Baker, R., Wolfe, R., & Morris, M. E. (2009). The reliability of three-dimensional kinematic gait measurements: A systematic review. *Gait and Posture*.
<https://doi.org/10.1016/j.gaitpost.2008.09.003>

Monheit, G., & Badler, N. I. (1991). A kinematic model of the human spine and torso. *IEEE Computer Graphics and Applications*. <https://doi.org/10.1109/38.75588>

Naumann, A., & Roetting, M. (2007). Digital Human Modeling for Design and Evaluation of Human-Machine Systems. *MMI-Interaktiv*, (12), 27–35.

- Nelson, A., & Baptiste, A. S. (2004). Evidence-based practices for safe patient handling and movement. *Online Journal of Issues in Nursing*. <https://doi.org/10.1385/BMM:4:1:55>
- Nelson, A., Lloyd, J. D., Menzel, N., & Gross, C. (2003). Preventing nursing back injuries: redesigning patient handling tasks. *AAOHN*, *51*(3), 126–134.
- Nussbaum, M. a, & Zhang, X. (2000). Heuristics for locating upper extremity joint centres from a reduced set of surface markers. *Human Movement Science*, *19*(5), 797–816.
[https://doi.org/10.1016/S0167-9457\(00\)00020-8](https://doi.org/10.1016/S0167-9457(00)00020-8)
- OSHA. (2009). Ergonomics for the Prevention of Musculoskeletal Disorders. *U.S. Department of Labor*, *1*, 54. <https://doi.org/http://dx.doi.org/10.1016/B0-08-043076-7/03919-X>
- Papi, E., Osei-Kuffour, D., Chen, Y.-M. A., & McGregor, A. H. (2015). Use of wearable technology for performance assessment: a validation study. *Medical Engineering & Physics*, *37*(7), 698–704. <https://doi.org/10.1016/j.medengphy.2015.03.017>
- Patel, D. R., & Kinsella, E. (2017). Evaluation and management of lower back pain in young athletes. *Translational Pediatrics*. <https://doi.org/10.21037/tp.2017.06.01>
- Paul, G., & Quintero-Duran, M. (2015). Ergonomic assessment of hospital bed moving using DHM Siemens JACK. *Proceedings of the 19th Triennial Congress of the International Ergonomics Association*, 9–14. Retrieved from <http://eprints.qut.edu.au/86239/3/86239.pdf>
- Plamondon, A., Gagnon, M., & Desjardins, P. (1996). Validation of two 3D segment models to calculate the net reaction forces and moments at the L5/S1 joint in lifting. *Clinical Biomechanics*, *11*(2), 101–110.
- Pompeii, L. A., Lipscomb, H. J., Schoenfisch, A. L., & Dement, J. M. (2009). Musculoskeletal

- injuries resulting from patient handling tasks among hospital workers. *American Journal of Industrial Medicine*, 52(7), 571–578. <https://doi.org/10.1002/ajim.20704>
- Potvin, J. (2017). an Ergonomics Simulation Study of a Clinical Recliner, Chair, and Bed During Sit-To-Stand Patient Lifting. *International Journal of Safe Patient Handling & Mobility (SPHM)*, 7(2), 64–73. Retrieved from <http://search.ebscohost.com/login.aspx?direct=true&db=ccm&AN=124173991&lang=es&site=ehost-live&scope=site>
- Punnett, L., Fine, L. J., Keyserling, W. M., Herrin, G. D., & Chaffin, D. B. (1991). Back disorders and nonneutral trunk postures of automobile assembly worker. *Scandinavian Journal of Work, Environment and Health*, 17(5), 337–346. <https://doi.org/10.5271/sjweh.1700>
- Punnett, L., Fine, L. J., Monroe Keyserling, W., Herrin, G. D., & Chaffin, D. B. (2000). Shoulder disorders and postural stress in automobile assembly work. *Scandinavian Journal of Work, Environment and Health*, 26(4), 283–291. <https://doi.org/10.5271/sjweh.544>
- Quintero-Duran, M., & Gunther, P. (2016). Comparison of Two Different DHM Systems for the Ergonomic Assessment of a Physical Task. In *The 4th International Digital Human Modeling Symposium* (pp. 15–17).
- Raghunathan, R., & R, S. (2016). Review of Recent Developments in Ergonomic Design and Digital Human Models. *Industrial Engineering & Management*, 5(2), 1–7. <https://doi.org/10.4172/2169-0316.1000186>
- Rajput, V., Kalra, P., & Singh, J. (2013). Digital Human Modeling Approach in Ergonomic Evaluations. *International Journal of Science and Research*, 2(6), 156–158.

- Rao, G., Amarantini, D., Berton, E., & Favier, D. (2006). Influence of body segments' parameters estimation models on inverse dynamics solutions during gait. *Journal of Biomechanics*. <https://doi.org/10.1016/j.jbiomech.2005.04.014>
- Raschke, U., Martin, B. J., & Chaffin, D. B. (1996). Distributed moment histogram: a neurophysiology based method of agonist and antagonist trunk muscle activity prediction. *Journal of Biomechanics*, 29(12), 1587–1596.
- Raschke, U., Schutte, L. M., & Chaffin, D. B. (2000). Ergonomics in Digital Environments. In *Handbook of Industrial Engineering* (pp. 1111–1130). <https://doi.org/10.1002/9780470172339.ch41>
- Reed, M. P., Faraway, J., Chaffin, D. B., & Martin, B. J. (2006). The HUMOSIM Ergonomics Framework : A New Approach to Digital Human Simulation for Ergonomic Analysis. *Society of Automotive Engineers, Inc.*, 01-2365(724). <https://doi.org/10.4271/2006-01-2365>
- Reed, M. P., & Huang, S. (2008). Modeling Vehicle Ingress and Egress Using the Human Motion Simulation Framework. *Digital Human Modeling for Design and Engineering Symposium*, 1–12. <https://doi.org/10.4271/2008-01-1896>
- Reeves, N. P., & Cholewicki, J. (2003). Modeling the human lumbar spine for assessing spinal loads, stability, and risk of injury. *Critical Reviews in Biomedical Engineering*. <https://doi.org/10.1615/CritRevBiomedEng.v31.i12.30>
- Regazzoni, D., & Rizzi, C. (2013). Digital Human Models and Virtual Ergonomics to Improve Maintainability. *Computer-Aided Design and Applications*, 11(1), 10–19. <https://doi.org/10.1080/16864360.2013.834130>

- Riemer, R., & Hsiao-Wecksler, E. T. (2008). Improving joint torque calculations: Optimization-based inverse dynamics to reduce the effect of motion errors. *Journal of Biomechanics*.
<https://doi.org/10.1016/j.jbiomech.2008.02.011>
- Robinette, K., Blackwell, S., Daanen, H., Boehmer, M., Fleming, S., Brill, T., ... Burnside, D. (1991). Civilian American and European Surface Anthropometry Resource (Ceasar). *SAE International*, 5(December).
- Rune, S., Hongjun, X., & Bifeng, S. (2008). Ergonomic assessment method for cockpit layout of civil aircraft based on virtual design. *ICAS International Council of Aeronautical Sciences*, 1–8. Retrieved from
http://www.icas.org/ICAS_ARCHIVE/ICAS2008/PAPERS/002.PDF
http://www.icas.org/ICAS_ARCHIVE_CD1998-2010/ICAS2008/PAPERS/002.PDF
- Ruspa, C., Quattrocchio, S., & Bertolino, D. (2007). Virtual Tool for the Evaluation of the Visibility during Critical Driving Tasks. *Virtual Reality*, (724).
<https://doi.org/10.4271/2007-01-2499>
- Samson, A., & Khasawneh, M. T. (2009). Digital human modeling for ergonomic assessment of patient lifting by paramedics. *Graduate School of Binghamton University, Master of*, 164.
- Sanjog, J., Karmakar, S., Patel, T., & Chowdhury, A. (2015). Towards virtual ergonomics: aviation and aerospace. *Aircraft Engineering and Aerospace Technology*, 87(3), 266–273.
<https://doi.org/10.1108/AEAT-05-2013-0094>
- Santoshuman Inc. Software. (2009). Software™ Engine - Software User Guide V1.0.
- Satheeshkumar, M., & Krishnakummar, K. (2014). Digital Human Modeling Approach in

Ergonomic Design and Evaluation - A Review. *International Journal of Scientific & Engineering Research*, 5(7), 2229–5518.

Schibye, B., Hansen, A. F., Hye-Knudsen, C. T., Essendrop, M., Böcher, M., & Skotte, J. (2003). Biomechanical analysis of the effect of changing patient-handling technique. *Applied Ergonomics*, 34(2), 115–123. [https://doi.org/10.1016/S0003-6870\(03\)00003-6](https://doi.org/10.1016/S0003-6870(03)00003-6)

Siemens PLM Software. (2016). Jack User Manual Version 8.4. Retrieved from <http://inition.co.uk/3D-Technologies/productsection/43>

Skotte, J., Essendrop, M., Hansen, A., & Schibye, B. (2002). A dynamic 3D biomechanical evaluation of the load on the low back during different patient-handling tasks. *Journal of Biomechanics*, 35(10), 1357–1366. [https://doi.org/10.1016/S0021-9290\(02\)00181-1](https://doi.org/10.1016/S0021-9290(02)00181-1)

Skotte, J., & Fallentin, N. (2008). Low back injury risk during repositioning of patients in bed: the influence of handling technique, patient weight and disability. *Ergonomics*, 51(March 2015), 1042–1052. <https://doi.org/10.1080/00140130801915253>

Sun, X., Gao, F., Yuan, X., & Zhao, J. (2011). Application of Human Modeling in Multi-crew Cockpit Design. In V. G. Duffy (Ed.), *Digital Human Modeling: Third International Conference, ICDHM 2011, Held as Part of HCI International 2011, Orlando, FL, USA July 9-14, 2011. Proceedings* (pp. 204–209). Berlin, Heidelberg: Springer Berlin Heidelberg. https://doi.org/10.1007/978-3-642-21799-9_23

Sutherland, C. a., Albert, W. J., Wrigley, A. T., & Callaghan, J. P. (2008). A validation of a posture matching approach for the determination of 3D cumulative back loads. *Applied Ergonomics*, 39(2), 199–208. <https://doi.org/10.1016/j.apergo.2007.05.004>

- Takagi, Y., Oi, T., Tanaka, H., Inui, H., Fujioka, H., Tanaka, J., ... Nobuhara, K. (2014). Increased horizontal shoulder abduction is associated with an increase in shoulder joint load in baseball pitching. *Journal of Shoulder and Elbow Surgery*.
<https://doi.org/10.1016/j.jse.2014.03.005>
- Theilmeyer, A., Jordan, C., Luttmann, A., & Jäger, M. (2010). Measurement of action forces and posture to determine the lumbar load of healthcare workers during care activities with patient transfers. *Annals of Occupational Hygiene*, 54(8), 923–933.
<https://doi.org/10.1093/annhyg/meq063>
- Ulin, S. S., Chaffin, D. B., Patellos, C. L., Blitz, S. G., Emerick, C. A., Lundy, F., & Misher, L. (1997). A biomechanical analysis of methods used for transferring totally dependent patients. *American Association of Spinal Cord Injury Nurses*, 14(1), 19–27. Retrieved from <http://eutils.ncbi.nlm.nih.gov/entrez/eutils/elink.fcgi?dbfrom=pubmed&id=9165952∓retmode=ref&cmd=prlinks>
- Van Kampen, D. A., Willems, W. J., van Beers, L. W. A. H., Castelein, R. M., Scholtes, V. A. B., & Terwee, C. B. (2013). Determination and comparison of the smallest detectable change (SDC) and the minimal important change (MIC) of four-shoulder patient-reported outcome measures (PROMs). *Journal of Orthopaedic Surgery and Research*, 8(1), 1–9.
<https://doi.org/10.1186/1749-799X-8-40>
- Vicon. (2016). Vicon Nexus User Guide.
- Warburton, D. E. R., Jamnik, V. K., Bredin, S. S. D., Burr, J., Charlesworth, S., Chilibeck, P., ... Gledhill, N. (2011). Executive Summary The 2011 Physical Activity Readiness Questionnaire for Everyone (PAR--Q+) and the Electronic Physical Activity Readiness

Medical Examination (ePARmed--X+). *Health & Fitness Journal of Canada*.

Waters, T. R., Putz-Anderson, V., Garg, a, & Fine, L. J. (1993). Revised NIOSH equation for the design and evaluation of manual lifting tasks. *Ergonomics*, *36*(7), 749–776.

<https://doi.org/10.1080/00140139308967940>

Wegner, D., Chiang, J., Kemmer, B., Lämkuhl, D., & Roll, R. (2007). Digital Human Modeling Requirements and Standardization. *SAE International*, 151–159.

Weiner, C., Alperovitch-Najenson, D., Ribak, J., & Kalichman, L. (2015). Prevention of Nurses' Work-Related Musculoskeletal Disorders Resulting From Repositioning Patients in Bed. *Workplace Health & Safety*, *63*(5), 226–232. <https://doi.org/10.1177/2165079915580037>

Weiner, C., Kalichman, L., Ribak, J., & Alperovitch-Najenson, D. (2017). Repositioning a passive patient in bed: Choosing an ergonomically advantageous assistive device. *Applied Ergonomics*, *60*, 22–29. <https://doi.org/10.1016/j.apergo.2016.10.007>

Winkel, J., & Mathiassen, S. E. (1994). Assessment of physical work load in epidemiologic studies: concepts, issues and operational considerations. *Ergonomics*, *37*(6), 979–988. <https://doi.org/10.1080/00140139408963711>

Woldstad, J. C. (2006). Digital Human Models for Ergonomics. In *International Encyclopedia of Ergonomics and Human Factors* (pp. 3093–3096).

Wu, G., Siegler, S., Allard, P., Kirtley, C., Leardini, A., Rosenbaum, D., ... Stokes, I. (2002). ISB recommendation on definitions of joint coordinate system of various joints for the reporting of human joint motion—part I: ankle, hip, and spine. *Journal of Biomechanics*, *35*(4), 543–548. [https://doi.org/10.1016/S0021-9290\(01\)00222-6](https://doi.org/10.1016/S0021-9290(01)00222-6)

- Wu, G., Van Der Helm, F. C. T., Veeger, H. E. J., Makhsous, M., Van Roy, P., Anglin, C., ...
Buchholz, B. (2005). ISB recommendation on definitions of joint coordinate systems of
various joints for the reporting of human joint motion - Part II: Shoulder, elbow, wrist and
hand. *Journal of Biomechanics*, 38(5), 981–992.
<https://doi.org/10.1016/j.jbiomech.2004.05.042>
- Xia, S., & Gunther, P. (2011). Determinants of Driver vs . Second Row Occupant Posture
Modelling. In *1st International Symposium on Digital Human Modelling* (pp. 14–16).
- Yamamoto, I., Panjabi, M. M., & Oxland, T. (1989). Three-dimensional movements of the whole
lumbar spine and lumbosacral joint. *Spine*. <https://doi.org/10.1097/00007632-198911000-00020>
- Yang, J., Kim, J. H., Abdel-Malek, K., Marler, T., Beck, S., & Kopp, G. R. (2007). A new digital
human environment and assessment of vehicle interior design. *Computer-Aided Design*, 39,
548–558. <https://doi.org/10.1016/j.cad.2006.11.007>
- Yang, J., Rahmatalla, S., Marler, T., & Abdel-malek, K. (2007). Validation of Predicted Posture
for the Virtual Human Santos™. *Hcii, LNCS 4561*(Digit. Hum. Model.), 500–510.
Retrieved from
[http://www.springerlink.com/index/E312574437V91Q11.pdf%5Cnpapers2://publication/uu
id/A787ECAA-1FFD-411C-8376-2453F7F78D76](http://www.springerlink.com/index/E312574437V91Q11.pdf%5Cnpapers2://publication/uuid/A787ECAA-1FFD-411C-8376-2453F7F78D76)
- Zatsiorsky, V. M. M. (1998). Kinematics of Human Motion. *American Journal of Human
Biology*. <https://doi.org/99.1998/zatsiorsky.0880116765>
- Zhang, L., Niu, J., Feng, X., Xu, S., & Li, X. (2013). Digital Human Modeling for
Musculoskeletal Disorder Ergonomics Researches In Healthcare. In *The 19th International*

Conference on Industrial Engineering and Engineering Management (pp. 1149–1156).

<https://doi.org/10.1007/978-3-642-38442-4>

Zhang, X., & Chaffin, D. B. (2006). Digital human modeling for computer-aided ergonomics.

Interventions, Controls, and Applications in Occupational Ergonomics, Chapter 10.

Retrieved from

<http://www.mechse.uiuc.edu/research/xudong/Preprint/ChapterPreprint.pdf%5Cnpapers2://publication/uuid/C4E7FBEF-23D7-4DE2-8A96-5DE82A131ADE>

Zhang, X., Xue, L., Li, S., & Kim, F. J. (2013). Digital human modeling for ergonomic

evaluation of patient table height. *Robotics and Biomimetics (ROBIO), 2013 IEEE*

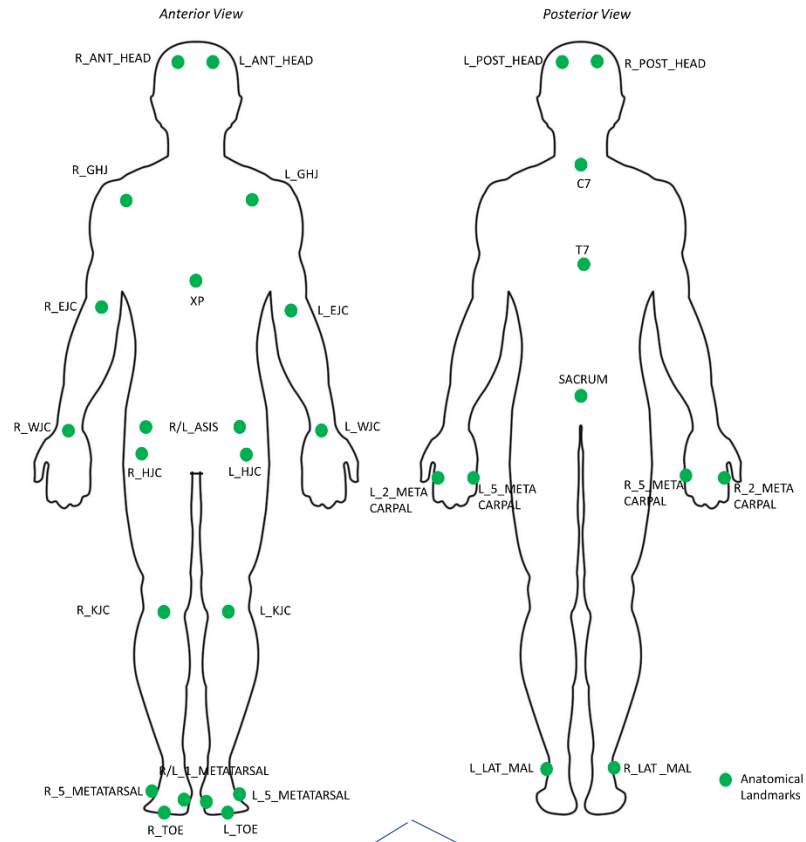
International Conference On, (December), 1480–1485.

Zhao, J., & Badler, N. I. (1994). Inverse kinematics positioning using nonlinear programming for highly articulated figures. *ACM Transactions on Graphics*.

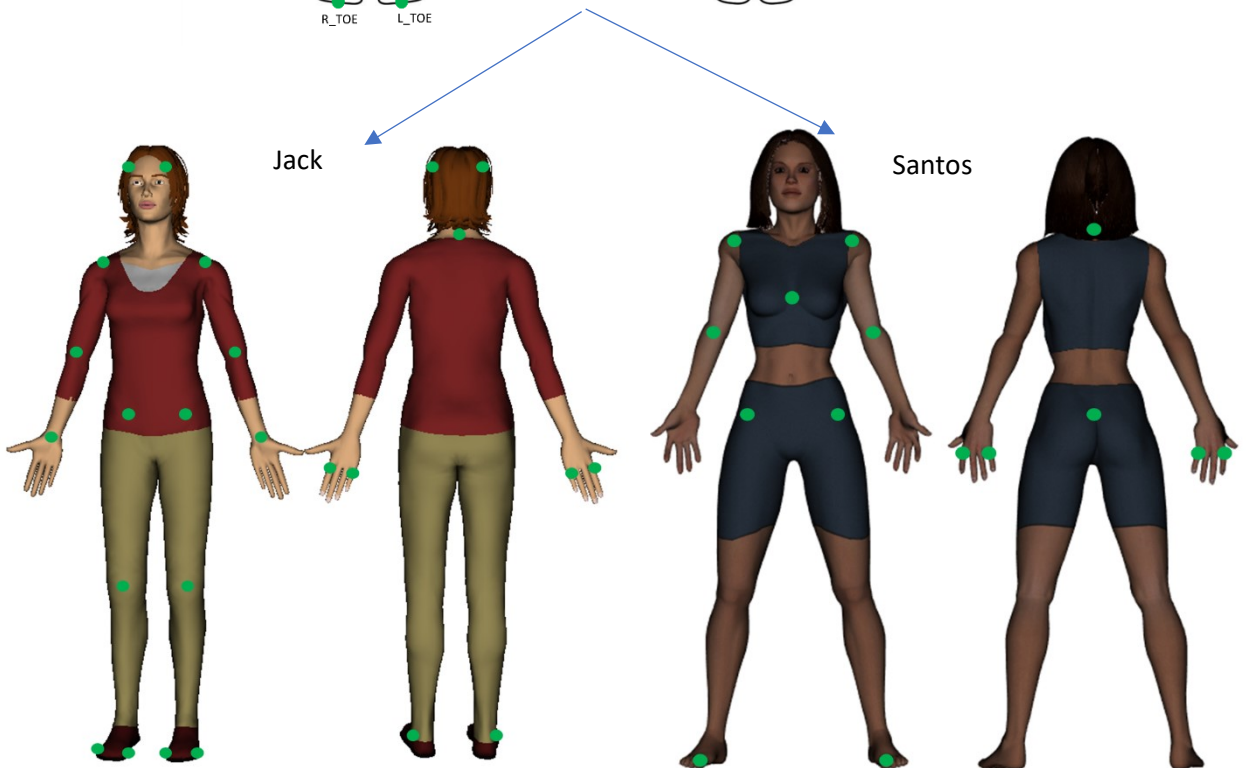
<https://doi.org/10.1145/195826.195827>

Appendix I

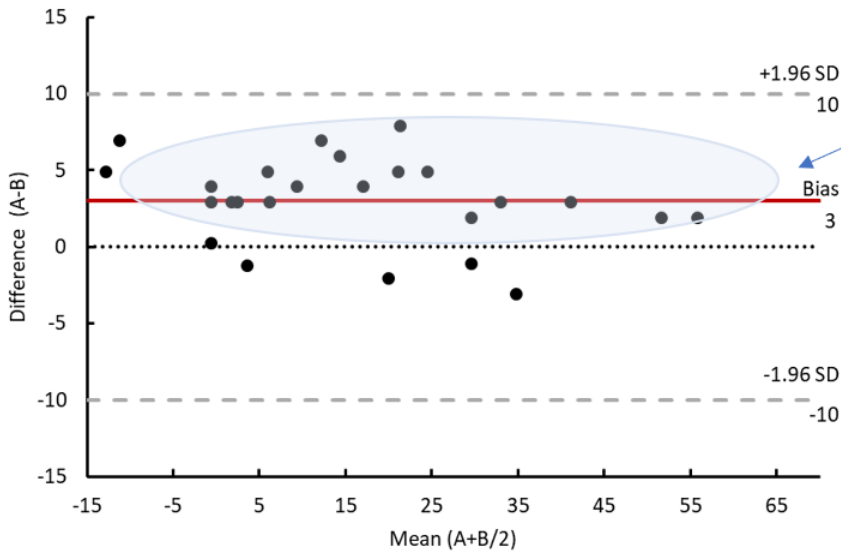
Lab-based rigid-linked model joint centers of rotation and segment landmarks



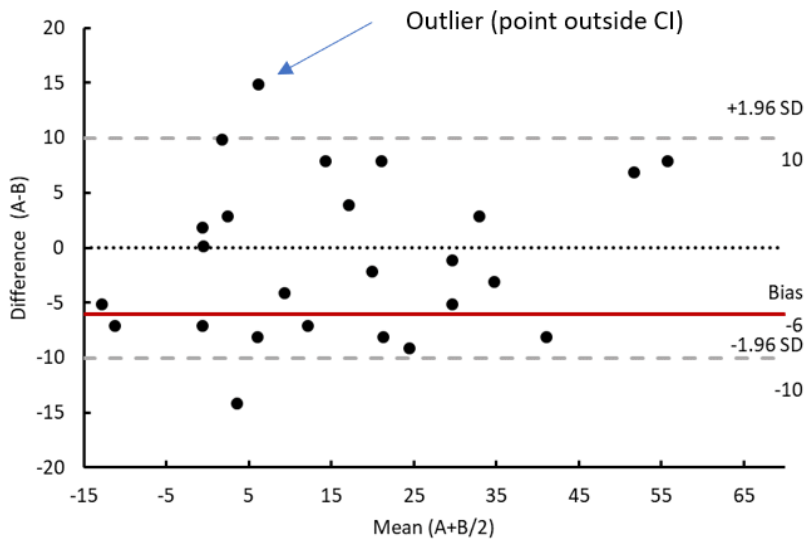
Select joint/segment position data from the lab-based model were mapped onto the corresponding joints/segments of the avatar in the DHM where permissible



Appendix II

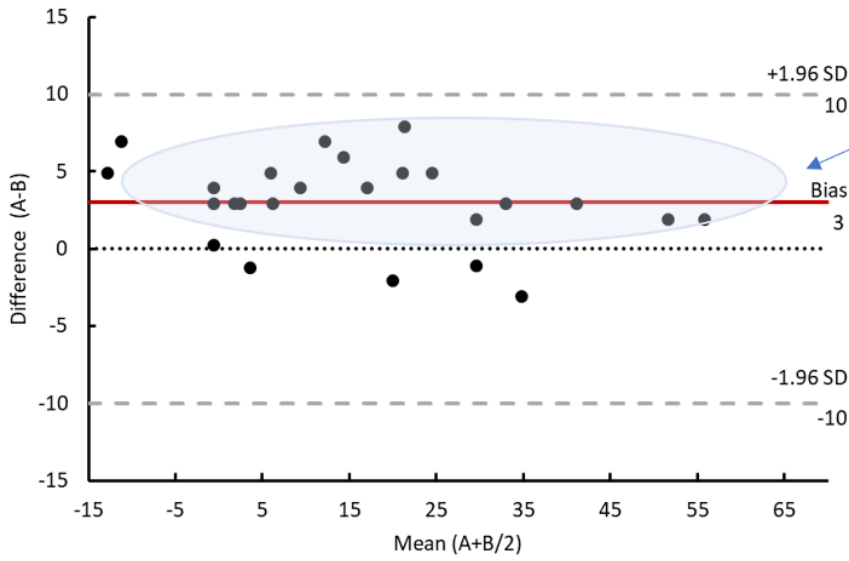


Majority of differences are above the line of equality, showing that B is **underestimating** measures relative to A. Differences are near the line of equality, and equally spread, showing **moderate agreement**

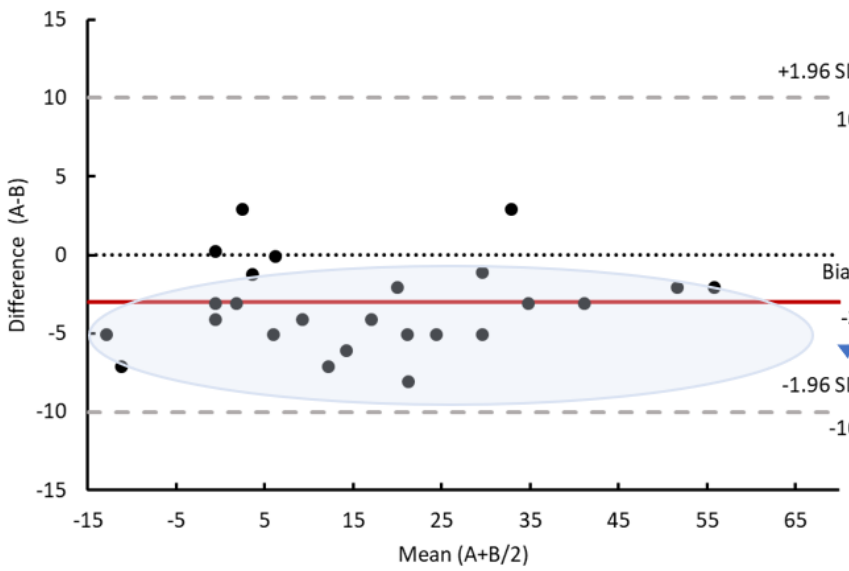


Differences are not near the line of equality. Variance around the line is not constant and there is a large bias and outliers showing **poor agreement** (disagreement between A and B)

Large bias



Majority of differences are above the line of equality, showing that B is **underestimating** measures relative to A. Differences are near the line of equality, and equally spread, showing **moderate agreement**



Majority of differences are below the line of equality, showing that B is **overestimating** measures relative to A. Differences are near the line of equality, and equally spread, showing **moderate agreement**

Appendix III

Summary of multiple regression statistics for the Independent variables (Mean outputs) to Dependent variables (Mean difference outputs)

Manual

Independent Variable	Unstandardized Coefficients		Standardized Coefficients	
	B	Std. Error	β	t
Jack L4-L5 Moment	0.22	0.08	0.47	2.54*
Santos L4-L5 Moment	0.69	0.11	0.79	6.15*
Jack Shoulder Moment	0.11	0.36	0.06	0.30
Santos Shoulder Moment	1.28	0.31	0.65	4.15*
Jack Trunk Angle	0.17	0.68	0.05	0.24
Santos Trunk Angle	1.73	0.25	0.83	7.02*
Jack Shoulder Angle	-0.66	0.14	-0.71	-4.85*
Santos Shoulder Angle	0.04	0.08	0.10	0.47

*p<0.05

Posture Prediction

Independent Variable	Unstandardized Coefficients		Standardized Coefficients	
	B	Std. Error	β	t
Jack L4-L5 Moment	1.33	0.20	0.81	6.56*
Santos L4-L5 Moment	1.59	0.17	0.89	9.54*
Jack Shoulder Moment	0.07	0.27	0.05	0.26
Santos Shoulder Moment	0.51	0.37	0.28	1.38
Jack Trunk Angle	1.40	0.23	0.78	5.96*
Santos Trunk Angle	1.71	0.11	0.96	16.28*
Jack Shoulder Angle	0.85	0.34	0.47	2.53*
Santos Shoulder Angle	1.13	0.35	0.56	3.20*

*p<0.05

Motion Capture

Independent Variable	Unstandardized Coefficients		Standardized Coefficients	
	B	St. Error	β	t
Jack L4-L5 Moment	0.44	0.18	0.45	2.40*
Santos L4-L5 Moment	1.55	0.12	0.94	12.77*
Jack Shoulder Moment	-0.05	0.41	-0.03	-0.13
Santos Shoulder Moment	0.41	0.36	0.23	1.14
Jack Trunk Angle	1.07	0.20	0.75	5.38*
Santos Trunk Angle	0.35	0.22	0.31	1.59
Jack Shoulder Angle	0.17	0.16	0.22	1.08
Santos Shoulder Angle	1.52	0.14	0.92	10.95*

*p<0.05